Assessment and improvement of TELEMAC-2D routines for urban flood simulation

By

Ruijie Chen

A thesis submitted to the University of Ottawa

In partial fulfillment of the requirements

for the Master of Applied Science in Civil Engineering

Department of Civil Engineering

Faculty of Engineering

University of Ottawa

Abstract

Pluvial flood is a natural hazard that severely threatens people's property and safety. With the development of algorithms and computer technologies, numerical modeling has emerged as an effective tool for predicting the impacts of floods. Despite being one of the most costly types of floods in West Africa, pluvial flooding has not been studied as extensively as riverine flooding, probably because modeling runoff across urban areas remains a challenge. Recently, a module based on the SCS Curve Number Method is incorporated in the open-source software TELEAMC-2D, which provides a possibility to model the infiltration process dynamically. TELEMAC-2D is one of the first hydraulic models to consider hydrologic parameters. Although the update is expected to increase the suitability of TELAMC-2D in pluvial flood modeling, the infiltration routine has not yet been tested in a real situation in a semi-arid area. This study aims to investigate the capability of TELEMAC-2D in simulating the rainfall-runoff process during a pluvial flood event in a semi-arid urban area, Niamey city in west Africa. Due to the lack of calibration data, a hydrological model SWAT is used to evaluate the performance of TELEMAC-2D. Through the comparison between the runoffs generated by the two models, it is found that TELEMAC-2D has a similar trend with SWAT in runoff simulation. However, TELEMAC-2D significantly overestimates the runoff magnitude despite having the same SCS values as SWAT. The reason for the overestimation is TELEMAC-2D that does not properly consider evaporation. Two suggestions are made to improve pluvial floods simulations using TELEMAC-2D in semi-arid areas: 1) couple TELEMAC-2D with a hydrologic model, and use net rainfall generated by the hydrologic model as precipitation input; 2) provide functions in infiltration subroutine that calculate rainfall abstractions by other hydrologic phenomena in addition to the infiltration process.

Acknowledgments

I would like to take this opportunity to express my gratitude and appreciation to all the people who have provided support during my master's study and helped me grow professionally.

First, I owe my sincerest gratitude to my supervisors Dr. Ousmane Seidou and Dr. Majid Mohammadian, for offering me the opportunity to study Civil Engineering at UOttawa. Their research achievements have greatly inspired me to continue to explore the field of numerical modeling. My supervisors always offer me guidance when I encounter difficulties or make mistakes in my study, which helped me develop the ability to think independently and critically. It also boosted my confidence in my chances to study in Canada as an international student successfully.

I also feel grateful for all the professors in the Department of Civil Engineering. They offer great lectures that are informative and interesting. The completion of this thesis would not have been possible without the background developed by attending their courses.

A big 'THANK YOU' should also go to all the staff members at UOttawa who ensure that all the resources are available to us students, especially during this trying time.

Last but not least, I would like to thank my friends and my parents who are always there for me. It is always a pleasure to discuss my learning experience with them. I know their critical feedback has been an excellent help to me. Your support means everything to me.

Table of Contents

List of Figures

List of Tables

List of Abbreviations and Acronyms

1D: One dimensional

2D: Two dimensional

3D: Three dimensional

AI: Artificial Intelligence

AMC: Antecedent Moisture Condition

AMC1: Dry Antecedent Moisture Condition

AMC2: Normal Antecedent Moisture Condition

AMC3: Wet Antecedent Moisture Condition

ANN: Artificial Neural Network

ARD: Accumulated Rainfall Depth

C: Contoured

CA: Cellular Automate

CN: Curve Number

CN (I): Curve Number in Dry Antecedent Moisture.

CN (II): Curve Number in Normal Antecedent Moisture.

CN (III): Curve Number in Wet Antecedent Moisture.

CR: Crop Residue Cover

C&T: Contoured and Terraced

DEM: Digital Elevation Model

DSM: Digital Surface Model

F: Actual Retention

FAO: Food and Agriculture Organization

FDM: Finite Differential Method

FEM: Finite Element Method

FFS: Flood Forecasting System

FMS: Flood Monitoring System

FVM: Finite Volume Method

IA: Initial Abstraction

LIDAR: Light Detection and Raging

NRCS: U.S Natural Resource Conservation Service

PDE: Partial Differential Equation

SCS: Soil Conservation Service

SPS: Ensemble Prediction System

SR: Strait Row

SRTM: Shuttle Radar Topographic Mission

SWAT: Soil and Water Assessment Tool

SWE: Shallow Water Equation

TDR: Time Domain Reflectometry

USDA: United States Department of Agriculture

USGS: United States Geological Survey

WD: Wetting and Drying

List of symbols

b	Viscous drag coefficient
F	Actual retention [mm]
f	Coriolis coefficient associated with the Coriolis force
g	Acceleration due to gravity [m^2/s]
H	Mean height of the horizontal pressure surface [m]
h	Height deviation of the horizontal pressure surface from its mean height H [m]
I_a	Initial abstraction [mm]
P	Rainfall depth for the day [mm]
Q	Accumulated surface runoff [mm]
S	Maximum potential retention [mm]
t	Time [s]
u	Velocity in the x-direction [m/s]
$\vec{u}$	Velocity vector
v	Velocity in the y-direction [m/s]
x	Horizontal Space Coordinates
y	Horizontal Space Coordinates
Z	Free Surface [m]
η	Total fluid column height [m]
ν	Kinematic viscosity [m^2/s]
λ	Constant coefficient in SCS Curve Number Method

Chapter 1 Introduction

Over the last few decades, the frequency and intensity of floods have increased dramatically. Floods are a major contributor to personal injury and property damage and can strike with little warning. According to the data collected by the Munich Reinsurance Company, fatalities caused by flooding lead to half of the fatalities related to natural disasters (Kron, 2005). Meanwhile, one-third of economic losses incurred from natural hazards are directly connected to floods: for example, around one trillion economic losses and 220,000 fatalities were ascribed to flooding between 1980 and 2013 (Hoch et al., 2018). Latest investigation showed that 47% of natural hazards occurring during 1995-2015 were floods-related, affecting 2.3 billion people worldwide and causing 662 billion dollars damage during this period (UNISDR 2015). Even though flood causes tremendous damage, research on the nature of flood and flood management is still insufficient. Pluvial flood occurs when precipitation or snowmelt can not be discharged by drainage systems, forcing water to stay on the ground (Carter 1996). Due to climate change and urbanization, pluvial flooding has been striking urban areas more frequently and has caused important damage to life and property (Bulti & Abebe, 2020; Grahn & Nyberg, 2017; Rosenzweig et al., 2018). According to Hochrainer-Stigler et al. (2016), economic and life losses related to rainfall-induced flooding will continuously increase in the future. Urban flood occurs when surface runoff generation exceeds infiltration rates and drainage capacity (Rosenzweig et al., 2018). Urban districts are prone to suffer more significant flooding due to heavy rainfalls, the number of constructions, ground surface of low permeability, and drainage systems that lack adequate

management. Pluvial flood research is required to understand the nature of flood and flood coping mechanisms in urban areas and help minimize these losses.

1.1 Background

With the acceleration of urbanization, pluvial flooding is now acknowledged as one of the most common and destructive natural hazards in urban areas(Huang, Wang et al. 2017, Pradhan-Salike and Pokharel 2017, Rosenzweig, McPhillips et al. 2018). The predominance of highly impermeable surfaces and lack of water storage in typical urban districts makes them more vulnerable to heavy rainfall (Rehman et al., 2019). The situation could worsen when pluvial flooding is combined with fluvial flooding (Apel et al., 2016). In the past 50 years, our understanding of floods has improved to a great extend (Merkuryeva et al., 2015). However, most studies focused on riverine flooding, which is relatively simpler to model than rainfall-reduced flooding. Due to a lack of appropriate topographic data, complex footpaths, and computational challenges, the study of pluvial flooding has been challenging for half a century.

As pluvial floods appear more frequently and the consequences are getting more serious, policymakers are paying additional attention to urban flood hazards. With the fast improvement of computer technologies and remotely sensed technologies, numerical models show great potential to be an effective and economical tool to study this urban flood issue (Xing et al., 2019). An accurate representation of the terrain and a comprehensive understanding of the rainfall-runoff process is required to mimic the flow propagation in urban areas realistically. Previously, conventional analyses based on empirical methods were inadequate to simulate hydraulic variables

in urban catchments dynamically (Bulti & Abebe, 2020). With the progress in computing facilities in the last decade, several hydrodynamic models have been developed in hazard and risk assessment. They can realistically model flow motion by solving physically based equations and dynamically provide inundation information for real-life flood events.

Currently, the most widely used numerical hydrodynamical models are 1D (one dimensional) and 2D (two dimensional) models because 3D (three dimensional) models are costly and require more computational effort. With 1D models, terrains are presented as a succession of cross-sections, and flows are simulated to approximate the average velocity and water depth at every cross-section. One core assumption of 1D models is that velocities only have longitudinal direction along the channel, and at each cross-section, the nodes have the same value. Based on this assumption, roughness is considered the main factor that influences the flow pattern of 1D models. 1D models are advantageous in simulating in-channel flow, but they are not as effective as 2D models to simulate floodplain flows. As a Result, 1D models are usually used to simulate drainage systems during urban flood events.

With the increased availability of high-resolution DEMs (Digital Elevation Models), 2D models are now frequently used to compute free surface flow. They consider the two orthogonal flow velocities on a structured or unstructured mesh at each time interval, using 2D Saint-Venant depth-averaged equations. In the past, 2D flood inundation research was hampered due to the lack of detailed topographic information (Bates et al., 1992). Nowadays, the simulation environment has improved as topographic resources availability has increased with advanced remote sensing technology. Even though 2D models have many advantages over 1D models, the trade-off is that

2D models require more preparation in building meshes and more computation time. Fortunately, the computation time has recently been reduced significantly with the enhancement of computational facilities.

Not all rainfall becomes runoff during a storm because initial abstraction and continuous abstraction reduce the rainfall volume. When precipitation exceeds a certain threshold value, rainfall that is not absorbed by soil becomes direct runoff. Hydrologic rainfall-runoff modeling plays a significant role in urban flood modeling to foster a better understanding of flooding in urban areas. Hydrological models can be categorized into three main models: data-driven, conceptual, and process-driven. Data-driven models are used most frequently in the simulation due to the simplicity of the model. However, conceptual models and process-driven models require more knowledge in hydrologic data (Sitterson et al., 2018). Despite the existing limitations in data-driven models, they have become an accurate and reliable tool for rainfall-runoff transformation.

Teng et al. (2017) analyzed the related uncertainties in hydrodynamic and hydrological modeling, and critically examined the advantages and disadvantages of each type of model. Their study showed that a model which applies to all research scenarios is unavailable. Therefore, it is critical to choose a model that meets the specific requirements of a study. For example, the simplified route runoffs and wave propagation in rainfall-runoff models are unable to present some common phenomena such as backwater effects (Hsie, 1974). In such a situation, more comprehensive hydrodynamic models are required to avoid misestimation of the impact of flooding.

TELEMAC-2D shows great potential in simulating urban area flooding among numerous packages. TELEMAC-2D is an open-source program developed by the R&D group of Électricité de France, which solves full Saint-Venant equations on unstructured meshes. The open-source code also allows researchers to program Fortran language in subroutines to meet their specific requirements, which is helpful to develop a realistic model for pluvial urban floods (Ligier, 2016). Another benefit of TELEMAC-2D is that users can adjust the density of the mesh according to the demand. For example, a dense mesh can be used in urban areas where the environment is complicated. In contrast, a sparse mesh can be used for non-urban areas where geometric characteristics are relatively simple. The flexible mesh strategy could significantly reduce the computation time.

Moreover, the parallel version is also available to allow users to activate multiple processors to accelerate the computation. Since version v7p2, released in 2017, an infiltration process has been added as a subroutine in the TELEMAC-2D package, allowing it to model the infiltration process dynamically. Infiltration is one of the most important processes during an urban rainfall event, as ignoring infiltration can lead to the overestimation of surface runoff (Wallach et al., 1997). The new update makes TELEMAC-2D more suitable in urban pluvial flood modeling.

Even though TELEMAC-2D has many obvious advantages, and the new infiltration routine makes it even more attractive, the model may perform in every situation. For example, the SCS Curve Number Method incorporated in TELEMAC-2D was developed using American field data, which may bring some uncertainty when applying this approach in different regions. Besides, the SCS Curve Number Method is very sensitive to antecedent moisture conditions (AMC), and there is no clear guidance for classification (Ponce & Hawkins, 1996). Furthermore, given that in infiltration module is new, it has to be tested to check if its output is in line with observations.

Consequently, the applicability, correctness, limits, and potential of the novel hydro-inundation model in a semi-arid area are particularly worth examining and thus are the subject of this study.

1.2 Objectives of the Study

Urban flood is one of the most common natural disasters which cause tremendous loss to property and life. Most of the floods are caused by natural precipitation that can not be discharged in time. Rainfall-related flood is a complex phenomenon affected by a series of factors such as flow paths, drainage systems, and the built environment. TELEMAC-2D is a tool for urban flood simulations and has routines for calculating time-varying rainfall and infiltration with SCS Curve Number Method. This study aims to test the ability of TELEMAC-2D to simulate urban runoff in the city of Niamey, Niger. A hydrological model SWAT (Soil and Water Assessment Tool) is selected to compare the runoffs generated by SWAT and TELEMAC-2D. The infiltration subroutine in TELEMAC-2D is examined, and suggestions are given to improve the subroutine.

1.3 Novelty of the Study

At present, a lot of benchmark studies of flood modeling are conducted in Europe and America. Only recently, the southeast Asian area has become a research focus because this area is often affected by intense rainfall. On the other hand, West Africa has rarely been paid enough attention, yet this region is one of the areas that flood disasters have most severely struck (Ekeu-wei and Blackburn 2018). One of the reasons for the lack of study in this area is that data preparation for running numerical models remains one major challenge. The present study is one of the first attempts to compare rainfall-runoff simulated by a hydrological and a hydraulic model using online data for flood modeling. Meanwhile, the present research is one of the first studies to evaluate

rainfall-related flood simulation by TELEMC-2D in a real-life situation. Due to the lack of measured data, calibrations and validations are required in future work.

1.4 Scope of the Study

Previous research on using 1D and 2D models for pluvial modeling is discussed in the literature review, while 3D models are not covered during this study. In the present study, a 2-D hydrodynamic model was developed to simulate a major rainfall-related flood event in Niamey city in 2019. Given that very limited streamflow observations are available in the study area, the TELECMAC 2D simulations will be compared to the output of a SWAT (Soil and Water Assessment Tool) model using default parameters. SWAT is an established rainfall-runoff model that is used worldwide, including in Africa. The study primarily focuses on testing the impact of the space-varying Curve Number. Because infiltration in SWAT is simulated using the SCS CN method, it is expected that if the same CN values are used in SWAT and TELEMAC, the runoff values should be similar.

1.5 Outline of the Thesis

This thesis consists of five chapters. Chapter 1 is the introduction, providing the general information on urban pluvial flood and flood analysis. In chapter 2, previous research on the applications of hydraulic models and hydrologic models in flood simulations is reviewed. Chapter 3 introduces the methods and the materials used to conduct the simulation of the study area.

Chapter 4 demonstrates the research processes and the discussion of results obtained from TELEMAC-2D and SWAT models. To be more specific, the generated runoffs are compared to improve the TELEMAC-2D model in further detail. The benefits and forfeits of hydraulic and hydrologic models in the rainfall-runoff simulation are also discussed in this chapter. Chapter 5 presents the conclusion along with suggestions for future research.

1.6 Contribution of the Study

The study examines the applicability of the new SCS CN infiltration routine in TELEMAC 2D. Results show that additional work is required before TELEMAC 2D could be used to realistically assess urban floods in Niamey. A SWAT model of the study area was also developed and used to simulate runoff in the 2019 flood event in Niamey city using the TELEMAC-2D hydrodynamic model. Despite the identified limitations, the result of the simulation of both models can provide practical and empirical implications for flood management in the city. Once the recommended improvement to the TELEMAC routines is implemented, the impacts of pluvial processes across west Africa can be assessed. Particularly, visualizing the runoff distribution at different stages during a flood event will indicate the timing at which a certain area is likely to be affected so that timely reactions can be taken. In addition, modeling surface runoff dynamically in a hydraulic model can provide more detailed evidence for decision-makers to make decisions for flood emergency management as well as property management.

Chapter 2 Literature Review

2.1 Impacts of Flood Disasters

Flood is one of the most common disasters that cause significant adverse impacts to human life and properties (Doocy et al., 2013; Jha et al., 2012; UNISDR2015). As one of the most devastating hazards, flood is considered a consequence of climate change and anthropogenic factors that increase the occurrence of flood and its severity (Salami et al., 2017). Climate change, such as intense rainfall, snowmelt, and high tides, contributes to the natural causes of floods. Meanwhile, anthropogenic factors, including unabated urbanization, improper land use, and poor drainage system maintenance, make humans more vulnerable when a flood occurs (Tingsanchali, 2012; Wong, 2015).

2.2 Flood Management

More and more evidence has been obtained in recent years that show that increasing extreme rainfall's frequency and intensity are crucial factors contributing to urban floods (Abaje et al., 2015; Tarhule, 2005; Vojinovic, 2015). Compared with rural areas, urban areas are more prone to rainfall-induced flood inundation because of limited infiltration, low-lying terrain, insufficient drainage systems, and massive construction that reduces the capacity of the ground to absorb excessive rainfall (Pauleit & Duhme, 2000). Consequently, urban areas suffer greater life and property losses during flood events. On the other hand, people undergo considerable challenges caused by floods in less developed countries due to insufficient knowledge about flood and flood coping systems (Winsemius et al., 2016). Therefore, in-depth analysis to better understand flood

as a human security issue should be prioritized in underdeveloped areas. In recent years, a constant endeavor has been made to increase the awareness of floods worldwide.

Meanwhile, various approaches such as flood monitoring, flood forecasting, and flood modeling have been implemented to improve flood management. Flood Monitoring System (FMS) plays an essential role in providing early warnings for people to respond timely during flood events. To be more specific, FMS is used to provide information on hydrologic variables such as water level, flood extent, precipitation, distribution through gauge stations, and satellite images (Marin-Perez et al., 2012; Revilla-Romero et al., 2015). At the same time, FMS is often affected by the limited distribution of gauge stations and satellite cycles (Andreadis & Schumann, 2014; Di Baldassarre et al., 2009; Yamazaki et al., 2014). Flood Forecasting System (FFS) provides a critical approach to notify people of flood events. While Ensemble Predictions Systems (EPS) (Cloke & Pappenberger, 2009; Demeritt et al., 2007; Demeritt et al., 2010) and Artificial Intelligence (AI) (Chau et al., 2005; Wu & Chau, 2006) technologies are two promising methods used in flood forecasting, the accuracy of FFS is affected by the lack of real-time data assimilation (Goonetilleke & Jenkins, 1999; Teng et al., 2017) and the limited amount of data input (Al-Sabhan et al., 2003; Merkuryeva et al., 2015). Flood modeling serves as a non-structural flood management approach used to simulate the evolution of a flood event and assess the possibility of inundation under a specific condition. Even though flood modeling provides a straightforward illustration of floods, the substantial computation time required in flood modeling is considered a major constraint (Kalyanapu et al., 2011). Since flood monitoring, flood forecasting, and flood modeling have their advantages and disadvantages in predicting flood phenomena and mitigating the negative impacts of flood disasters, it has become essential to consider the context when determining the optimal approach (Teng et al., 2017).

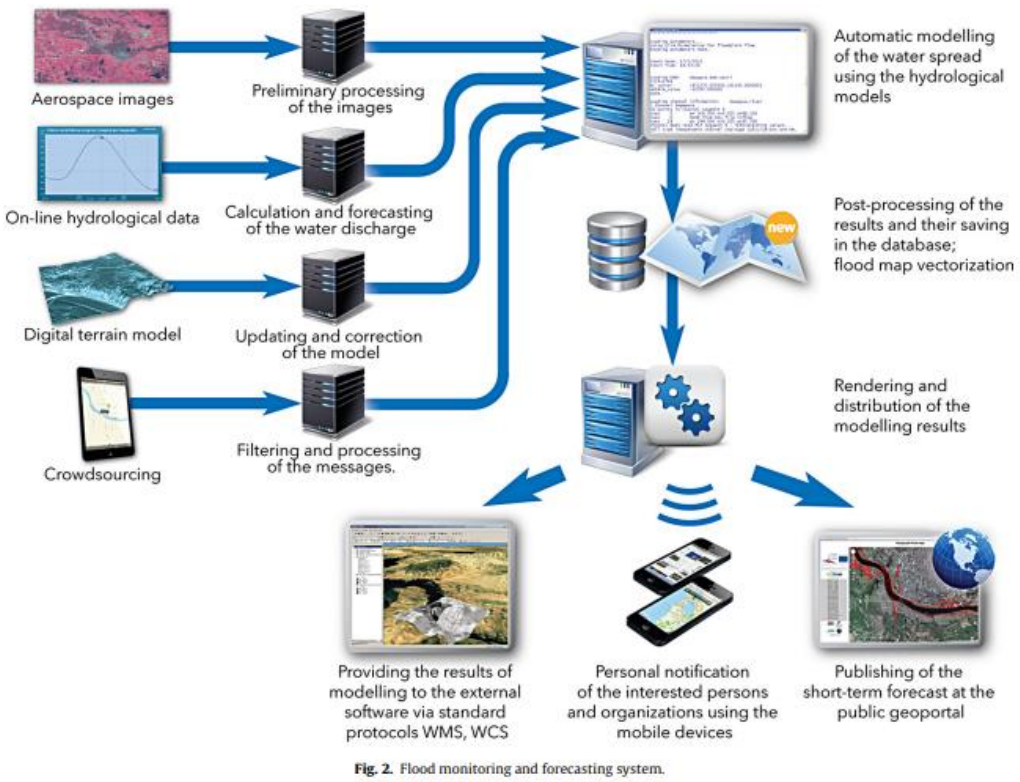

Figure 2. 1 Flood monitoring and forecasting system (Merkuryeva et al., 2015).

2.3 Flood Hazard Mapping

Flood hazard maps have been used to identify areas that are likely to be exposed to flooding. Due to drastic climate change and rapid urbanization especially, the identification of areas that are at high risk of flood disaster is imperative for minimizing flood induced losses in these areas (Büchele et al., 2006; Ghimire, 2013; Meng et al., 2019; Tsubaki & Fujita, 2010).

2.3.1 Statistical Models

In the past, statistical models were primarily utilized to generate hazard maps (Al-Sabhan et al., 2003; Fernández & Lutz, 2010; Kourgialas & Karatzas, 2011; Manfreda et al., 2008; Nandi et al., 2016; Sanyal & Lu, 2006; Termeh et al., 2018; Xiao et al., 2017). For example, Sanyal and Lu (2006) created a hazard map in India by evaluating variables related to geomorphic,

topographic, and demography to provide evidence for classifying areas under different levels of flood severity. Fernández and Lutz (2010) used multicriteria analysis to rank urban areas in Argentina by considering their variables which control flow routing when the flow exceeds the drainage capacity. Da Costa et al. (2019) developed a data-driven web-based application to delineate flood-prone zones in Europe. Although the statistical models could provide useful information for flood hazard mapping, these data-based models could not model dynamic conditions, such as water flow velocity and water depth (da Costa et al., 2019).

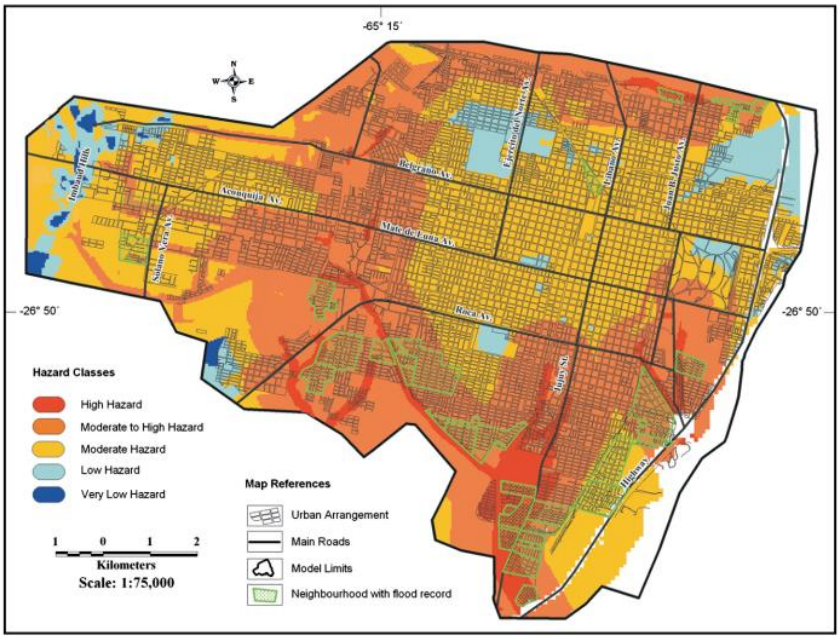

Figure 2. 2 Flood hazard map created by multi-criteria method (Fernández & Lutz, 2010).

2.3.2 Hydrodynamic Modeling

With the progress of computation facilities and remotely sensed technology, hydrodynamic models have been developed to overcome the limitations of data-based models (Schumann et al., 2009; Smith, 1997). Hydrodynamic modeling is an emerging approach that uses governing equations to

study fluids in motion (Abbott & Basco, 1989). As hydrodynamic models describe flows in the real world, models are often categorized into 1D, 2D, and 3D models by the dimensional features of the flow in the area (Teng et al., 2017).

2.3.2.1 1D Hydrodynamic Modeling

1D models solve one-dimensional Saint-Venant Equations between two adjacent cross-sections (Pramanik et al., 2010; Samuels, 1990) and are widely used to simulate flow in channels (Huţanu et al., 2020; Pappenberger et al., 2008; Pramanik et al., 2010; Romali et al., 2018) and flow in confined pipes (Axworthy et al., 2000; Mark et al., 2004; Santoro et al., 2018). While the major advantage of 1D modeling is that it is time-efficient and it produces reliable results when simulating 1D flows, the drawback becomes obvious in modeling overland flow because 1D model is not appropriate to simulate lateral diffusion of the flood waves (Bates & De Roo, 2000; Hunter et al., 2007). Mark et al. (2004) studied the advantages and disadvantages of the 1D model in urban flood modeling and concluded that inaccurate representation of surface flow led to an overestimated water depth.

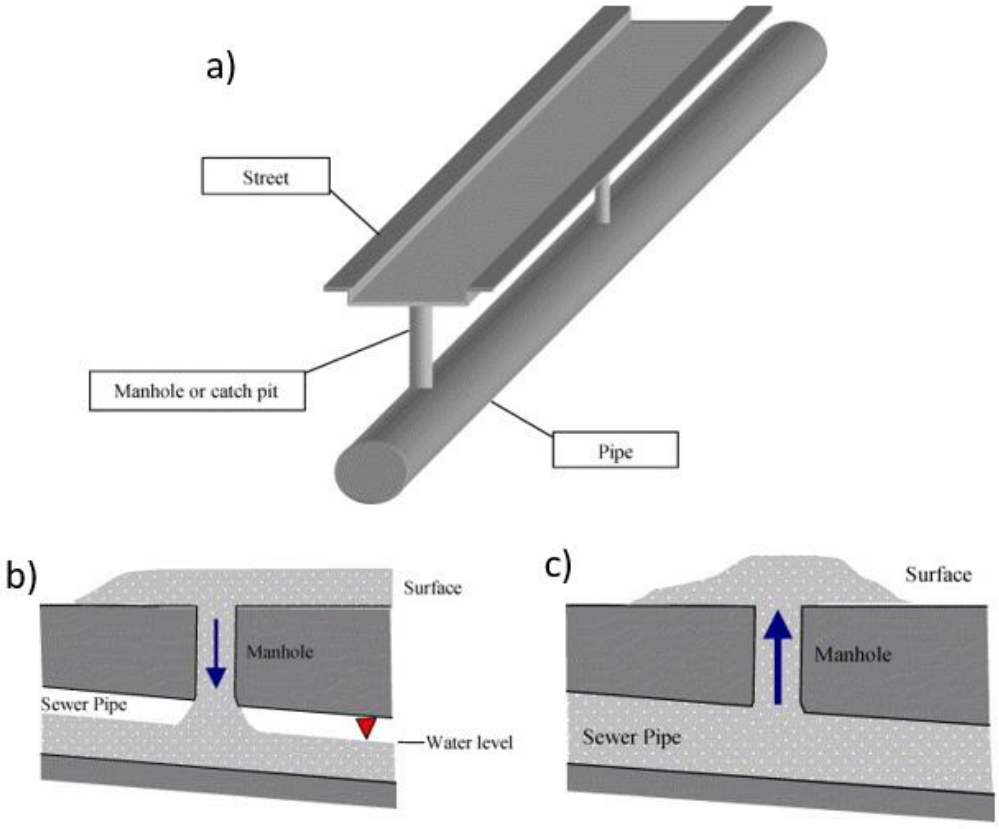

Figure 2. 3 Dual-drainage system (Mark et al., 2004): a) Layout of pipe and street system; b) Flow from the street system into a partly full pipe; c) Flow to the streets from a pipe system with insufficient capacity.

To develop inundation maps, Cook and Merwade (2009) used six DEMs in the 1D HEC-RAS model and 2D FESWMS model. The results reported that the inundation maps were overestimated when using HEC-RAS. This conclusion has been validated by similar studies that compared the ability of 1D and 2D HEC-RAS models to simulate a flood event (Ghimire et al., 2020; Tayefi et al., 2007). Although 1D model has obvious limitations, it plays a significant role in flood modeling, and recent studies have been conducted using 1D modeling (Abdessamed & Abderrazak, 2019; Hunter et al., 2007; Loi et al., 2019; Pappenberger et al., 2008; Pramanik et al., 2010). Based on the results obtained by coupling 1D hydraulic model HEC-RAS and hydrological model HEC-HMS, Abdessamed and Abderrazak (2019) provided suggestions on

the specific location of concrete walls to be used to prevent floods. Loi et al. (2019) integrated the HEC-RAS model with the SWAT model to link the rainfall-runoff process and river hydraulics for real-time flood forecasting in Vietnam. The result demonstrated that the predicted stream flow aligned well with the measured outflow. Pappenberger et al. (2008) carried out a sensitivity analysis of the 1D flood inundation model on River Alzatte by employing five sensitivity analysis methods; the results indicated that the model's parameters were prioritized differently in each method. Pramanik et al. (2010) investigated the viability of simulating riverine flood with free online DEM SRTM (Shuttle Radar Topographic Mission) in MIKE11; in this study, a similar stage-discharge relationship was obtained from DEM-extracted cross-sections and measured cross-sections. Hunter et al. (2007) discussed the feasibility of employing 'reduced complexity 1D models' to simulate floodplain inundation and reported that 1D modeling, as a simplified version of 2D and 3D modeling play a part in predicting flood inundation in real-world scenarios.

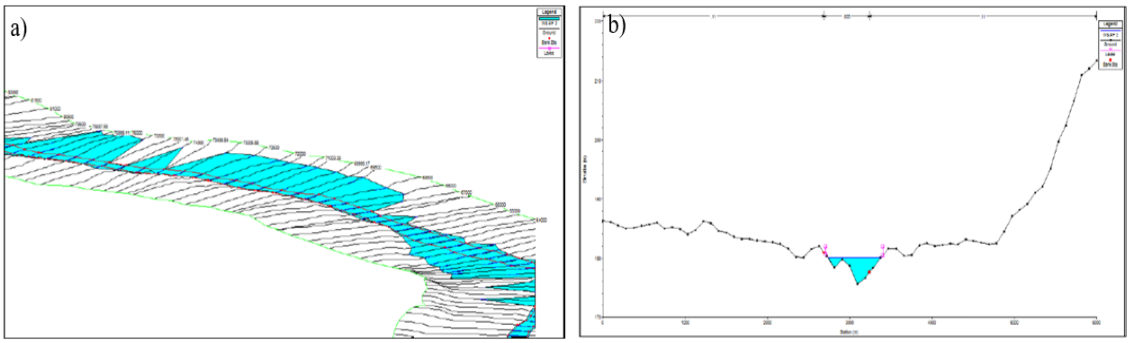

Figure 2. 4 Channeling flow simulated by HEC-RAS (Kheradmand et al., 2018): a) Cross sections of Niamey River in HEC-RAS; b) One cross-section along the Niamey river in HEC-RAS.

2.3.2.2 2D Hydrodynamic Model

2.3.2.2.1 Advantages of 2D Hydrodynamic Models

The core assumption of 1D model is that the flow moves in the longitudinal direction exclusively, so 1D models are best suited in pipe flow or in-channel flow modeling (Bates et al., 1992). However, when it comes to more complex conditions, multi-dimensional models are required to obtain more accurate simulation results. Compared with 1D models, 2D models provide more information on flow distribution, velocity distribution, and water depth distribution with less assumption and less modeling setup time, but the trade-off is that 2D models need more computation time (Bradbrook et al., 2004; Dimitriadis et al., 2016; Horritt & Bates, 2002; Seyoum et al., 2012).

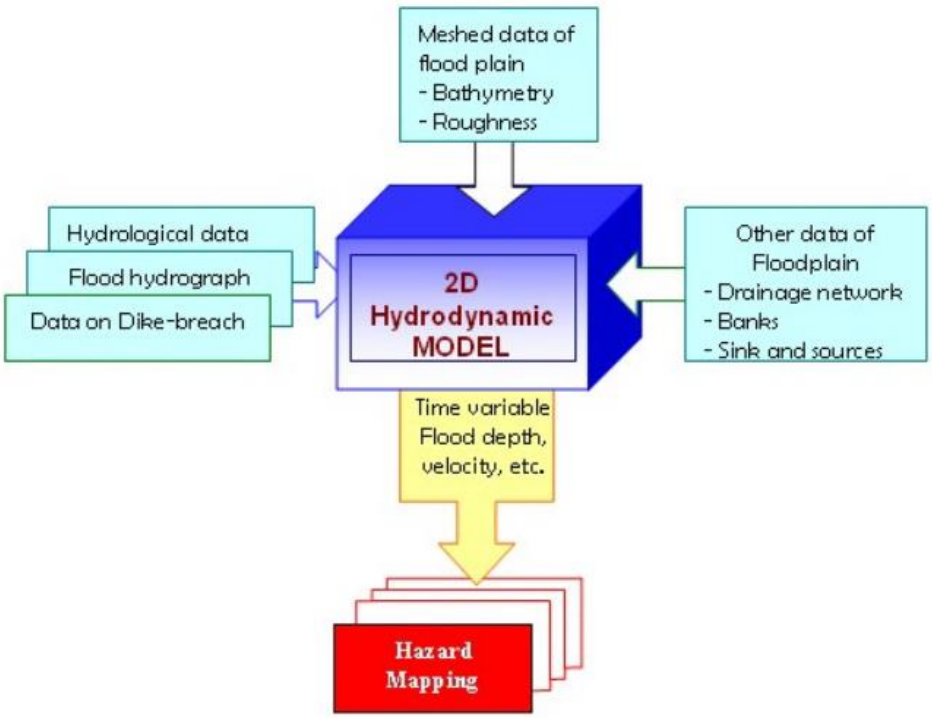

Figure 2. 5 Schematic of 2D models (Mens, 2008).

Similarly, although 3D models can also overcome the deficiencies of the 1D modeling, 3D models are computationally costly compared with 2D models. Besides, 3-D models require highly experienced users, and 3D models are designed to model complex conditions such as dam-break and embankment-failure flood situations where the vertical velocity of the flow is an essential feature (Stoesser et al., 2003; Wu et al., 2000). To conclude, 2D models are the most appropriate tools for modeling fluvial and pluvial flood phenomena, the two most common flood scenarios.

2.3.2.2.2 Application of 2D models

2D hydrodynamic modeling has received increased attention in recent decades. A variety of 2D modeling software has been applied to solve riverine and urban flood problems. Some of the prevailing packages are HEC-RAS 2D, LISFLOOD-FP, MIKE 21, TELEMAC-2D, etc., and research on using these packages to simulate floods has increased in literature. Shustikova et al. (2019) investigated the effects of different DEM resolutions on creating flood inundation maps through a case study in Italy. In their study, the initial DEM resolution was 1m and then averaged to 25m, 50m, and 100m. The result showed that while acceptable results could be obtained with 25m DEM resolution. Results obtained using 50m, and 100m DEM resolution were relatively ambiguous in large-scale modeling (Shustikova et al., 2019). Carr and Smith (2007) integrated MIKE 21, a 2D hydraulic model with a 1D sewer model, and used this combination to simulate urban flood environment; “secondary flow paths” and “cross-flows” become apparent compared with results from traditional 1D models (Carr & Smith, 2007). HEC-

RAS 2D and TELEMAC-2D were used to simulate a hypothetical dam-break flood event by Pilotti et al. (2020). The study reported a consistency between the numerical results and the results obtained from the laboratory-scaled modeling. The results further confirmed the performance of 2D numerical models in flood modeling. Teng et al. (2017) reviewed a variety of popular 2D hydrodynamic software, describing each software by the shallow water equation used, numerical methods, and discretization of time and space. TELEMAC-2D (Hervouet, 1999) solves full dynamic shallow water equations on unstructured mesh with finite element method (FEM) or finite volume method (FVM). On the other hand, LIS-FLOOD uses the finite differential method (FDM) to solve simplified shallow water equations in which the advection terms are not considered on a structured mesh. Some 2D hydraulic software solves either full shallow-water equations or simplified shallow water equations. For example, Costabile et al. (2020) compared the performance of 2D fully dynamic equations and 2D diffusion wave equations in modeling rainfall-related floods with HEC-RAS 2D model. The validation of the study concluded that the results obtained when using 2D fully dynamic equations, compared with 2D diffusion wave equations, align more closely with the measurements.

Table 2. 1 Some commonly used 2D software.

Model	Developer	Mesh/Grid	Status	Website
TELEMAC-2D	Électricité de France	Mesh	Open Source	https://www.telemac2d.org
LISFLOOD-FP	University of Bristol	Grid	Research	http://www.bristol.ac.uk/geography/research/hydrology/models/lisflood
MIKE-21	DHI	Grid	Commercial	https://www.mikepoweredbydhi.com/
HEC-RAS 2D	US Army Corps of Engineers	Grid	Free	http://www.hec.usace.army.mil/software/hec-ras

2D TUFLOW	BMT WBM	Flexible	Commercial	https://www.tuflow.com/
XP2D	XP Solutions	Grid	Commercial	http://lagasys.com/watermngmt/xp2D.html
SOBEK 2DFLOW	DELTARES	Grid	Commercial	https://www.deltares.nl/en/software/module/sobek-2dflow-overland-flow/

2.3.2.2.3. Comparison between 1D and 2D Models

As an increasing number of open-source 2D models became available for simulating shallow water flow, scholars have conducted numerous studies that compare the latest 2D models with long-standing 1D models for the optimal model in different situations. Vojinovic and Tutulic (2009) analyzed the differences between using 1D and 1D-2D coupled models in assessing urban flood damage in a case study in St Maarten, NA. The results showed that while the 1D model can be sufficient for predicting the flow along channels, the 1D model cannot map flows into 2D dimensions because the 1D model does not treat terrain as a continuous surface (Vojinovic & Tutulic, 2009). Bohorquez and Darby (2008) reconstructed glacial outburst flooding with 1D and 2D shallow water techniques and found the 2D model gave more reliable results compared with the 1D model even in complex terrains. Tayefi et al. (2007) used three methods (cross-sections, storage cells, and explicit 2D representation) to describe floodplains in a riverine flood event in the UK; among the three methods, the 2D representation was found the best in terms of accuracy and sensitivity to floodplain friction. Costabile et al. (2015) employed high-resolution air-borne Lidar data to obtain an improved description of the topography and examined to what degree the gaps between 1D and 2D models can be reduced. The experiment showed that the predicted inundation areas were comparable when using high-resolution DEM in 1D or 2D models;

however, obvious differences exist in the maximum velocity and water depth. In conclusion, evidence has shown that the inherent limitation of 1D modeling is a major factor that hinders hazard assessment, and 2D modeling is a more sophisticated method that can replace 1D models in simulating various flood phenomena.

Table 2. 2 Comparison between 1D and 2D models.

Features	1D Hydraulic Model	2D Hydraulic Model
Governing Equations	1D Shallow water equations	2D Shallow water equations
Velocity	Uniform velocity perpendicular to cross-sections	Depth-averaged velocity with different directions
Spatial Discretization	Cross sections	Mesh/grid/hybrid
Application	Pipe flow, in-channel flow	Overland flow
Setup Time	Long	Short
Computation Time	Short	Long
Accuracy	Depends on section numbers	Depends on mesh resolution
Turbulence	Not available	Available
Complex River Structures	Suitable	Not Suitable
Urban Flood Plain	Not suitable	Suitable
Source of Instability	Cross section's spacing	Sensitivity of full momentum equations

2.3.2.2.4 Improvements and Challenges of 2D Models

Over the decades, modifications have been made to improve 2D models. For example, Bates et al. (2010) developed a 2D model that decoupled flows in X and Y directions to reduce computational cost. Soares-Frazão et al. (2008) modified the source terms of shallow water

equations to calculate head losses. Tsakiris and Bellos (2014) developed an in-house model with the McCormack numerical scheme to capture shocks in flow propagation in complex terrain. Wetting and Drying (WD) algorithms are crucial for modeling inundation accurately. Nowadays, estimating wetting and drying still presents a challenge for modelers because the numerical model determines the WD algorithm, and hence it is difficult to generalize the algorithm (Medeiros & Hagen, 2013).

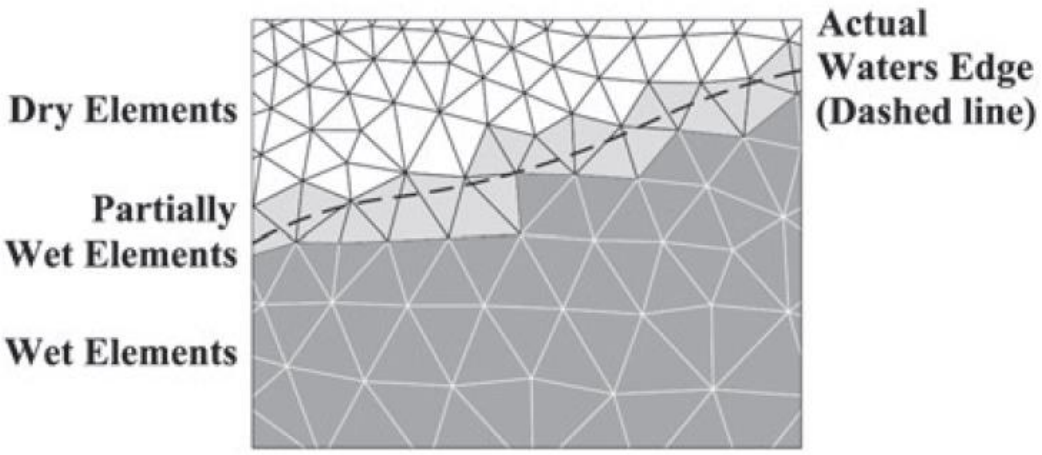

Figure 2. 6 Unstructured triangular mesh illustrating wetting front in reality and as seen by a numerical model (Medeiros & Hagen, 2013).

Mesh generation is considered another critical factor in numerical modeling because mesh type and mesh size are essential for modeling accuracy and running time (Kim et al., 2014). Recently, modelers have attempted to incorporate flexible meshes for finer resolution and less computation cost (Castro Gama et al., 2013; Hoch et al., 2018). Three methods for reducing computation time have been proposed in recent years. First, computation time can be reduced significantly by enhanced graphical processing units (Castro et al., 2011; Lacasta et al., 2015; Neal et al., 2010; Sanders et al., 2010), especially for large-domain simulation (Kalyanapu et al., 2011).

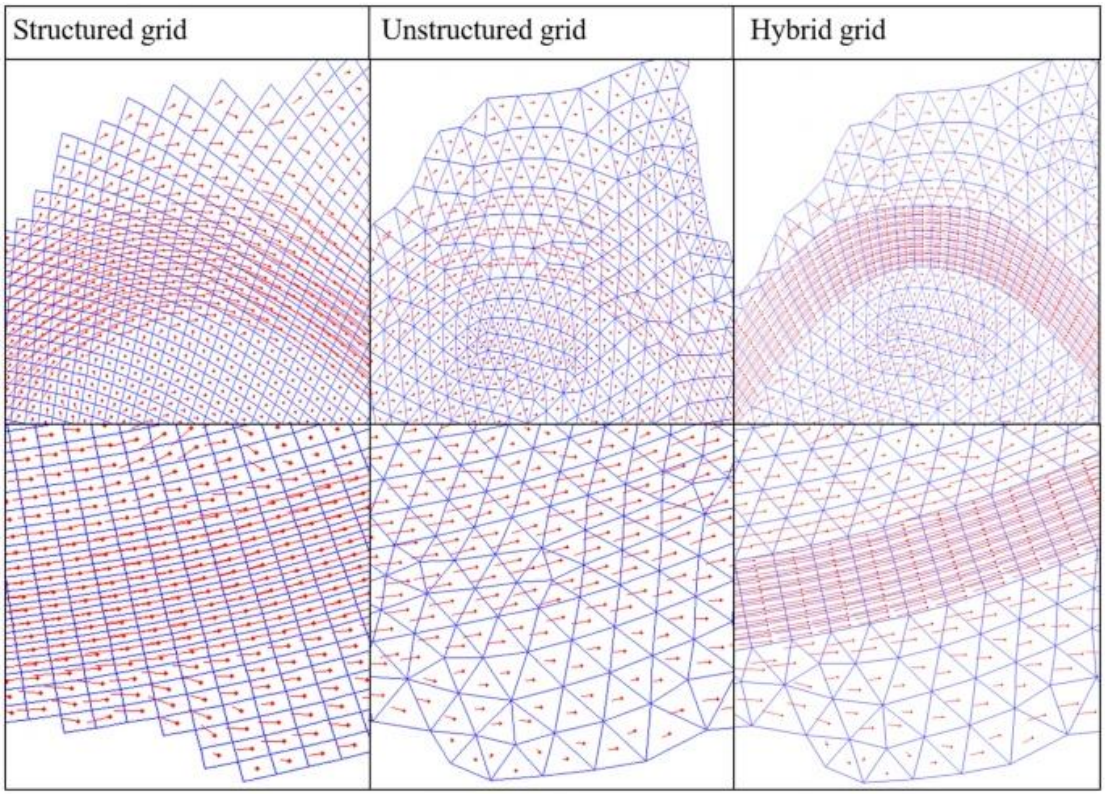

Figure 2. 7 Illustration of structured, unstructured, and hybrid grids (Bomers et al., 2019).

Second, explicit numerical schemes make parallelization of codes easier (Pau & Sanders, 2006; Yu, 2010). Third, simplified 2D models that use Cellular Automate (CA) approach have merged (Dottori et al., 2013; Ghimire et al., 2013). Although full 2D models are required for detailed risk management, these simplified approaches can provide acceptable results with faster computation, and therefore prove useful for flood modeling in various scenarios.

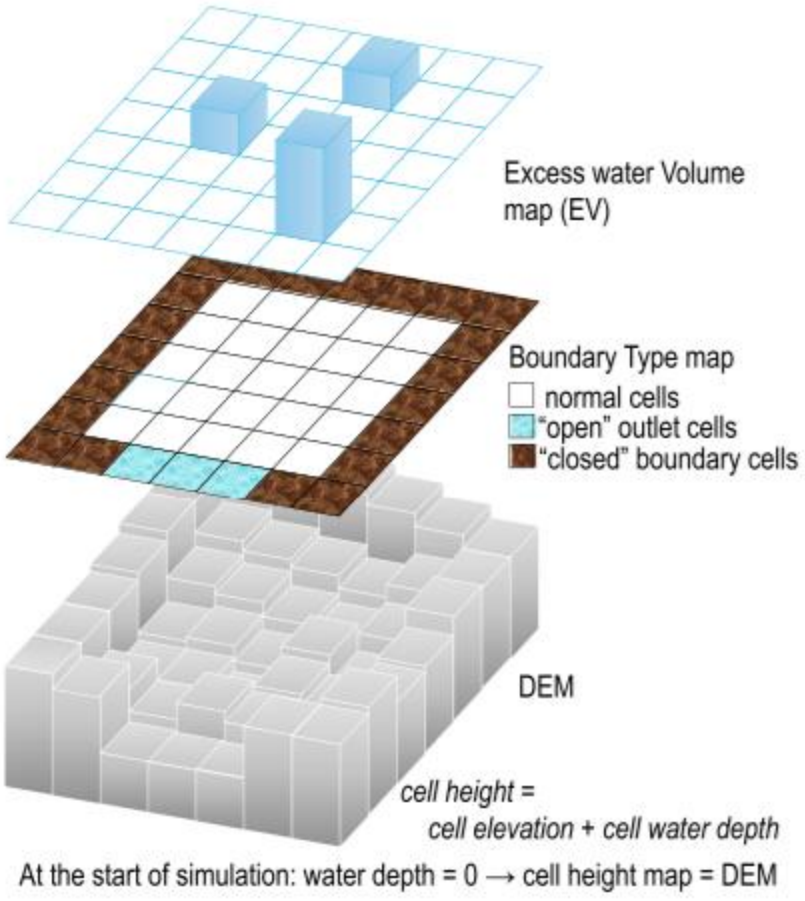

Figure 2. 8 Schematic of cellular approach algorithm (Jamali et al., 2019).

2.4 Pluvial Floods Modeling

2.4.1 Mechanisms of Pluvial Flood

By far, the most extensively studied flood type is fluvial flooding that occurs when the stream rises above the channel (Rosenzweig et al., 2021). Many studies have been conducted on fluvial flood modeling using both 1D and 2D modeling techniques. However, despite being a natural disaster that poses a significant threat to life and property in urban areas, the pluvial flood has not been well studied (Gaitan et al., 2016). Pluvial flooding occurs when rainfall-runoff cannot be discharged by drainage systems in time, thus staying on ground surfaces (Houston et al., 2011).

As the driving factor and mechanisms of pluvial floods are different from those of fluvial floods (Sörensen & Mobini, 2017), they need to be explicitly addressed through appropriate modeling techniques. In urban areas, drainage systems can be generally categorized in two components: major and minor systems (Zhu et al., 2018). Pluvial flooding occurs when the amount of rainfall-runoff exceeds the capacity of the minor system. Compared with rural areas, urban structures such as roads, buildings, and drainage systems have nonnegligible impacts on flood patterns. Therefore, thorough preparation is required in the setting up for pluvial modeling.

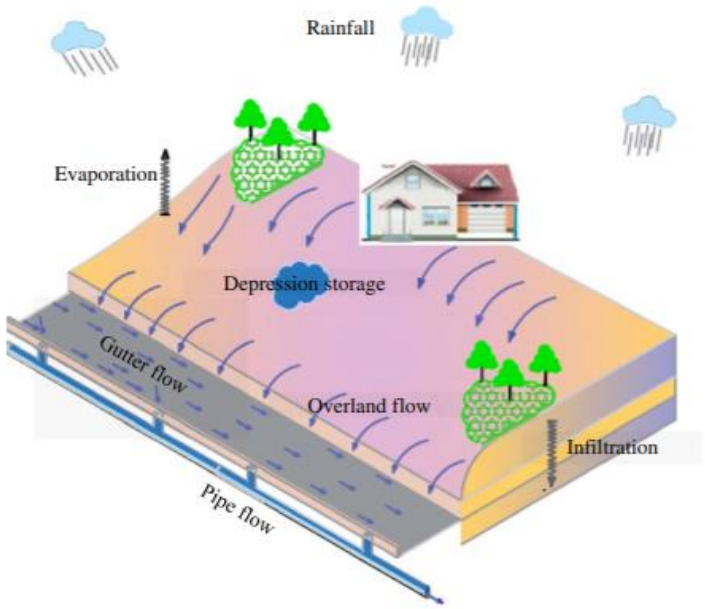

Figure 2. 9 Schematic of rainfall-runoff process in urban areas (Bulti & Abebe, 2020).

2.4.2 Numerical Models of Pluvial Floods

Traditionally, conceptual models for pluvial modeling consider the following components: rational formula, time of concentration, and linear urban catchment (Maksimović et al., 2009). To better understand the flow dynamics in urban areas, numerical modeling has arisen in this regard. Djordjević et al. (1991) proposed a concept of a "dual-drainage" model to simulate the

minor and the major drainage system behaviors simultaneously. At the early stage of their study, the surface flow was approximated as a water column overtopping the manhole (Maksimović et al., 2009). In 2004, Mark et al. (2004) developed a 1D/1D dual-drainage system consisting of a 1D sewer network model and a 1D surface flow routing model. The authors found that the system's limitation is that the 1D surface model was only efficient for simulating water remaining within the street profile; consequently, the authors suggested that the 2D model should represent surface flow and provide a more detailed representation of surface flows.

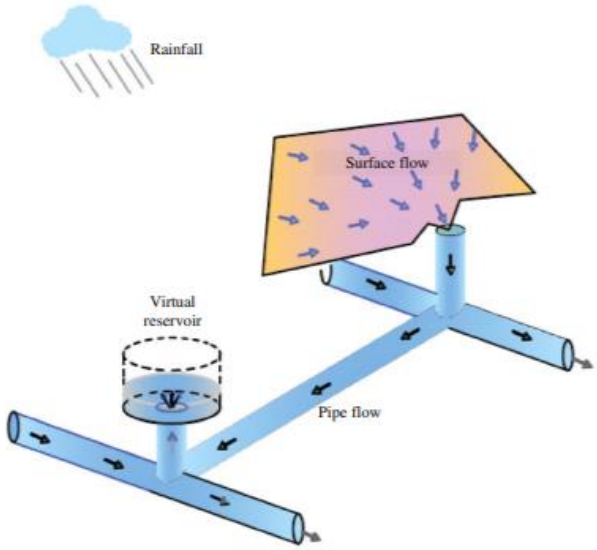

Figure 2. 10 Illustration of 1D-1D coupled model (Bulti & Abebe, 2020).

Carr and Smith (2007) enhanced the model in Mark's study (Mark et al., 2004) by developing a 1D-2D approach that integrates sewer with 2D surface flow models. The integrated model allowed the surface flow to take preferential paths in urban catchments. The 1D-2D coupled model has received attention from many researchers and has become one of the principal ways to research urban floods (Chen et al., 2005; Chen et al., 2007; Löwe et al., 2017; Pina et al., 2016).

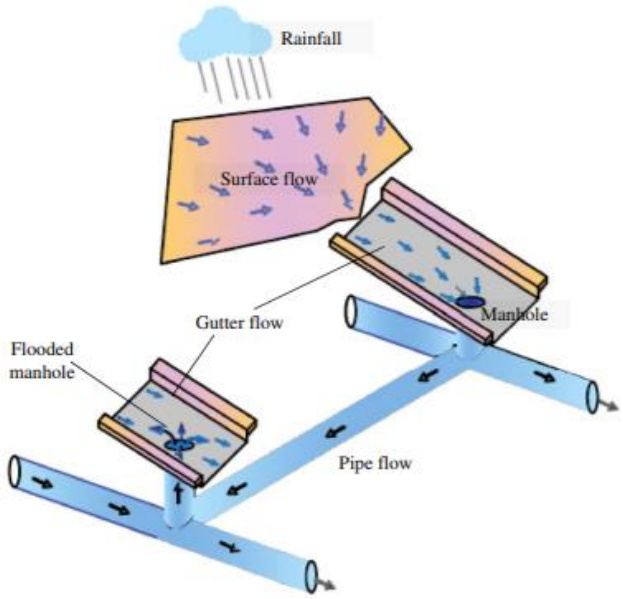

Figure 2. 11 Illustration of 1D-2D coupled model (Bulti & Abebe, 2020).

2.4.3 2D Surface Flow Model in Pluvial Flood Modeling

Given that 1D-2D integration requires consideration of several factors, including the study area, data availability, model parameterization, and budget (Maksimović et al., 2009), 2D surface flow models are extensively used for urban flood modeling (Yu & Lane, 2006). van Dijk et al. (2014) investigated 1D-2D and 2D modeling techniques in an extreme rainfall event. The primary conclusion of this research is that 2D surface models can serve as an efficient alternative for the 1D-2D coupled model in flat and hilly areas where the minor drainage system has less impact on the identification of flood-prone areas. Hofmann and Schüttrumpf (2020) integrated a 2D model with risk-based solutions to forecast pluvial floods in real-time, which is an innovative way of using hydrodynamic models in flood forecasting. Ghimire et al. (2013) used the CA approach, a 2D model with reduced computation time, to simulate the spatio-temporal evolution of pluvial

flooding in the UK. The result was consistent with the result from the hydraulic fracturing model.

Meanwhile, 2D surface modeling and experimental modeling have been used to examine the effects of urban structures on the flow movement during an urban flood. Testa et al. (2007) placed concrete blocks in an instrumented physical model to simulate floods in a simple urban district; the results suggested the physical model measurements can be used to validate numerical models. Dottori and Todini (2013) evaluated the performance of a simplified 2D diffusive model to model urban inundation by comparing the simulated water level with the measured water level from an urban district physical model. The 2D diffusive model captured the main flow processes; however, some local flows were poorly simulated. Kadir et al. (2019) applied an experimental physical model to calibrate the numerical simulation of an urban flood inundation modeled by HEC-RAS 2D. During his research, changes in geometry were found the cause that led to the turbulence phenomenon (Kadir et al., 2019). In 2D surface flow modeling, an approach to simplify drainage systems assumes that the amount of water drained away equals the drainage capacity (Yin et al., 2016; Yu & Coulthard, 2015). Other ways to simplify drainage systems include increasing net rainfall amount (Bruwier et al., 2020) and excluding the impacts of the drainage system where it is poorly engineered or maintained (Huang et al., 2017). Although the drainage system is simplified in 2D surface models, the accuracy and reliability of the result are not compromised. Hence, 2D surface modeling can be widely used in areas when drainage systems are insufficient.

2.5 Rainfall-runoff Modeling

Rainfall-runoff is a major process in the hydrological cycle that connects precipitation and surface water. Runoff occurs when excessive precipitation cannot infiltrate into the soil and flows on the ground (Sitterson et al., 2018). Rainfall-runoff modeling offers detailed information on hydrological phenomena in flood simulation (Sitterson et al., 2018; Vaze et al., 2011; Xu & Small, 2002). Rainfall-runoff models can be grouped into empirical, conceptual, and physically-based models based on the algorithm and the structure. Empirical models are commonly used worldwide due to their simplicity, stability, and predictability (Vaze et al., 2011).

2.5.1 The SCS Curve Number Method in Rainfall-runoff Modeling

One well-known empirical model for calculating runoff from rainfall is SCS Curve Number Method. The main assumption of the SCS Curve Number method is that the ratio of actual runoff to potential runoff equals the ratio of actual retention to potential retention (Beven, 2011). CN relates to soil type, land use, and antecedent moisture condition. SCS Curve Number Method is applicable for runoff under varying land uses and soil types with a few parameters required in the model setup. Therefore, the advantage of the SCS Curve Number Method has been documented in various studies. In their research, Merz and Blöschl (2009) and Bennett et al. (2018) suggested that rainfall intensity and rainfall patterns can impact flood magnitude, but AMC can also have a strong influence on flood volume. Four soil moisture indicators, including TDR (Time Domain Reflectometry) measurements, modeled soil moisture, antecedent precipitation, and baseflow, were compared by Tramblay et al. (2010) to reduce the uncertainties related to AMC. The result suggested that measured soil moisture was most helpful for setting the initial conditions for a simplified event-based rainfall-runoff model in a small basin (Tramblay et al., 2010). Tramblay et al. (2011) investigated the impact of lumped and distributed rainfall input on rainfall-runoff

modeling and found distributed rainfall input was more efficient. King et al. (1999) and Jeong et al. (2010) concluded that one disadvantage of using the SCS Curve Number Method was that rainfall-runoff was calculated simply based on the total rainfall volume while the rainfall intensity and duration were disregarded, which may lead to inaccurate results. Rozalis et al. (2010) employed the SCS Curve Number model with a flow routing model to simulate excess rainfall, and the authors pointed out two weak points of the SCS Curve Number method were that the drying process is not represented in the model and the sensitivity of the model depended on sole CN parameter. To date, The CN method has been modified and incorporated in much hydrological software, such as HEC-HMS, EPIC, and SWAT, to calculate rainfall-runoff (Grimaldi et al., 2013).

2.5.2 Modeling Rainfall-runoff by SWAT Hydrological Model

SWAT (Soil and Water Assessment Tool) was first designed and developed by Jeff Arnold in 1990 for the Agricultural Research Service (Ghaffari et al., 2010). In previous studies, SWAT has been demonstrated as a successful semi-distributed hydrological model to simulate runoff (Easton et al., 2010; Lin et al., 2015; Rostamian et al., 2008). As a physical hydrological model, SWAT provides detailed information on the hydrologic cycle of the watershed. In 1994, multiple Hydrologic Response Units were incorporated in the SWAT model, which allows subbasins to be split up into different HRUs with unique land use, soil, and management strategy, and subsequently, the accuracy of SWAT model is significantly increased. As a physical model, SWAT yields more accurate output than conceptual models as SWAT uses input data that directly represents the conditions in the real world (Arnold et al., 2012), including DEM, weather, land use, soil, etc.

SWAT partitions the catchment into sub-areas which are further divided into hydraulic response units by overlaying soil map, land use map, and digital elevation, and the application of which has been demonstrated in numerous studies (Bingner, 1996; Deng et al., 2015; Dessu & Melesse, 2012; Fereidoon et al., 2019; Ndomba et al., 2008; Vu et al., 2012; Zakizadeh et al., 2020). Dessu and Melesse (2012) evaluated the applicability of the SWAT model for long-term rainfall-runoff simulation in the Mara River Basin. The results demonstrated the potential of SWAT to simulate the runoff process. Similarly, Fereidoon et al. (2019) tested SWAT in simulating runoff with estimated rainfall data based on soil moisture measurements; each runoff reproduced by SWAT at six gauges had good agreement with the measured runoff. Ndomba et al. (2008) and Vu et al. (2012) confirmed the significance of SWAT to generate reliable simulation results in data-scarce areas. Zakizadeh et al. (2020) used SWAT and ANN (Artificial Neural Network) models to simulate rainfall-runoff in an urban watershed. Though both models gave good runoff simulating results, SWAT was found more appropriate in situations with no gauge station in the upper watershed. Zhang et al. (2019) obtained an effective simulation of daily runoff in China with SWAT model. Numerous studies have proved that SWAT is a practical hydrological model for simulation runoff during a flood event. As mass and momentum conservations are not considered in most hydrological rainfall-runoff models, these models are not applicable for the prediction of flood inundation.

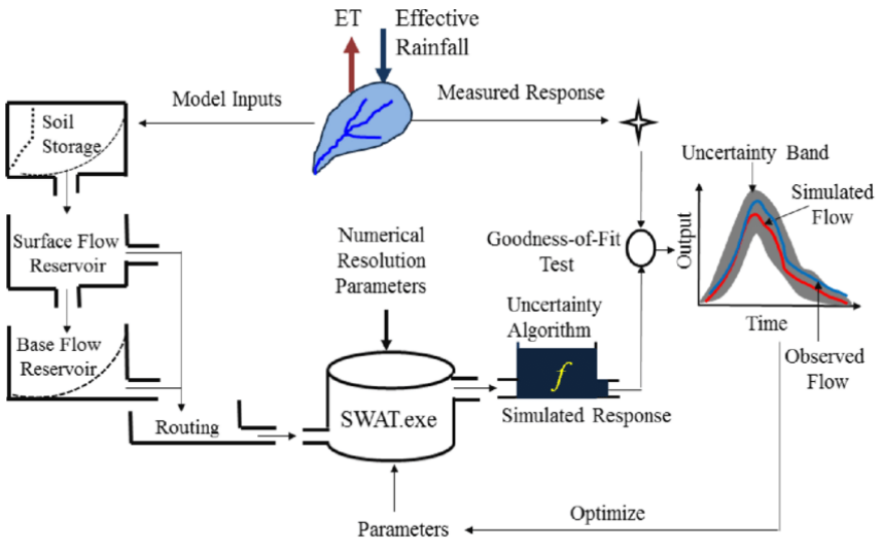

Figure 2. 12 The rainfall-runoff process of SWAT hydrological model (Samadi et al., 2017).

2.6 Integration of Hydrological Process in Hydrodynamic Models

Recently, 2D models combined with rainfall-runoff models have been investigated as a new technique that interlinks hydrological process and inundation to simulate urban pluvial flood, and the benefits of which were confirmed by researchers (Caviedes-Voullième et al., 2020; Ming et al., 2020; Sayama et al., 2012). In addition, the infiltration process, which was previously studied in isolation, is now considered in hydrodynamic models to simulate urban flood events due to the advancement in computational technology (Yu & Coulthard, 2015).

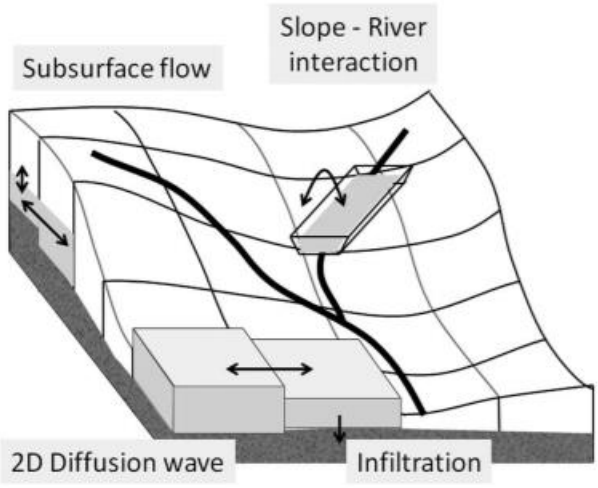

Figure 2. 13 Schematic of modeling rainfall-runoff process by 2D models (Choo et al., 2020).

2.6.1 An Emerging Hydro-inundation Model: TELEMAC-2D

The infiltration module opens new possibilities to enhance the suitability of hydrodynamic models for urban flood applications. TELEMAC-2D is emerging as a solid hydraulic software that incorporates the SCS Curve Number runoff module and provides the possibility to model the infiltration process during a rainfall event dynamically. In TELEMAC-2D, spatially varying CN values are defined at each computational node and used to calculate infiltration locally (Ligier, 2016).

2.6.2 Applications of TELEMAC-2D in Fluvial Flood Modeling

At present, studies on TELEMAC-2D primarily focus on riverine flood simulation. For instance, the study by Bates, Bates et al. (1992) was the first to employ TELEMAC-2D in a riverine flood simulation in the UK. The study highlighted the potential of 2D FEM schemes in flood

modeling, especially for simulating flood inundation extent. Vu et al. (2015) applied TELEMAC-2D in a flood inundation modeling of the Mekong River in Cambodia and validated the result with MODIS satellite images. Although the simulated inundation extent is consistent with the satellite images during the flood peak, the inundation extent was not accurately predicted during pre and post-periods. In addition, activating parallelization was reported to reduce computation time significantly; more specifically, the time was 60% down when four processors were utilized (Vu et al., 2015). Haque et al. (2020) employed TELEMAC-2D to dynamically investigate the relationship between water levels and inundation extents in the Niger delta. Di Baldassarre et al. (2010) examined the advantages and disadvantages of deterministic and probabilistic approaches in inundation mapping. In their study, a fully 2D finite element model TELEMAC-2D and simple raster-based inundation model LIS-FLOOD were applied to mimic the 1-in-100 flood event in 2006 in the UK; While TELEMAC-2D was found to be less sensitive than LIS-FLOOD, TELEMAC-2D employed only one "best-fit" model which may lead to inaccurate simulation results while LIS-FLOOD uses multiple behavioral models which can improve the accuracy of the simulation (Di Baldassarre et al., 2010).

2.6.3 Applications of TELEMAC-2D in Pluvial Flood Modeling

The application of TELEMAC-2D in urban flooding scenarios has emerged as a new research area. Li et al. (2019) used building-hole, building-block, and building resistance methods to examine the effects of two types of buildings arrangement modes on urban simulation and compared the numerical results with laboratory results. The numerical results followed the laboratory results, proving that TELEMAC-2D was applicable to simulate urban flood events (Li et al., 2019). In addition, Manning's coefficient was regarded as a significant factor that controls water flows through the urban district. According to the study, unit-width water discharge and water depth

were only sensitive to Manning's coefficient when the Manning's coefficient was less than $10^{4}m^{-1/3}$ s. This conclusion could provide modelers guidance for model setup (Li et al., 2019). Ma et al. (2015) employed TELEMAC-2D and FULLSWOF-2D to study the effects of meshing strategies and numerical schemes on 2D models. While TELEMAC-2D uses the finite element method and FULLSWOF-2D uses the finite volume method, similar results were obtained from both models. Regarding the description of building shapes and flow paths, Ma et al., (2015) reported that non-structural meshing outperformed grid meshing. Liu et al. (2019) tested how an urban area responded to a pluvial flood scenario in 12 design storm rainfall events with different magnitudes. Liu et al. (2019) is one of the first studies to employ the infiltration module of TELEMAC-2D in an urban flood scenario. The results showed that rainfall intensity, compared with rainfall amount and duration, was the main factor influencing inundation extent (Liu et al., 2019). Zhu et al. (2018) integrated TELEMAC-2D, a drainage model SWMM, and an agent-based model to simulate traffic congestion situations under different magnitude storms in Lishui city in China. In their study, the impacts of rainfall with 10-year return periods and 20-year periods were insignificant. In contrast, the rainfall with 50-year return periods had a strong effect on traffic congestion, and the conclusion aligned with the study by the 2019 study of Liu et al. (Zhu et al., 2018). Abily et al. (2013) examined the strengths and weaknesses of the high-resolution Digital Surface Model (DSM) in runoff hazard assessments. The researchers pointed out that using 2D models to simulate runoff should receive thorough consideration in future studies (Abily et al., 2013). To conclude, while TELEMAC-2D has various strengths in riverine floods, the capacity of which in pluvial modeling needs further investigation along with the latest rainfall-runoff module.

2.7 Conclusions

In recent years, pluvial floods have become one of the most devastating natural disasters under the influence of climate change and urbanization globally (Doocy et al., 2013; Jha et al., 2012). the most used approaches to reduce the impacts of pluvial floods on human life and property are flood monitoring, flood forecasting, and flood modeling.

For over half a century, flood modeling has played a significant role in flood hazard mapping. However, compared with traditional statistical models, modern hydrodynamic models allow researchers to obtain more detailed information such as water depth, water velocity, distribution of flows, etc. This chapter reviews the fundamental theories, applications, advantages, and disadvantages of 1D and 2D models. While numerous studies have been conducted on fluvial floods, there is a lack of research on pluvial floods (Gaitan et al., 2016). This literature review focused on developing pluvial flood modeling and the feasibility of using 2D surface models to simulate rainfall-related flood routines in urban settings.

Previously, research on pluvial flooding either neglected the hydrological processes, which are key in urban flood modeling, or studied hydrological and hydraulic processes in isolation (Yu & Coulthard, 2015). The results would inevitably become misleading due to their inaccuracy. In pluvial flood modeling, the state-of-the-art consists of using hydro-inundation models in urban applications to interlink hydrological and hydraulic processes synchronically. TELEMAC-2D has emerged as a hydro-inundation model that incorporates rainfall-runoff infiltration routines. This added value of the new feature enables TELAMC-2D to calculate spatially distributed runoff with SCS Curve Number Method.

Chapter 3 Study area and Methodology

3.1 Study Area

Niamey is the capital of Niger, the economic and cultural center of the country. The city has experienced a massive enlargement between 1979 and 2014 and now covers an area of around 250 km^2. Niamey River divides the city into two parts. Most urban areas are concentrated on the east of the riverbank, while rural areas are on the west. A chain of fluviatile marshy islands suits in the middle of the river channel. The climate is hot semi-arid, with an expected rainfall of around 500 to 700 mm per year on average during the rainy season from June to September. Despite the heavy rainfall during summer, the dry season with almost no rainfall lasts from October to next May, accounting for the lack of well-designed and maintained drainage systems.

The city is subjected to severe flood inundation, suffering from significant life and property losses. The flood inundation hazard now has been an all-too-common phenomenon in this area. In 2012, more than 7.7 million people in Niger delta were affected by the floods. Specifically, 363 deaths were reported, and almost 600,000 houses were destroyed (Tiepolo and Braccio 2018). Due to climate change, Pluvial flood has become a new pattern affecting thousands people and properties (Massazza, Bacci et al. 2021). Besides, the frequency and intensity of precipitation in Niamey continue to increase, posing flood-related threats with increasing severity (Douglas et al., 2008). A 448.82 km^2 watershed of the Niger River basin, covering most of Niamey city is selected as the study area to simulate a two-month rainfall-runoff infiltration process during pluvial flooding period in 2012.

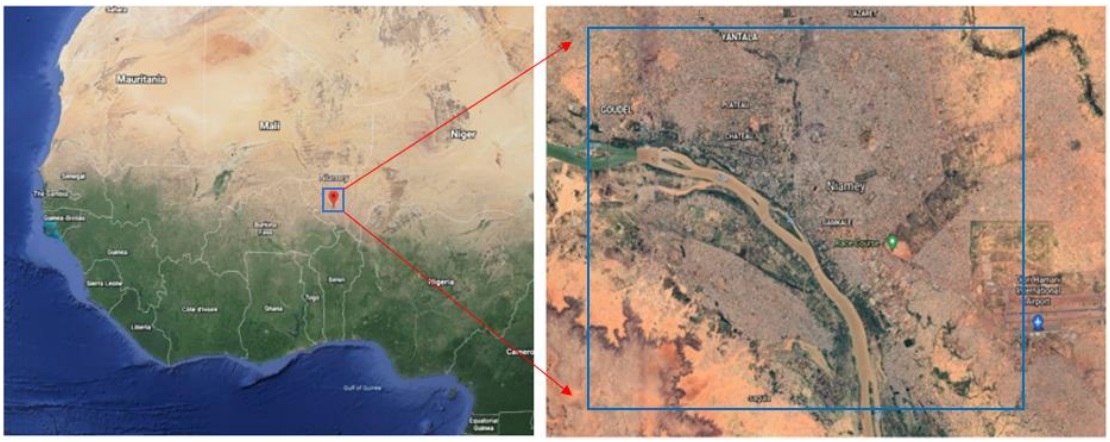

Figure 3. 1 Location of the study area.

3.2 Research Methodology

The thesis aims to check the applicability of the TELEMAC model to simulate pluvial flooding in a semi-arid area. Based on the SCS CN method, the new infiltration module is of particular importance for the exercise implemented in TELEMAC. The following steps were used to answer the research question:

1. A SWAT model of the study area was developed
2. The SWAT model was calibrated using available streamflow observations. These observations are very scarce (two rainfall events), so a validation exercise could not be conducted.
3. A TELEMAC model of the study area was developed
4. The calibrated CN values from the SWAT models were used in the TELEMAC model, and the same events were simulated using SWAT and TELAMAC
5. The runoff generated by the two models are compared.

6. The TELEMAC rainfall-runoff subroutine is examined to analyze the difference in the runoff from the TELEMAC 2D and SWAT.
7. The flow chart of the methodology is shown in Figure 3. 2.

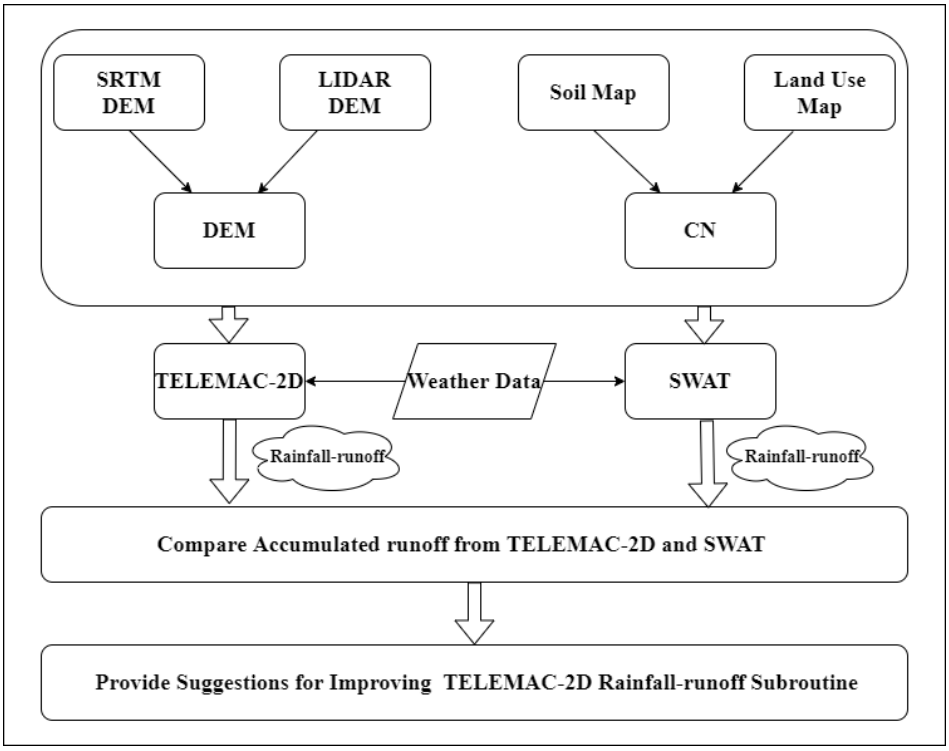

Figure 3. 2 Flow chart of the research methodology.

3.3 Modeling tools

As explained in the previous section, two models of the study area will be used:

1. The TELAMC 2D model, which calculates net rainfall using the SCS CN method, then solves Shallow Water Equations (SWEs) for simulating flow path
2. The SWAT model, which is a conceptual rainfall-runoff model

This section briefly introduces the main processes used in the two models.

3.3.1 Shallow-Water Equations (TELEMAC 2D)

The SWEs, also known as Saint-Venant equations, are hyperbolic or parabolic partial differential equations (PDEs) widely used to simulate fluid motion in rivers and channels in 2D hydrodynamic models (Bates et al., 2010; García-Navarro et al., 2019). The equations are derived from depth-integrating Navier-Stokes equations, and the typical feature of SWEs is that vertical depth scale is much less than horizontal length scale. Therefore, the vertical dimension is usually removed. Because Navier-Stokes equations are themselves derived from the equations of conservation of mass and conservation of momentum, the conservative form of 2D SWEs can be written as the following:

$$\frac{\partial(\rho\eta)}{\partial t}+\frac{\partial(\rho\eta u)}{\partial x}+\frac{\partial(\rho\eta v)}{\partial y}=0 \tag{2.1}$$

$$\frac{\partial(\rho\eta u)}{\partial t}+\frac{\partial}{\partial x}\left(\rho\eta u^2+\frac{1}{2}\rho g\eta^2\right)+\frac{\partial(\rho\eta uv)}{\partial y}=0 \tag{2.2}$$

$$\frac{\partial(\rho\eta v)}{\partial t}+\frac{\partial(\rho\eta uv)}{\partial x}+\frac{\partial}{\partial y}\left(\rho\eta v^2+\frac{1}{2}\rho g\eta^2\right)=0 \tag{2.3}$$

The non-conservative form can be written as:

$$\frac{\partial h}{\partial t}+\frac{\partial}{\partial x}\big((H+h)u\big)+\frac{\partial}{\partial y}\big((H+h)v\big)=0 \tag{2.4}$$

$$\frac{\partial u}{\partial t}+u\frac{\partial u}{\partial x}+v\frac{\partial u}{\partial y}-fv=-g\frac{\partial h}{\partial x}-bu+\nu\left(\frac{\partial^2 u}{\partial x^2}+\frac{\partial^2 u}{\partial y^2}\right) \tag{2.5}$$

$$\frac{\partial v}{\partial t}+u\frac{\partial v}{\partial x}+v\frac{\partial v}{\partial y}+fu=-g\frac{\partial h}{\partial y}-bv+\nu\left(\frac{\partial^2 v}{\partial x^2}+\frac{\partial^2 v}{\partial y^2}\right) \tag{2.6}$$

Where:

u (m/s) is velocity in the x-direction

v (m/s) is velocity in the y-direction

h (m) is height deviation of the horizontal pressure surface from its mean height H

H (m) is mean height of the horizontal pressure surface

η (m) is total fluid column height

g (m/s^2) is acceleration due to gravity

f is Coriolis coefficient associated with the Coriolis force

b is viscous drag coefficient

ν is kinematic viscosity (m2/s).

3.3.2 The SCS Curve Number Method (TELEMAC 2D and SWAT)

In the process of rain falls, part of the rainfall is intercepted by vegetation canopy, and the other part is held on the soil surface. A larger portion of the water on the soil surface will infiltrate the soil for plant uptake, ground water recharge, and soil moisture redistribution. In contrast, the water that can not infiltrate the soil will stay on the surface, flowing as runoff. On dry soil surface, infiltration equals precipitation. However, the rate of infiltration gradually decreases when the soil gets moisturized. In such a case, precipitation can not be fully absorbed by the soil, and hence runoff occurs.

The SCS Curve Number Method is an empirical model developed by the United States Department of Agriculture (USDA) Natural Resource Conservation Service in 1954 to estimate the rainfall-runoff amount under various land use and soil classes (Rallison & Miller, 1982). The main assumption of the SCS Curve Number Method is that the ratio of actual runoff to potential runoff equals the ratio of actual retention to potential retention (Beven, 2011).

$$\frac{F}{S} = \frac{Q}{P} \qquad (2.7)$$

where:

F (mm) is actual retention

S (mm) is potential retention

Q (mm) is accumulated runoff

P (mm) is rainfall depth for the day.

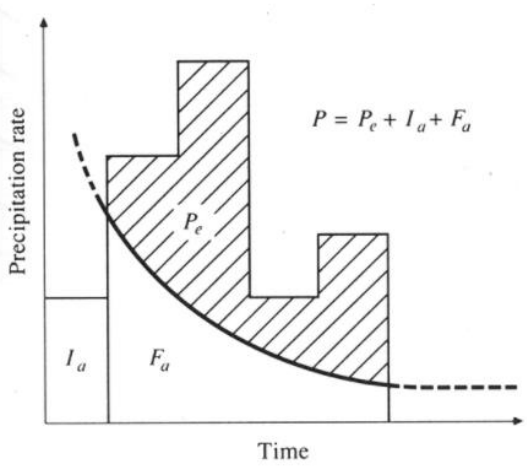

Figure 3. 3 Variables in the Curve Number model (Ligier, 2016).

In the SCS Curve Number Method, the surface storage, plant interception, and infiltration before runoff are defined as an initial abstraction. When rainfall exceeds initial abstraction, the surface begins to produce runoff, and excess rainfall starts to be stored in the maximum potential retention. Runoff commences when precipitation is greater than the initial abstraction of the day. The equation to calculate runoff is shown in equation (2.8):

$$Q = \frac{(P - I_a)^2}{(P - I_a + S)} \tag{2.8}$$

Where:

I_a (mm) is initial abstraction

S (mm) is maximum potential retention.

The maximum potential retention changes with the curve number (CN) calculated based on soil permeability, land use, and antecedent soil water condition, as shown in the equation below. Figure 3.3 demonstrate runoff calculated with different CN values or rainfalls,

$$S = 25.4\left(\frac{1000}{CN} - 10\right) \quad (2.9)$$

Where:

CN is the curve number ranging from 30 to 100.

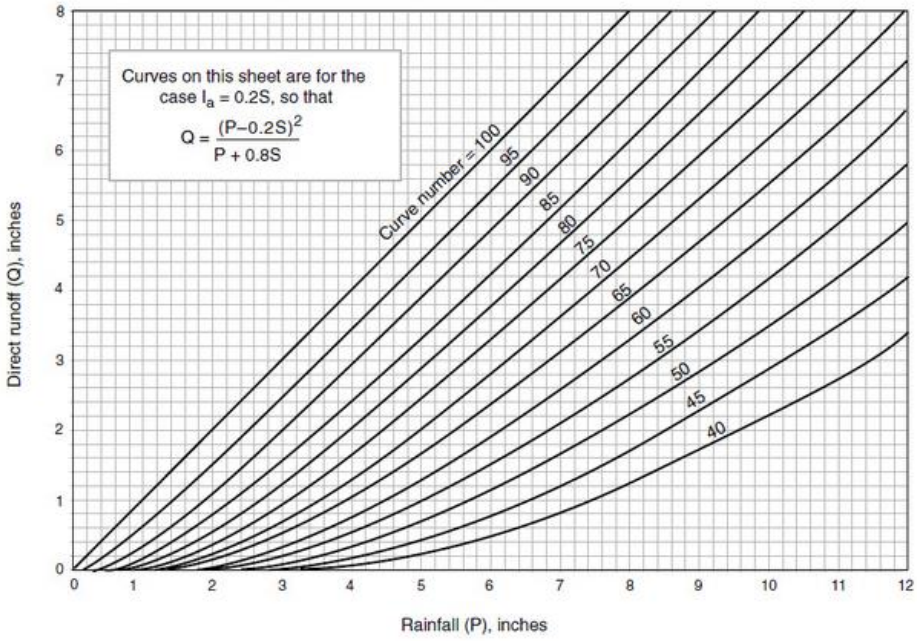

Figure 3. 4 Runoff under different CN values and rainfall amount (Ligier, 2016).

Four hydrologic soil groups (A, B, C, and D) were defined by The U.S Natural Resource Conservation Service (NRCS) according to their infiltration characteristics. Group A soil has a high infiltration rate and low runoff potential; group B has a moderate infiltration rate; group C

has a slow infiltration rate, and group D has an extremely low infiltration rate. Reference for soil group classification sees Appendix Table A. 1.

Antecedent moisture condition is the relative wetness or dryness of soil storage sponge before the rainfall. SCS Curve Number Method defines three antecedent moisture conditions: dry (AMC1), normal (AMC2), and wet (AMC3). Appendix Table A. 2 describes the rainfall each condition represents during the dormant and growing seasons. The Curve number for different moisture conditions are calculated with equation (2.10) and equation (2.11).

$$CN(I) = \frac{4.2 \cdot CN(II)}{10 - 0.058 \cdot CN(II)} \tag{2.10}$$

$$CN(III) = \frac{23 \cdot CN(II)}{10 + 0.13 \cdot CN(II)} \tag{2.11}$$

where:

$CN(I)$ is CN in dry antecedent moisture

$CN(II)$ is CN in normal antecedent moisture

$CN(III)$ is CN in wet antecedent moisture.

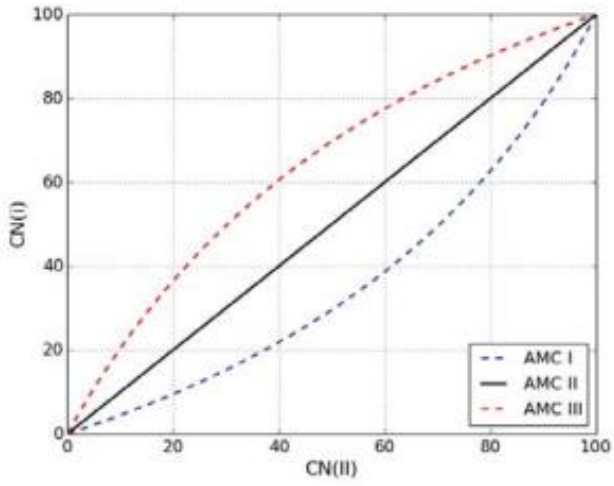

Figure 3. 5 Curve Number Conservation Based on AMC Classes (Ligier, 2016).

3.4. Available Data

In this project, two sets of data were used for the development of the hydrologic and hydraulic models: (1) geographic data including DEM, bathymetry data, satellite images, soil map, and land use map; (2) weather data including precipitation, wind speed, humidity, solar radiation, and flows. Table 3. 1. summarizes the available data for this project.

Table 3. 1 Available input data in this project.

Data	Accuracy	Source / Method
Flood Plain DEM	30m x 30m	SRTM from USGS
Bathymetry DEM	1m x 1m	LIDAR
Soil Map	1km x 1km	FAO
LNADSA8 Satellite Image	30m x 30m	USGS
Land Use Map	30m x 30m	Maximum Likelihood
Input Weather Data	Daily	OpenWeatherMap
Inflow Hydrograph	Daily	Manning's Equation

3.4.1 Geographic Data

In this study, geographic data includes floodplain DEM, bathymetry DEM, satellite images, soil map, and land use map. The geographic data are processed using ArcGIS software and projected on the UTM, Zone_31N projected coordinate system on the WGS 1984 datum.

As model accuracy is directly affected by DEM accuracy, LIDAR DEM obtained in 2014 using Ultralight Airplane and Photogrammetry is used in this project to accommodate SRTM for more accurate results. The 30m x 30m SRTM DEM (https://earthexplorer.usgs.gov/) provides elevation information for watershed delineation, stream delineation, and slope calculation.

Because SRTM DEM can not penetrate the water surface (Alsdorf et al., 2007), 1m x 1m LIDAR-based DEM is applied for water depth correction. The modified DEM infusion is then used for watershed delineation and further geographic processing.

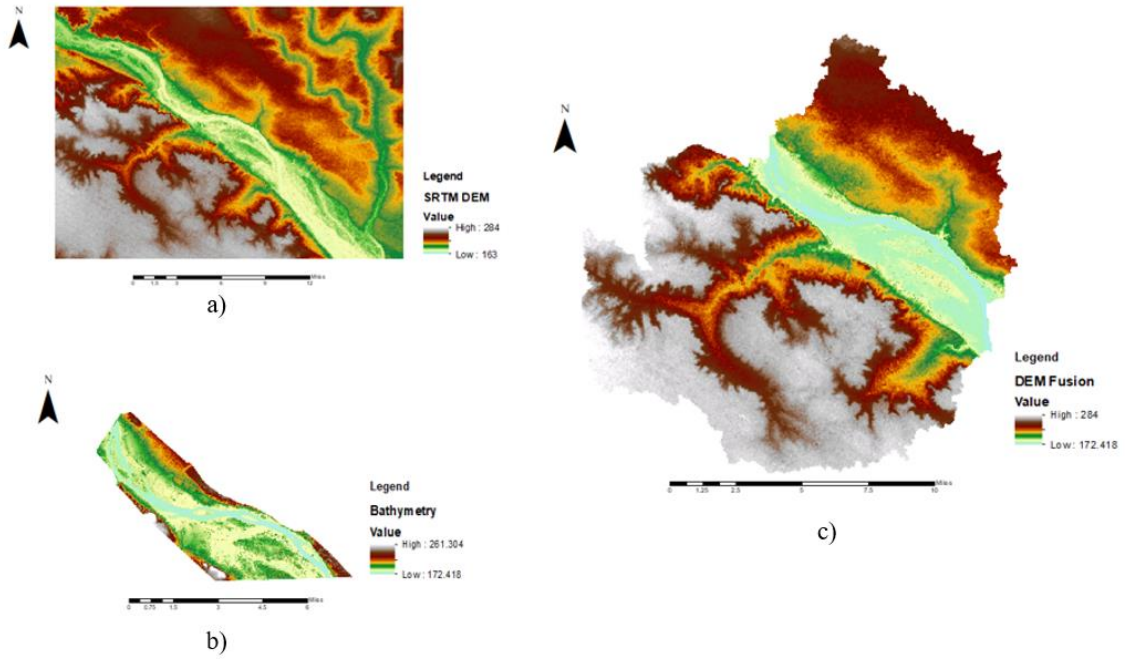

Figure 3. 6 Composite DEM: a) 30m x 30m SRTM DEM; b) 1m x 1m LIDAR DEM; c) Water depth corrected DEM.

The global scale soil map with 10km x 10km resolution from FAO (https://www.fao.org/soils-portal/data-hub/soil-maps-and-databases/faounesco-soil-map-of-the-world/en/) was downloaded for soil classification. Although the resolution of the soil map is low, it has been demonstrated that the difference in resolution will not significantly affect the model's accuracy (Ye et al., 2011). According to the FAO digital soil map, two types of soil exist in Niamey city. The first type is sand soil which covers an area of 326.59 km^2; the other is sandy loam, covering an area of 107.79 km^2. The FAO soil map provides comprehensive soil information, such as soil texture, hydraulic conductivity, hydro group, water content, etc. Given that SWAT cannot directly

identify the soil information provided by the FAO soil map, MAPWINDOW (https://www.mapwindow.org/) is employed as an intermediate step to solve the problem.

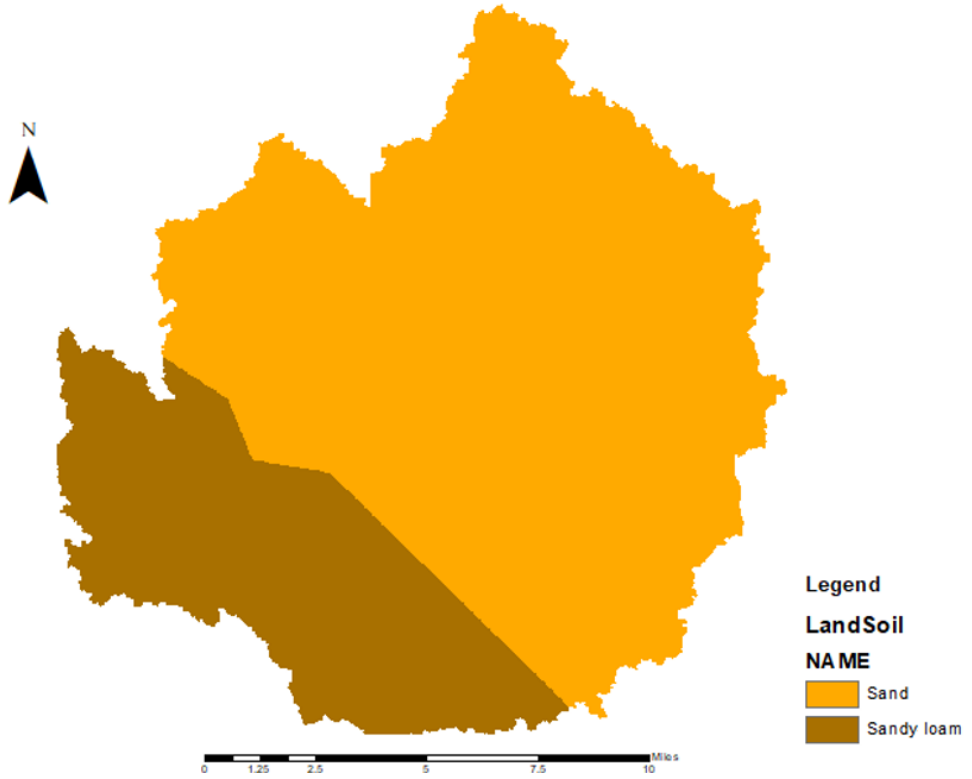

Figure 3. 7 Soil map of the study area.

Table 3. 2 Soil property of the study area.

Soil Type	Area (km^2)	Percent to Total	Hydro Group	SWAT Code
Sand	326.59	72.94%	B	Ql-1613
Sandy loam	107.79	27.06%	C	Ql-1617

The land use of the study area is determined according to the composite band of LANDSAT-8 satellite images from USGS, and a land-use map is created using the maximum likelihood approach to reflect how the land in this area is used for various purposes. In the maximum likelihood approach, the assumption is that the data for the land use types are normally

distributed in the bands; how a certain pixel belongs to a certain type is also calculated (Rawat & Kumar, 2015). The data is obtained from satellite images taken on June 26, 2019, to make sure land use remains comparable to the land use during the simulation period. In this study, four types of land use are identified: water body, wet-forest, mixed-forest, and low residential urban area, each of which occupies 8.71%, 3.64%, 19.6 %, and 68.04% of the total areas, respectively

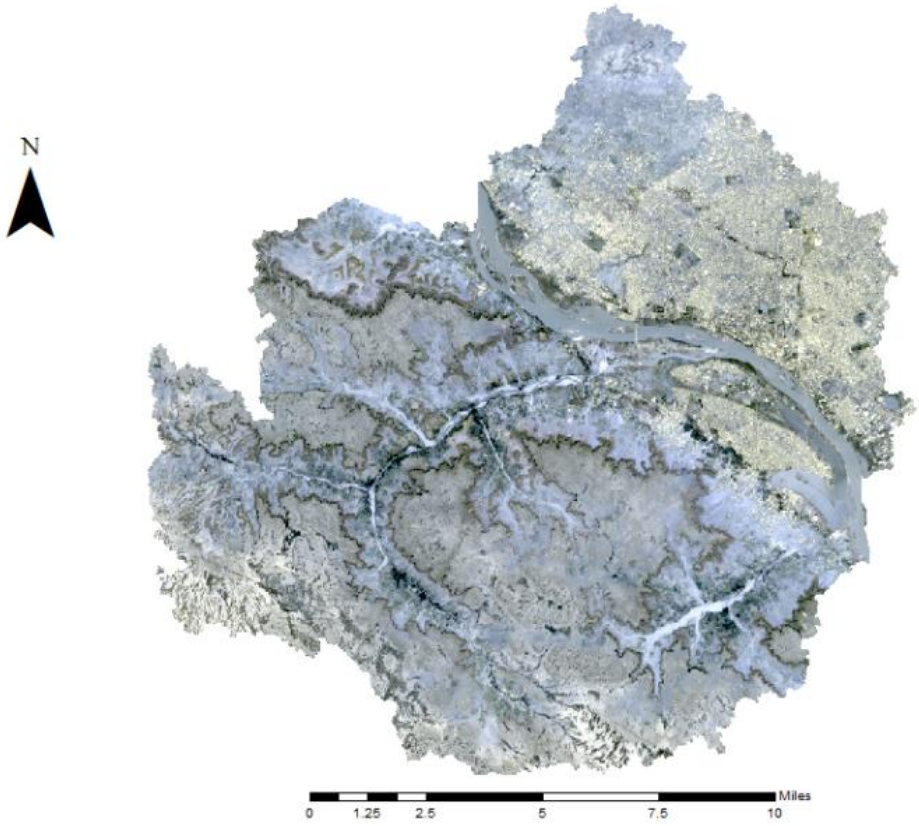

Figure 3. 8 LANDSAT-8 satellite image of the study area.

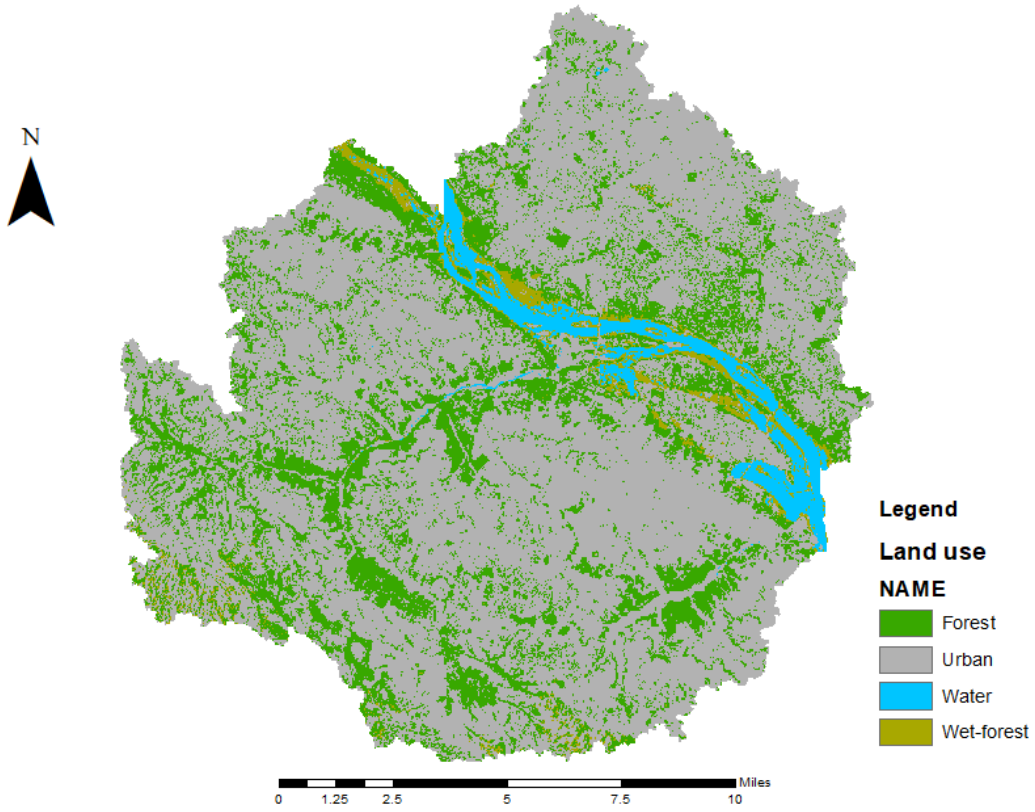

Figure 3. 9 Land use map of the study area.

Table 3. 3 Land use type of the study area.

Land Use Type	Area (km^2)	Percent to Total	SWAT Code
Water Body	38.97	8.71%	WATR
Wet Forest	16.31	3.64%	WETF
Forest	87.81	19.6%	FRST
Low Residential Urban Area	291.38	68.04%	URLD

3.4.2 Weather Data

In this study, weather data include precipitation, wind speed, humidity, solar radiation, and inlet flows, among which daily precipitation, wind speed, and humidity are historical data from OpenWeatherMap API (https://openweathermap.org/api) from the year 1979 to 2021. The inlet

flow rate provided by National Hydrological Service of Niger is converted from water level. Due to the unavailability of solar radiation data, simulated solar radiation data created by SWAT Weather Generator was used generating missing solar radiation data for the simulation period. The inlet hydrograph is shown in Figure 3. 9, and the weather data is shown in Table 3. 4.

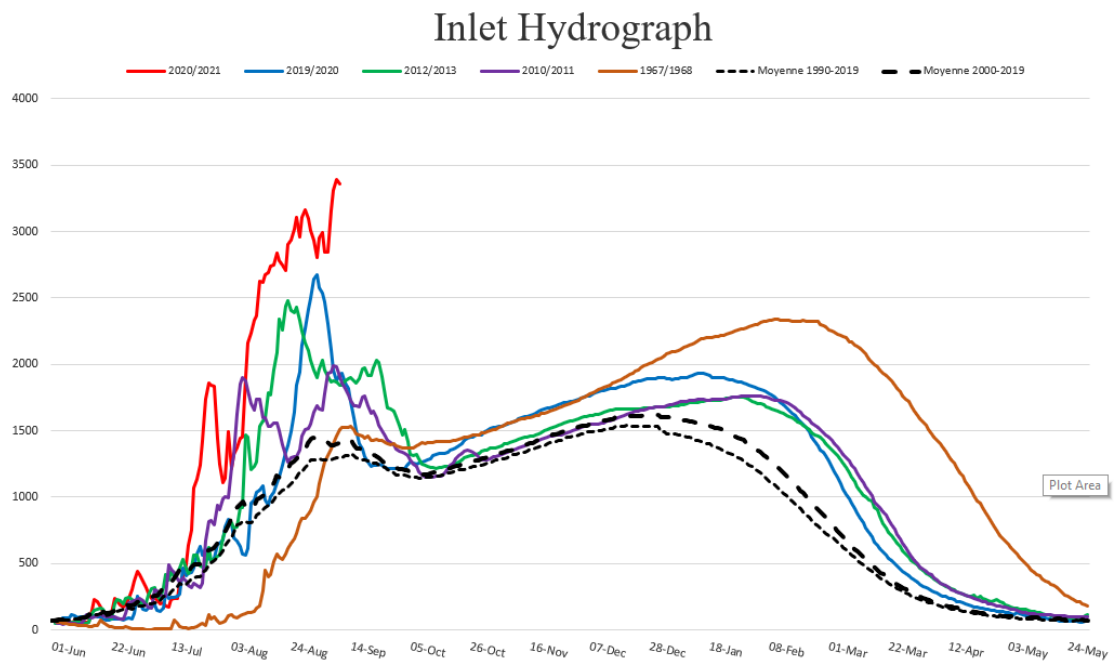

Figure 3. 10 Annual inlet hydrograph of Niamey River.

Table 3. 4 Available weather data.

Weather Input	Type	Periods	Data Range
Precipitation	Measured	1979-2021	0-65.79 mm
Wind Speed	Measured	1979-2021	1.18-7.55 m/s
Temperature	Measured	1979-2021	14.93-44.55℃
Solar Radiation	Simulated	1979-2021	11.71-28.46
Humidity	Measured	1979-2021	5.83-91.89

Chapter 4 Technical paper – Assessment and Improvement of TELEMAC Routines for Urban Flood Simulation

4.1 Introduction

Numerical simulation has been noted as an effective way to predict flood hazards with minimum cost (Bates et al., 2005; de Almeida et al., 2018; Kazama et al., 2010; van Dijk et al., 2014). Most studies have focused on fluvial flood because fluvial flood is regarded as a frequent and harmful flood type (Benito & Hudson, 2010; Bernhofen et al., 2018; Tariq & Van De Giesen, 2012). Research on fluvial flood have used both 1D and 2D modeling techniques extensively (Betsholtz & Nordlöf, 2017; Leandro et al., 2011). Recently, rapid urbanization and climate change have made pluvial flooding a major natural disaster that poses increasing threats to life and property for urban dwellers (Hammond et al., 2015). The acceleration of urbanization has increased impervious areas, which significantly reduces an urban's capacity to discharge rainfall runoff. On the other hand, heavier rainfall hits urban areas with increasing frequency because of global climate change, yielding increased runoff significantly (Tingsanchali, 2012; Wong, 2015). Although pluvial floods are as disastrous as fluvial floods, pluvial floods have not been thoroughly studied due to challenges such as complicated drainage systems, flow paths, and the built environment. In urban environments, drainage systems can be generally categorized as the major and minor systems (Zhu et al., 2018). Pluvial flooding occurs when the amount of rainfall-runoff exceeds the capacity of the minor system.

Typically, conceptual models are used for pluvial flood modeling. While conceptual models can simulate inundation efficiently, they do not simulate physical phenomena. As a result, numerical modeling has arisen for research on flow dynamics in urban areas, providing detailed flow information such as velocity, water depth, and runoff. Mark et al. (2004) developed a 1D-1D dual-drainage system which consists of a 1D sewer network model and a 1D surface flow routing model to simulate actual flow. Carr and Smith (2007) enhanced the model of Mark et al. (2004) by developing a 1D-2D approach that replaced the 1D surface model with a 2D surface model, introducing 1D-2D coupled models in pluvial flood modeling. According to Carr and Smith (2007), 2D modeling can provide more information on flow dynamics with fewer presumptions and less modeling setup time. Recently, the 1D-2D model has received considerable attention from researchers and has become one of the principal tools for research on urban pluvial floods.

2D models become an effective alternative for the 1D-2D integrated model when the minor drainage system has less impact on the identification of flood-prone areas (van Dijk et al., 2014). In 2D surface modeling, the minor drainage systems are usually simplified assuming that rainfall drains away at the drainage capacity (Yin et al., 2016) or by increasing the net rainfall amount (Bruwier et al., 2020). Experiments demonstrated that the accuracy of 2D models was not compromised when minor systems were simplified or neglected (Huang et al., 2017). Hence, 2D models can be widely used in areas where the data on drainage systems are insufficient.

In recent decades, various 2D modeling software have been applied to solve fluvial and pluvial flood problems. Some of the prevailing packages are HEC-RAS 2D, LISFLOOD-FP, MIKE 21, TELEMAC-2D, etc. With respect to model selection, the configuration of the study area should be the primary factor to be taken in consideration. In this study, TELEMAC-2D is employed to model the rainfall-runoff process. TELEMAC-2D is a fully two-dimensional flood model

developed by the French National Hydraulics and Environment Laboratory. Research has proved the efficiency of TELEMAC-2D in fluvial flood simulation (Forster et al., 2019; Robins & Davies, 2011; Yan et al., 2018); however, the application of TELEMAC-2D in pluvial simulation has not been studied extensively. Recently, the SCS Curve Number Rainfall-runoff module has been added into the TELEMAC-2D package, which enhanced the capability of TELEMAC-2D in the simulation of real flows.

The objective of this study is to examine the ability of TELEMAC-2D used to simulate urban runoff in the city of Niamey in July and August 2019. Meanwhile, SWAT (Soil and Water Assessment Tool) is employed to simulate the runoff as a reference to the results from TELAMC2D. Comparing rainfall-runoff generated by TELEMAC-2D (hydraulic model) and SWAT (hydrologic model) is an initiative for studies on this topic. Based on the differences in the simulated rainfall-runoff from the two models, the infiltration routines of TELEMAC-2D and SWAT are examined. The reasons for the discrepancies between the rainfall runoffs are further analyzed. Through the analysis, suggestions are provided to improve the accuracy of TELEMAC-2D used rainfall-runoff simulations.

4.2 Materials and Methods

4.2.1. Study Area

Niamey (13° 30′ 30.96″ N, 2° 6′ 39.96″ E) is the capital and the largest city of the Republic of Niger, with a population of more than one million. With a hot semi-arid climate, the city experiences, on average, rainfall around 500 to 700 mm per year during the rainy season from June to September, while the long dry season lasts from October till next May. Despite that the dry season often leads to draught in the area, the frequency and intensity of rainfall in the rain

season in Niamey continue to increase (Douglas et al., 2008), constantly leading the city to tremendous damages caused by floods. In this project, a watershed that covers most of the Niamey urban area is delineated to simulate the rainfall-runoff in Niamey city in July and August 2019 to understand the flood in the area better. The simulation results are expected to provide data-based evidence for flood management, allow policy makers to make informed decisions, and facilitate the understanding of floods among the public.

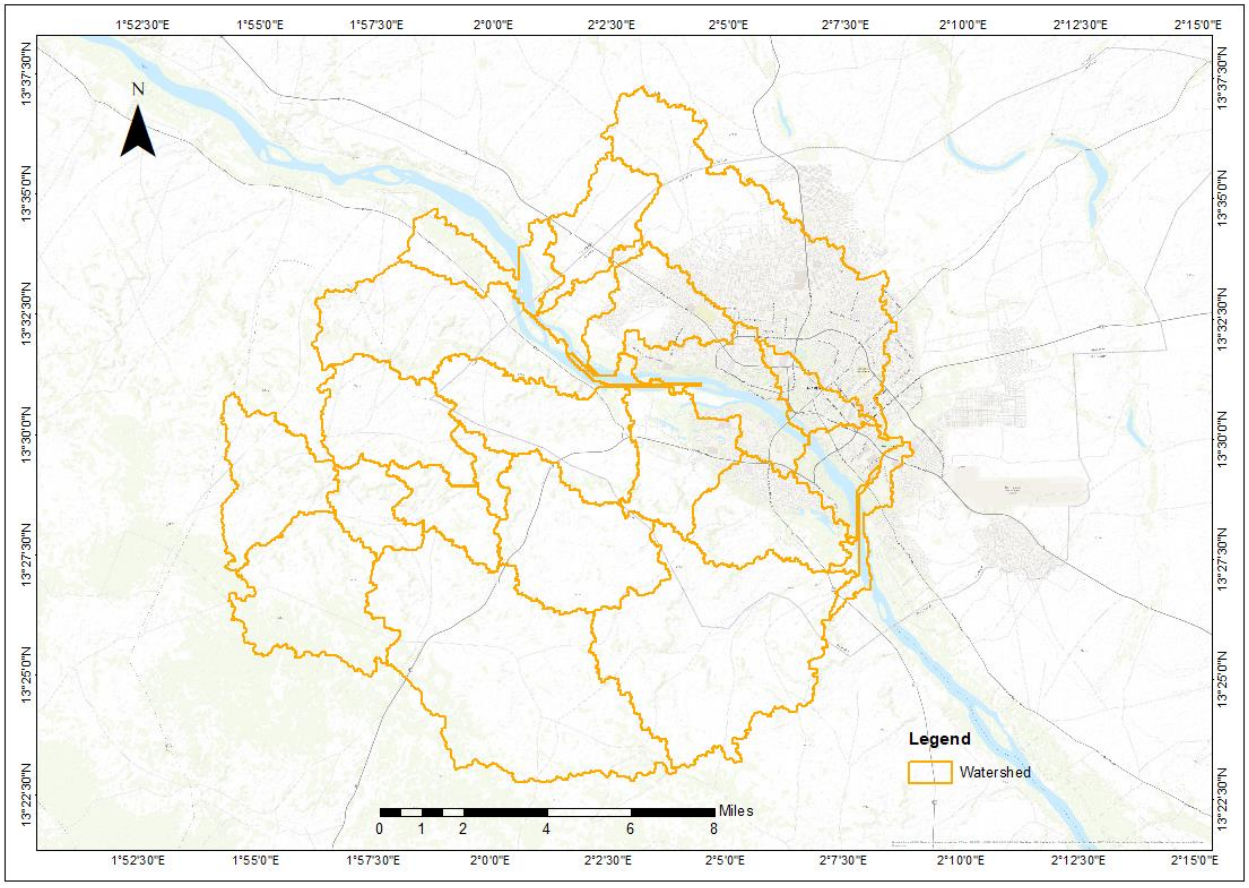

Figure 4. 1 Location of the watershed in the study area.

4.2.2. Methodology

The thesis aims to check the applicability of the TELEMAC model to simulate pluvial flooding in a semi-arid area. Based on the SCS CN method, the new infiltration module is of particular

importance for the exercise implemented in TELEMAC. The following steps were used to answer the research question:

1. A SWAT model of the study area was developed
2. The CN value of SWAT model was calibrated according to TR-55 table developed by USDA(https://www.nrcs.usda.gov/wps/portal/nrcs/site/national/home) . Because observations are very scarce (two rainfall events), so a validation exercise could not be conducted.
3. A TELEMAC model of the study area was developed
4. The calibrated CN values from the SWAT models were used in the TELEMAC model, and the same events were simulated using SWAT and TELAMAC
5. The runoff generated by the two models are compared.
6. The TELEMAC rainfall-runoff subroutine is examined to analyze the difference in the runoff from the TELEMAC 2D and SWAT.
7. The flow chart of the methodology is shown in Figure 4. 2.

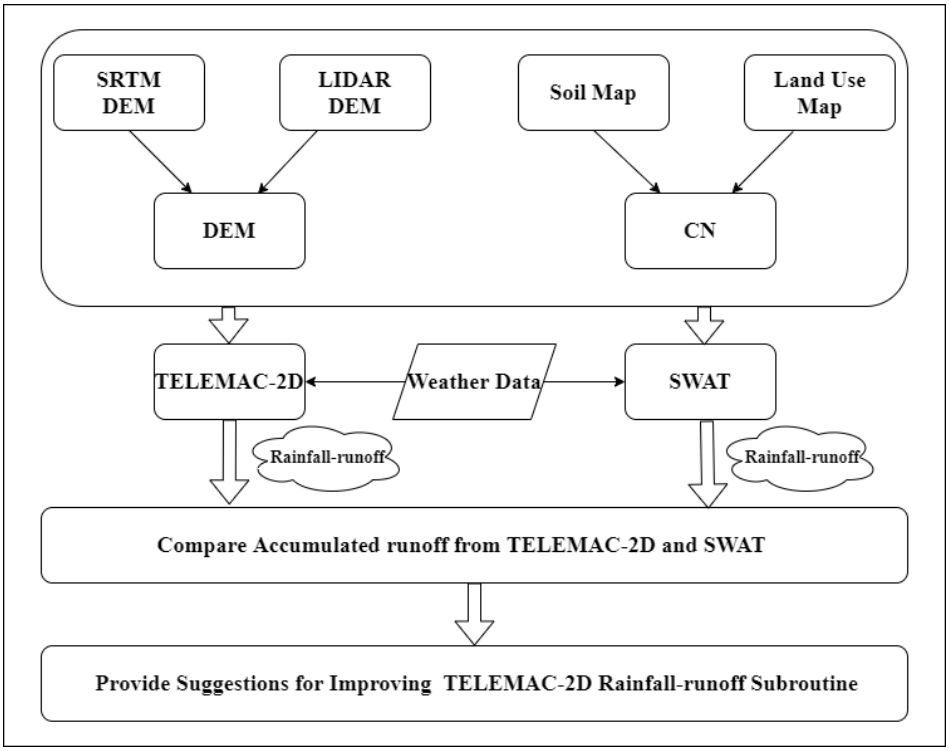

Figure 4. 2 Flow chart of the research methodology.

4.2.3. Modeling tools

4.2.3.1 Shallow Water Equations

Shallow water equations are a set of hyperbolic partial differential equations commonly used for the modeling of dynamic fluids in hydro static balance and constant density. The equations can be used for modeling fluids in a variety of conditions such as ocean, river estuary, coastal region, and river channel (Tan, 1992). In this project, TELEMAC-2D employs the Finite Element method to solve shallow water equations on unstructured meshes. The governing equations are written as:

$$\frac{\partial h}{\partial t} + \vec{u} \cdot \vec{\nabla}(h) + h div\left(\vec{u}\right) = S_h \quad (4.1)$$

$$\frac{\partial u}{\partial t} + \vec{u} \cdot \vec{\nabla}(u) = -g\frac{\partial Z}{\partial x} + S_x + \frac{1}{h}\text{div}\,(hv_t\vec{\nabla}u) \quad (4.2)$$

$$\frac{\partial v}{\partial t} + \vec{u} \cdot \vec{\nabla}(v) = -g\frac{\partial Z}{\partial y} + S_y + \frac{1}{h}\text{div}\,(hv_t\vec{\nabla}v) \quad (4.3)$$

where:

h (m) is water depth

$\vec{u}$ (m/s) is velocity vector

u and v (m/s) are velocity components

g (m/s^2) is gravity acceleration

x and y are horizontal space coordinates

Z (m) is free surface

t (s) is time

S_x and S_y (m/s^2) are sources or sink terms of momentum in dynamic momentum equations

S_h (m/s) is source or sink term of the fluid

v_t (m^2/s) is eddy viscosity

u, v ,and h (m) are unknowns.

4.2.3.2 SCS Curve Number Method

The SCS Curve Number Method, uniformly called the Curve Number Method, was developed by the USDA Natural Resources Conservation Service in 1954 (Boughton, 1989). The Curve Number method has been widely used to calculate rainfall-runoff in both agricultural and urban areas (Rizeei et al., 2018; Yao et al., 2018). The Curve Number Method relies on a single parameter CN to estimate surface runoff, making the Curve Number Method a simple and

practical way to simulate rainfall-runoff. CN is calculated with data about soil group, land use type, and hydrologic condition. Curve Number ranges from 30 to 100 where larger numbers stand for the greater potential that runoff occurs, and runoff is calculated by the following equations:

$$Q = \frac{(P - I_a)^2}{(P - I_a + S)} \quad (4.4)$$

$$S = 25.4 \times \left(\frac{1000}{CN} - 10\right) \quad (4,5)$$

$$I_a = \lambda \cdot S \quad (4.6)$$

where:

Q (mm) is surface runoff

P (mm) is the precipitation

I_a (mm) is the initial abstraction

S (mm) is the potential maximum retention

λ is the constant

CN is the curve number in normal antecedent moisture.

4.2.4 Simulation Setup

This section introduces the necessary process for building the hydraulic and hydrologic models from data preparation to model operation.

4.2.4.1 TELEMAC-2D Model Setup

BlueKenue (https://nrc.canada.ca/en/research-development/products-services/software-applications/blue-kenuetm-software-tool-hydraulic-modellers), a data preparation and visualization tool developed by National Research Council Canada, is used to generate unstructured mesh for the study area. The

unstructured mesh has 804,037 nodes and 1,602,901 triangle elements with two prescribed liquid boundaries. The inflow boundary is a prescribed discharge boundary where the flow rate is a function of time. The outflow boundary is a prescribed elevation boundary where the flow rate is a function of water elevation. A block-type hyetograph of rainfall from July 1st to August 31st, 2019, is defined for rainfall-runoff modeling. The CN value for runoff calculation is directly stocked in the geometry file as an additional variable. A part of the model's parameter is listed in Table 4. 4. The complete keywords activated in this study are provided in the Appendix. The four steps in development of the TELEMAC-2D model are shown in Figure 4. 2.

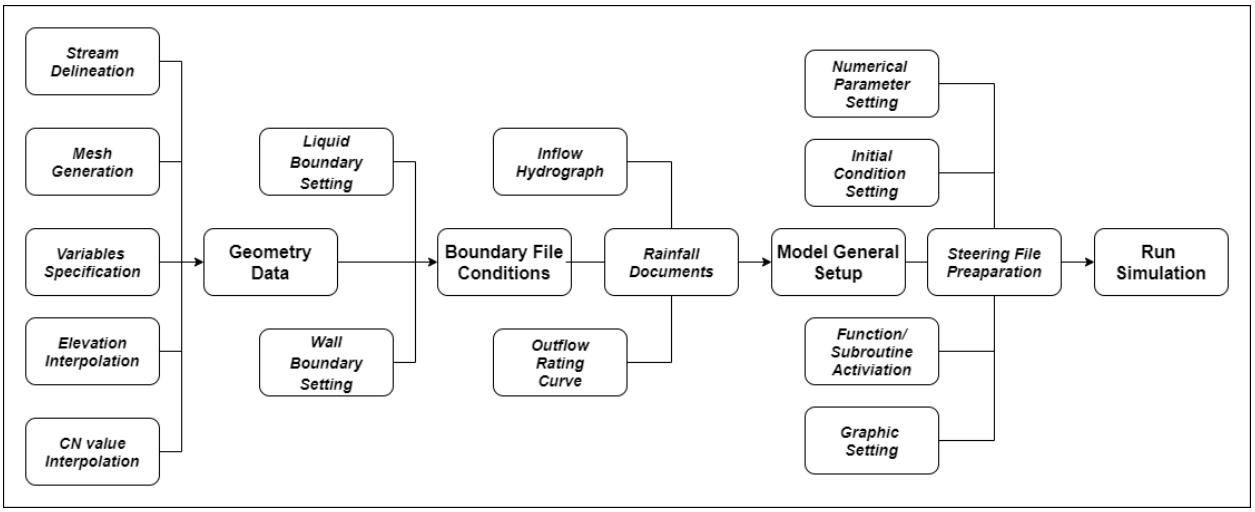

Figure 4. 3 Schematic of TELEMAC2D to simulate the rainfall-runoff process.

4.2.4.1.1 Geometrical Data

The watershed and the channels are delineated by a closed line and open lines separately. During the process of riverbank delineation, a series of marshy islands are found in the middle of Niger River. In previous studies, the marshy islands are generally considered to isolate river flows; in this study, however, five tributaries surrounding the islands are drawn to connect reaches to make the channel profile as realistic as possible. The location of each tributary is shown in Figure 4. 4. The final mesh comprises two parts: the first part contains meshes of Niamey River

and its tributaries. The second part is floodplain mesh. The two parts of meshes are combined to form the global mesh to stock variables. The properties of each mesh are listed in Table 4.1.

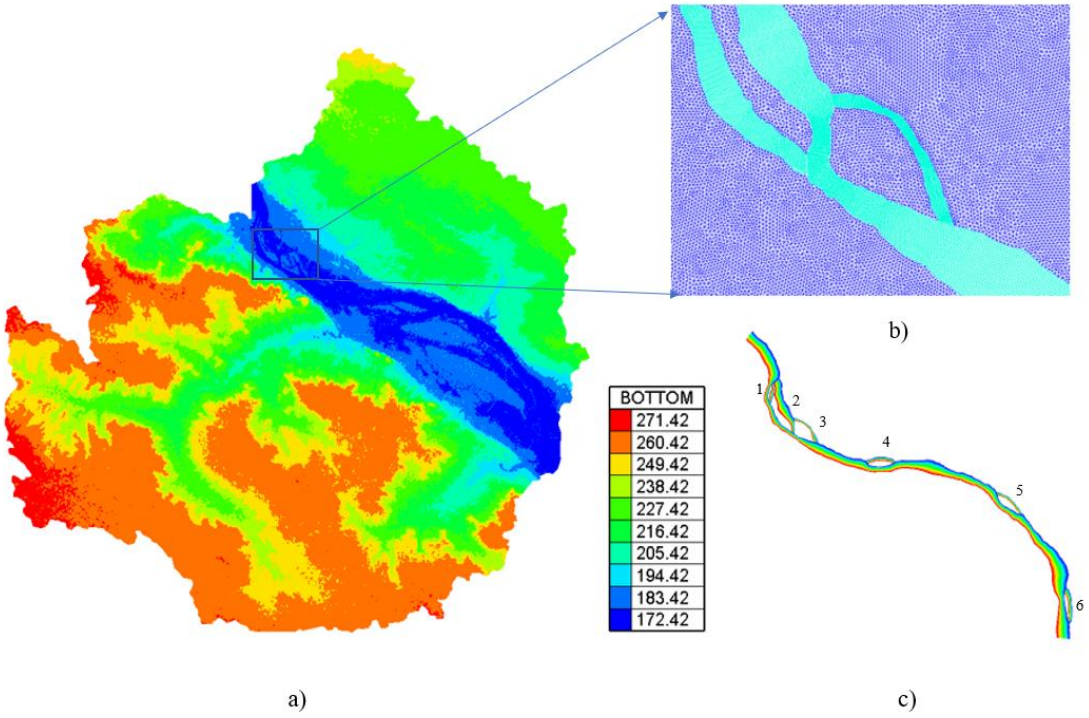

Figure 4. 4 Mesh generation of TELEMAC2D: a) Bottom elevation; b) Floodplain mesh; c) Channel mesh.

Table 4. 1 TELEMAC-2D mesh property.

Mesh	Nodes	Elements
Channel Mesh	32039	61883
Tributary1	2790	5180
Tributary2	1598	2599
Tributary3	1474	2724
Tributary4	991	1821
Tributary5	1403	2550
Floodplain Mesh	563892	1123118

TELEMAC-2D offers two options for defining the CN value in space: (1) setting constant CN in polygons with coordinates and (2) setting space-varied CN value as an additional variable in the geometry file, and the latter is adopted in this project. FAO soil map and the land-use map prepared are superimposed in the ArcGIS environment to calculate CN. The CN value is then linearly interpolated to the nodes on the global mesh in TELEMAC2D and stocked as an additional variable. The interpolated CN map is shown in Figure 4. 5. Table 4. 2 shows the specific CN value under different land-use types and soil classes in the city of Niamey.

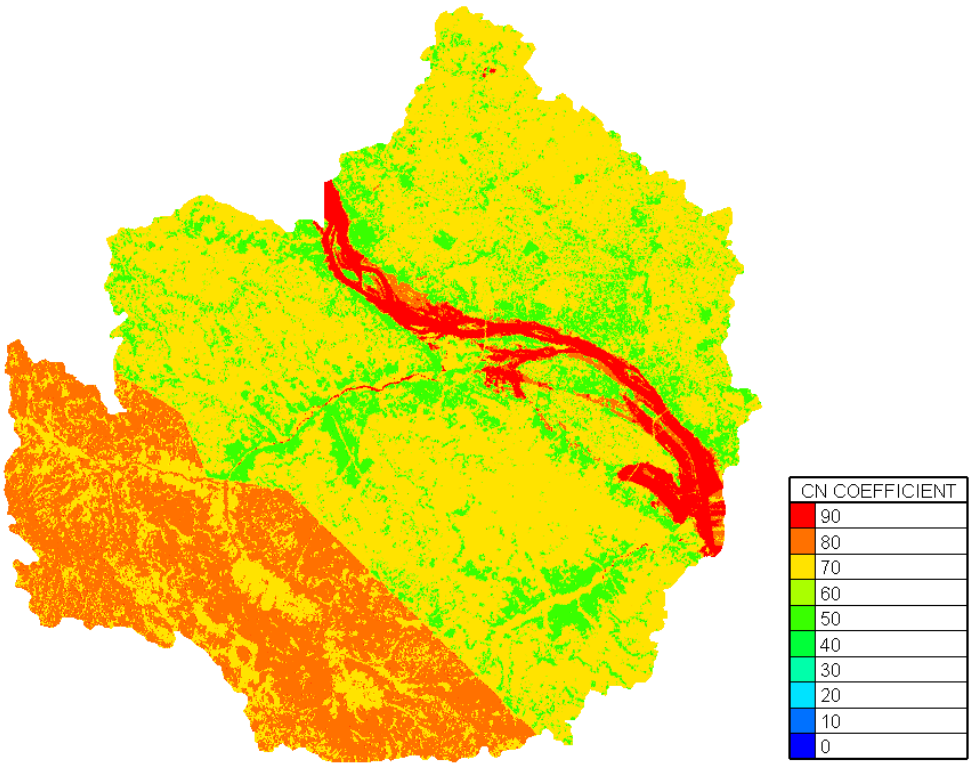

Figure 4. 5 CN map created by BlueKenue.

Table 4. 2 Reference for CN map generation.

Land Use Type	Soil Type	CN2 Value
Water	Sand	100

Water	Sandy Loam	100
Wet Forest	Sand	86
Forest	Sand	57
Forest	Sandy Loam	73
Low Residential Urban Area	Sand	75
Low Residential Urban Area	Sandy Loam	83

4.2.4.1.2 Boundary Conditions

Two liquid boundaries and two solid boundaries are set for the watershed. The inlet boundary is the first liquid boundary with a prescribed flow rate where the flow rate is a time series. The inflow rate is obtained using Manning's equation from the measured water level of this boundary containing the nodes from 792,491 to 80,403. The outlet boundary is the second liquid boundary with prescribed elevation where the flow rate is a function of water level. The outlet boundary contains nodes from 263,415 to 263,702. For each liquid boundary, velocity is set to be normal to the boundary. Subsequently, two wall boundaries are set in the domain to connect the inlet and the outlet boundaries. Figure 4. 6 shows the location of each boundary and the flow rates at each liquid boundary.

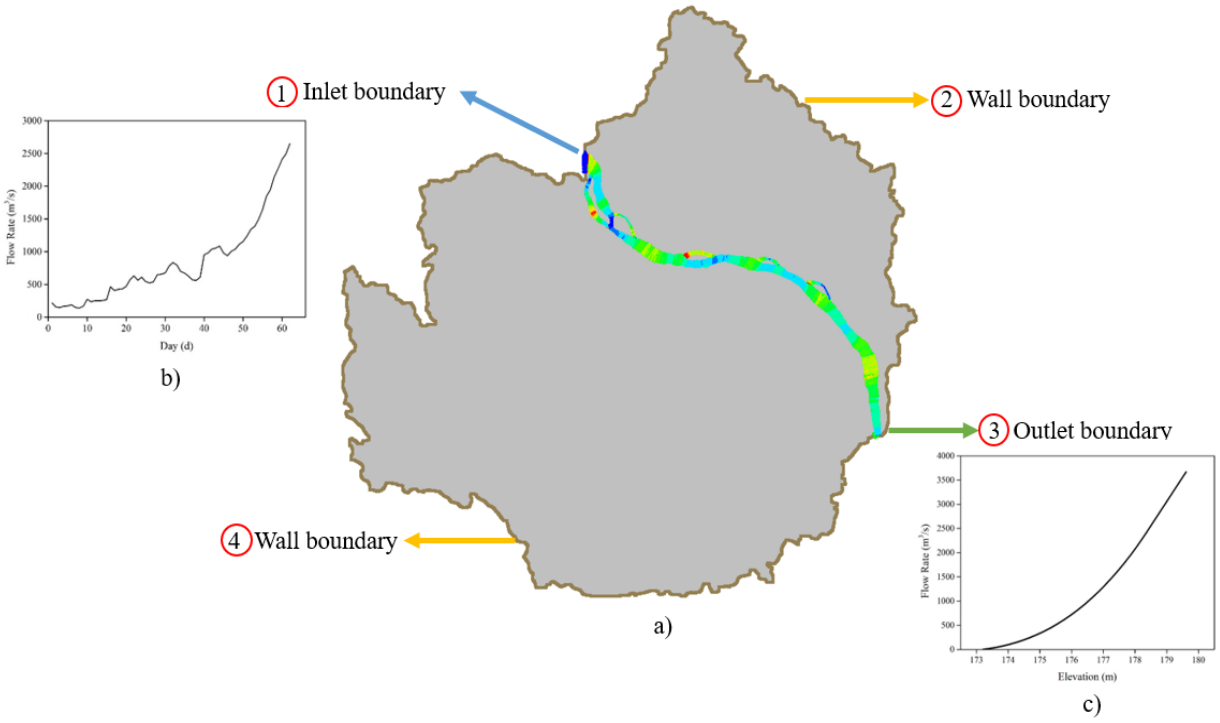

Figure 4. 6 Boundary conditions of TELEMAC-2D model.

Table 4. 3 Boundaries property of TELEMAC-2D.

Boundary Number	Boundary Type	Format
1	Liquid	Wall
2	Solid	Prescribed flow rate
3	Liquid	Prescribed elevation
4	Solid	Wall

4.2.4.1.3 Rainfall-runoff Data

According to the precipitation data obtained from OpenWeatherMap

(https://openweathermap.org/), the rainfall amount accumulated in five days from June 25th to

June 30th is 49.5mm, which is within the range of normal antecedent moisture condition. Consequently, the value for keyword ANTECEDENT MOISTURE CONDITION is set to 2 to present the normal AMC. TELEMAC-2D offers three options for rainfall definition: (1) standard rainfall type where rainfall is a constant each day; (2) Chicago Design Storm (CDS) with an Intensity-Duration-Frequency (IDF) curve; and (3) a block-type hyetograph applied in this project. With block-type hyetograph, rainfall depth is given as a time series in a formatted text file. The rainfall rate is assumed constant between two consecutive time steps, and the precipitation hyetograph is shown in Figure 4. 7.

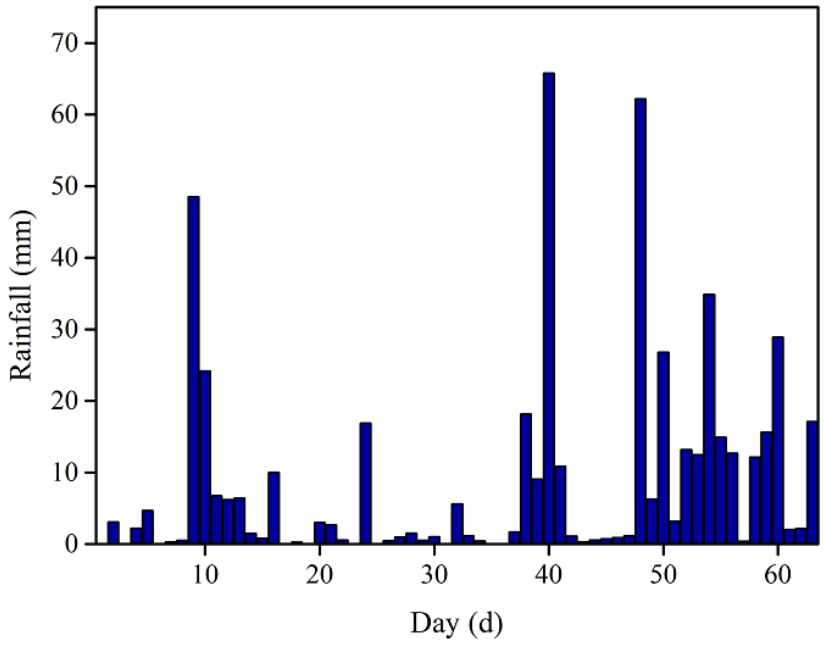

Figure 4. 7 Precipitation hydrograph.

4.2.4.1.4 Model General Setup

Telemac-2D offers FVM and FEM to solve the shallow water equations numerically. In this study, the FEM is adopted to simulate flow motions, with viscosity considered a constant and the turbulent viscosity set as 0.01 within the domain. Manning's law is used for the friction on the bottom with the friction coefficient set to 0.1 throughout the entire computation domain for the

definition of friction parameter. Because the watershed is relatively small compared with other regional-scale watersheds, and the bed levels remain consistent between upstream and the downstream, the initialization using constant water elevation is set at the downstream, while inflow is gradually introduced from upstream. Four private working arrays are added to the simulation to stock the SCS Curve Number Method variables.

Given that no complex turbulence model is involved in this project, hydrodynamic propagation becomes the primary factor accounting for selecting solvers., the time step is set to 4 seconds to keep Courant number below 1. TELEMAC-2D Parallel is set up to discretize the whole domain into eight sub-domains, with one sub-domain on each processor as the simulation is executed on a DELL Precision 3640 workstation. A segment of logical keywords is presented in Table 4. 4.

Table 4. 4 A segment of keywords used in the TELEMAC-2D steering file.

Keyword	Value	Description
TURBULENCE MODEL	1	Constant viscosity
VELOCITY DIFFUSIVITY	0.01	Viscosity coefficient
LAW OF BOTTOM	5	Manning's law
FRICTION COEFFICIENT	0.1	Friction coefficient
PRESCRIBED FLOWRATES	1;0	Inflow changes with Time
PRESCRIBED ELEVATIONS	0;1	Outflow changes with Elevation
INITIAL CONDITIONS	CONSTANT ELEVATION	Initial condition type
INITIAL ELEVATION	182	Elevation value
LIQUID BOUNDARIES FILE	INFLOW.txt	File of inflow
STAGE-DISCHARGE CURVES FILE	OUTFLOW.txt	File of outflow
FORTRAN FILE	RUNOFF_SCS_CN. f	Infiltration subroutine
FORMATTED DATA FILE 1	RAINFALL.txt	Precipitation Hydrograph

RAINFALL-RUNOFF MODEL	1	SCS Curve Number model
ANTECEDENT MOISTURE CONDITIONS	2	Normal AMC
OPTION FOR INITIAL ABSTRACTION RATIO	1	IA/S = 0.2
NUMBER OF PRIVATE ARRAYS	4	Variables in SCS Method
SUPG OPTION	4	Time step
TYPE OF ADVECTION	1;5	Triangular elements
DISCRETIZATION	11;11	Linear depth and velocity
SOLVER	1	Conjugate gradient method
SOLVER ACCURACY	$1.E^{-3}$	Required for propagation solution
TIME STEP	4	Time step

4.2.4.2 SWAT Model Setup

In this study, SWAT divides the watershed into 26 sub-watersheds and 69 HURs according to the geometry data, and the runoff generated on the sub-watersheds is compared with the runoff generated on the nodes in TELEMAC-2D.

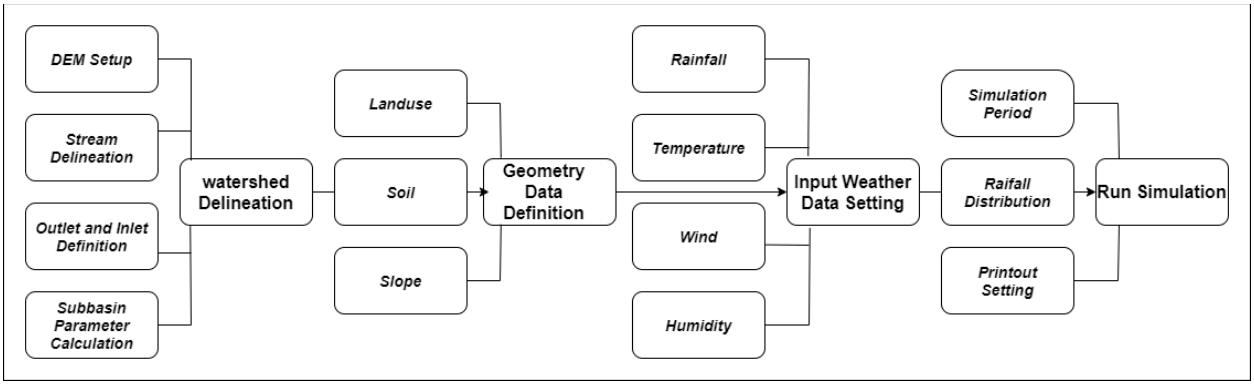

Figure 4. 8 Schematic of SWAT to simulate the rainfall-runoff process.

4.2.4.2.1 Watershed Delineation

The syncretic input DEM is an integration of the SRTM DEM with 30m resolution, showing floodplain elevation, and the LIDAR DEM with 1m resolution that describes the bathymetry. The syncretic DEM covers an area of 452 km^2, including most urban areas in Niamey city. The whole domain is divided into 26 subbasins and one inland. In Figure 4. 9, the inlet of the watershed is marked with a blue point, and the green points indicate the two outlets that are manually added. The green point at the right bottom indicates the outlet of the whole watershed, and the one at the right top is a flow monitoring station where the flow data on July 22nd and August 9th are obtained.

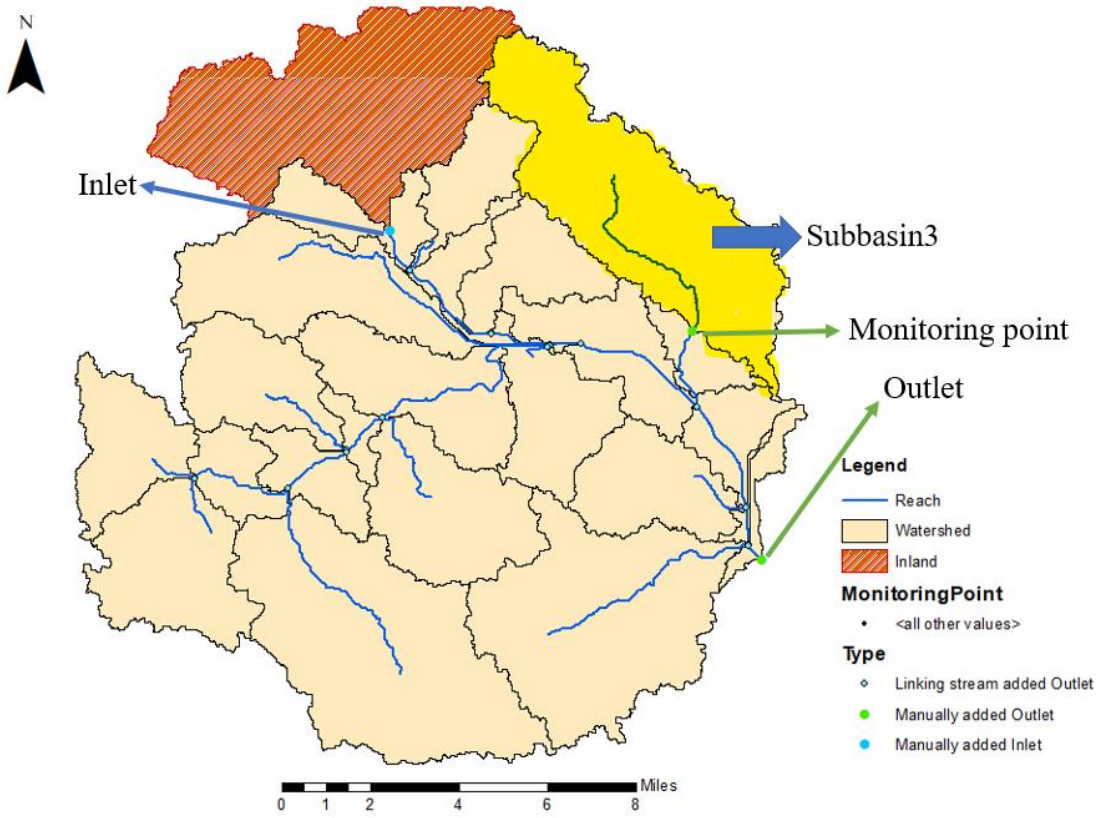

Figure 4. 9 Watershed delineation of the study area.

4.2.4.2.2 HRU Definition

Soil data, land use data, and slope data are overlayed to create HRU features. Sand soil covers two-third of the watershed, while the remaining one-third is covered by sandy loam. Four types of land use are found on sand soil, i.e., water body (WATR), wet forest (WETF), mixed forest (FRST), and low residential urban area (URLD). The sandy loam area contains two land use types: forest (FRST) and low density residential urban area (URLD). As the study area is flat terrain, one single slope segment is used in the SWAT model. The HRUs in each subbasin are shown in Table 4. 5.

Table 4. 5 HRU divisions in each subbasin.

Subbasin	Area	Soil texture	Land Use Type	HRU Numbers
1	10.99	Sand	WATR, WETF, FRST, URLD	4
2	12.33	Sand	FRST, URLD	2
3	55.11	Sand	FRST, URLD	2
4	5.97	Sand	WATR, WETF, FRST, URLD	4
5	14.27	Sand	FRST, URLD	2
6	1.48	Sand	WATR, WETF	2
7	30.52	Sand	FRST, URLD	2
8	0.23	Sand	WATR, WETF, FRST	3
9	0.04	Sand	WERF, FRST, URLD	3
10	16.75	Sand	FRST, URLD	2
11	17.70	Sand	WATR, WETF, FRST, URLD	4
12	6.24	Sand	FRST, URLD	2
13	24.28	Sand	FRST, URLD	2
14	18.74	Sand, Sandy Loam	FRST, URLD	3
15	3.56	Sand	FRST, URLD	2
16	16.88	Sandy Loam	FRST, URLD	2
17	9.22	Sand, Sandy Loam	FRST, URLD	4
18	8.36	Sandy Loam	FRST, URLD	2
19	25.97	Sand	FRST, URLD	2
20	8.85	Sand	WATR, WETF, FRST, URLD	4
21	18.23	Sand	WATR, FRST, URLD	3
22	25.08	Sandy Loam	FRST, URLD	2
23	1.12	Sand	WATR, WETF, FRST, URLD	4
24	0.39	Sand	WATR, FRST, URLD	3
25	53.53	Sand	FRST, URLD	2
26	62.74	Sandy Loam	FRST, URLD	2

4.2.4.2.3 Weather Data

SWAT model is a physical model which requires direct weather input. The precipitation, wind speed, temperature, and humidity are historical data from OpenWeatherMap. The solar radiation data is simulated by SWAT because the solar radiation date for the simulation period has not been recorded. SWAT requires a warming-up period to ensure the water volume is balanced

during the simulation, and therefore, a 5-year warming-up period is set up for the daily weather date from 2014- 2019.

4.3 Result and Discussion

Subbasin 3 is selected to illustrated runoff evolution because this area has a significant urban coverage, and that the runoff generated by TELEMAC 2D and SWAT is compared to exam the accuracy of TELEMAC 2D. In TELEMAC, nodes in the coordinate of the area corresponding to subbasin 3 were extracted by MATLAB code. Figure 4. 10 shows the sequence of the runoffs simulated by TELEMAC 2D, starting at various certain accumulated rainfall depths (ARD). When ARD increases, the sequence is demonstrated as in Table 4. 6.

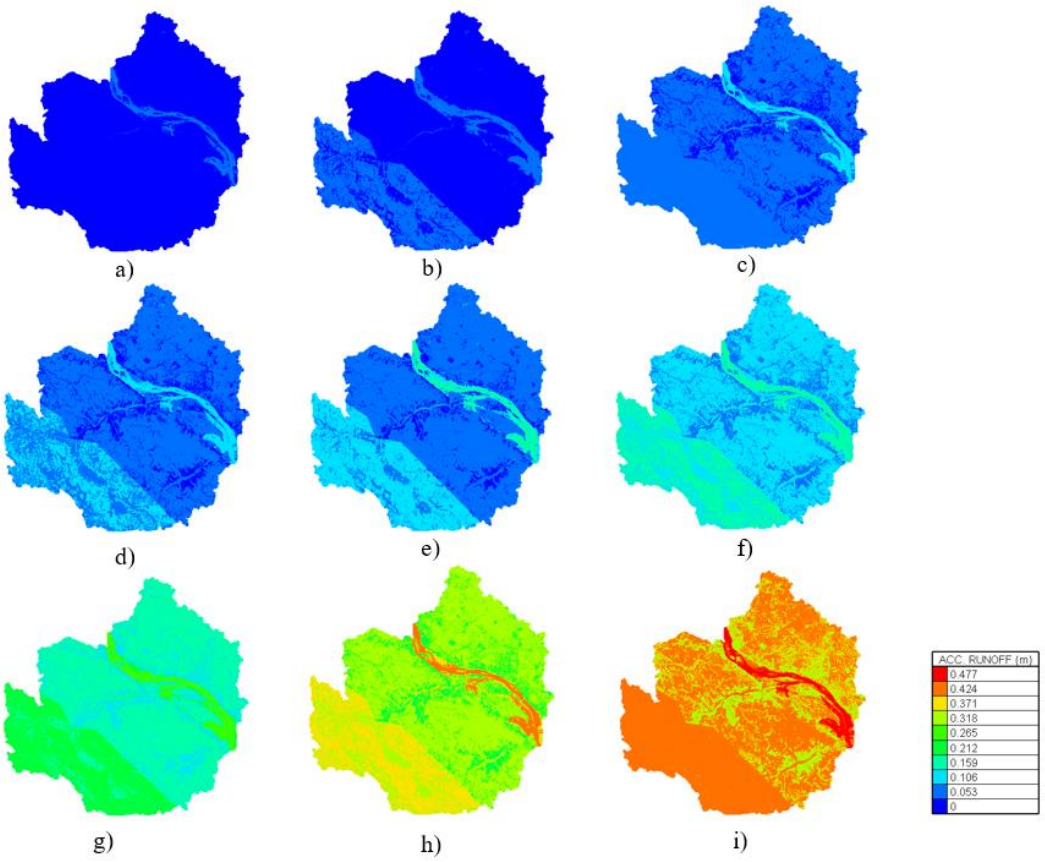

Figure 4. 10 Time series of rainfall-runoff simulated by TELEMAC-2D: a) Accumulated runoff at time = 7 days; b) Accumulated runoff at time =14 days; c) Accumulated runoff at time = 21 days; d) Accumulated runoff at time = 28 days; e): Accumulated runoff at time = 35 days; f) Accumulated runoff at time = 42 days; g) Accumulated runoff at time = 49 days; h) Accumulated runoff at time = 56 days; i) Accumulated runoff at time = 62 days.

Table 4. 6 Runoff occurring time in different areas.

Areas	Runoff Occurring Time	Accumulated Rainfall
Urban areas + Sandy loam	2019/07/11	90mm
Wet forest + Sand	2019/07/12	99mm
Forest + Sandy loam	2019/07/16	115mm
Urban areas + Sand	2019/07/20	120mm
Forest + Sand	2019/08/07	174mm

Figure 4. 11 shows the rainfall and runoff simulated by SWAT in subbasin 3. The runoff amount is categorized into four stages: (1) the initial stage from day 1 to day 6 of the simulation in which runoff amounts close to 0; (2) Stage II from day 8 to day 38, where the runoff has a sharp increase from 0- 19.63 mm during the first three days and then stays stable; (3) stage III starts from day 39 and ends at day 46 during which the runoff increases substantially to 66.26 mm from day 39 to day 40 and then remained stable; (4) the last stage is from day 47 to the end of the simulation, and the runoff increases steadily.

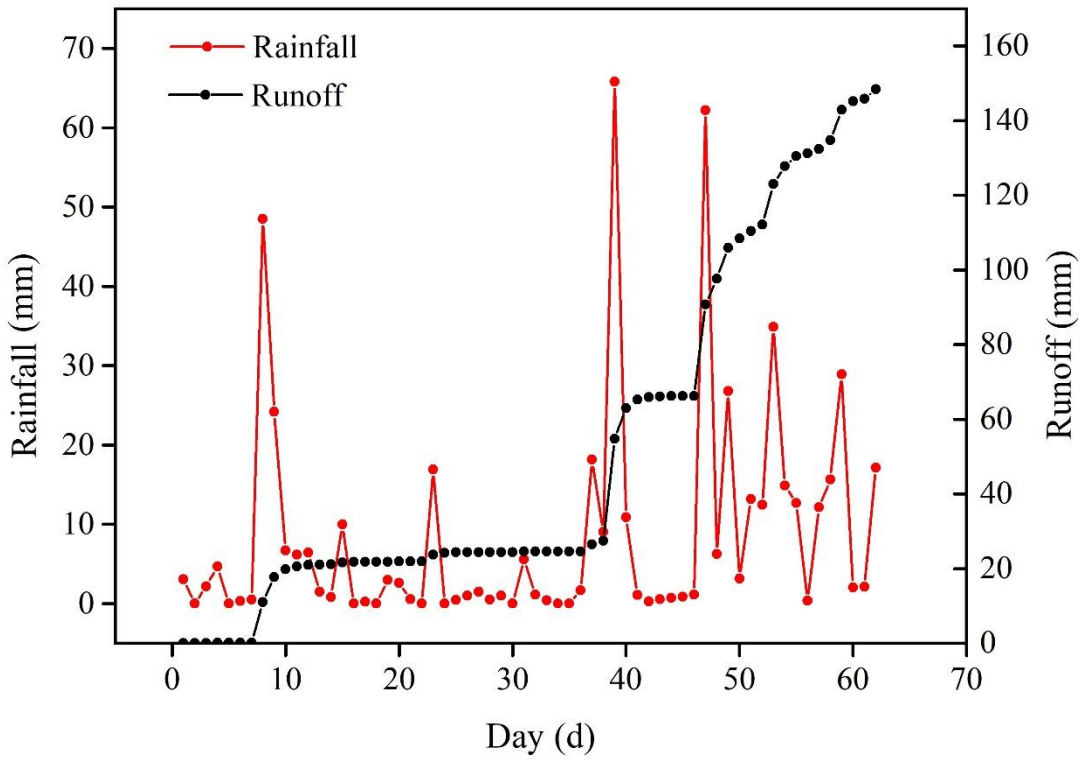

Figure 4. 11 Rainfall-runoff simulated by SWAT.

Figure 4. 12 shows the rainfall and runoff simulated by TELEMAC. The curve indicates that the runoff increases over the simulation period and has a similar tendency to the curve for runoff generated by SWAT. However, it is worth mentioning that during stage II from day 8 to day 38, the runoff from TELEMAC has a steady increase from 0- 88.80mm. In contrast, the runoff from SWAT has a steep increase during the first three days of stage II and then remains stable, with the runoff increasing to 27.47 mm at the end of the stage.

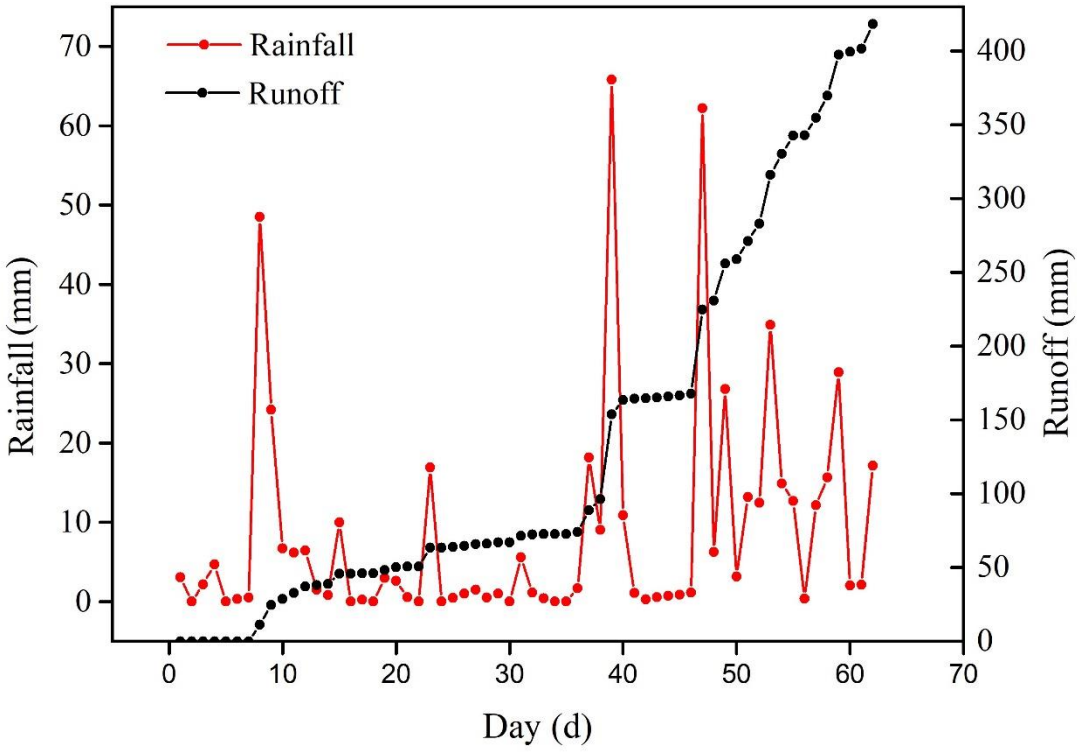

Figure 4. 12 Rainfall-runoff simulated by TELEMAC-2D.

Figure 4. 13 provides an overview of the runoffs generated by SWAT and TELEMAC with the rainfall amount. From day 1 to day 46 (July 1 to August 15), the average rainfall amounted to 5.65 mm; however, this area had a rainfall of 12.69 mm on average from day 48 to day 62 (August 16 to August 31). In terms of the relationship between rainfall and runoff, it is noticeable that the runoff during stage I in both models is close to 0, and this is because the soil was dry after the dry season. Hence, the infiltration rate is significantly higher than the precipitation rate. In addition, as shown in Figure 4. 12, intense rainfall is always followed by a sharp increase in the runoff.

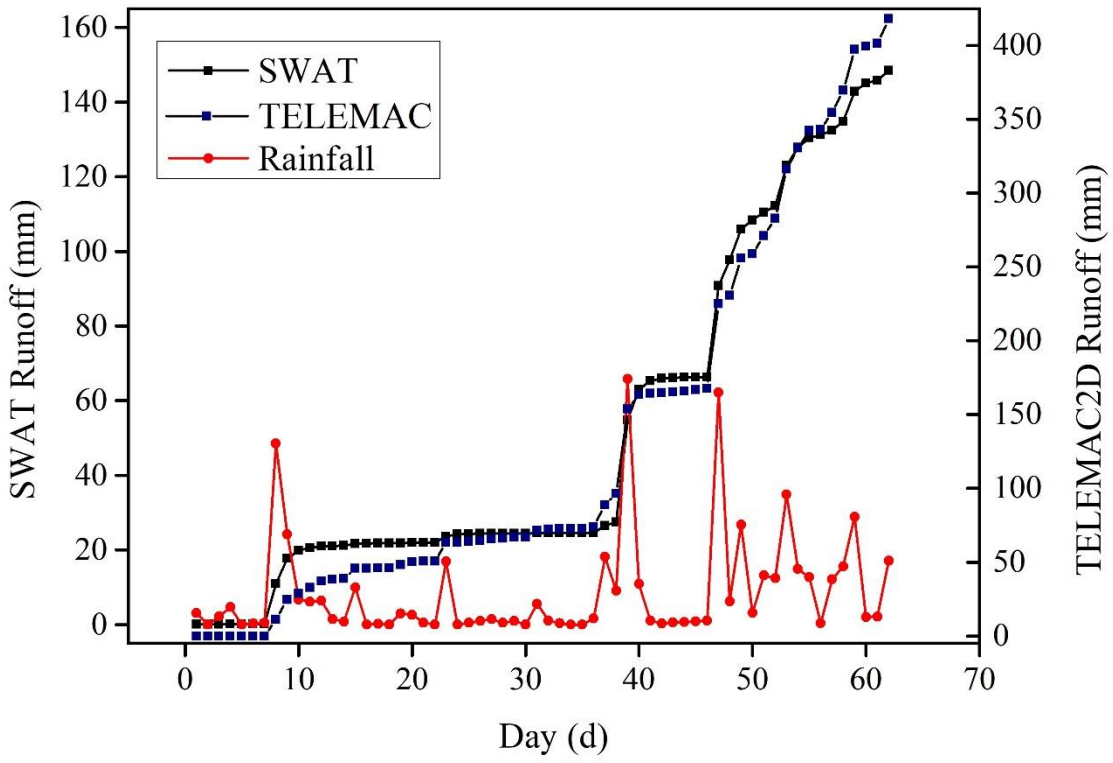

Figure 4. 13 Rainfall-runoff comparison between SWAT and TELEMAC-2D.

According to the SWAT outputs, the rainfall in Niamey was consumed by five major hydrologic phenomena: evaporation and transpiration took up 70.28%; plant uptake, soil moisture redistribution, and infiltration add up to 15.72% of the total rainfall ;14% was consumed by surface runoff.

Table 4. 7 Hydrology phenomena simulated by SWAT.

Hydrology Phenomena	Average Annual Amount (mm)	Percent to rainfall
Precipitation	641.6	100.00%
Evaporation and transpiration	450.9	70.28%
Infiltration		

Plant uptake Soil moisture redistribution	100.83	15.72%
Surface runoff	89.87	14.00%

A probable explanation for the difference in the runoff magnitudes between the two models is that infiltration is the sole factor considered for the hydrologic process in TELEMAC-2D. Therefore, in areas with intense evaporation, the runoff will be significantly overestimated as the evaporation rate substantially impacts runoff. As such, it is suggested that the improvement of TELEMAC-2D should start by considering a complete hydrological cycle. a hydrologic model such as SWAT can be used to estimate net rainfall in area with significant evaporation, which can provide data for TELEMAC-2D to simulate runoff and other variables more accurately during a flood event.

Flow rate is often used to validate the simulated flow rates with different models. A line perpendicular to the direction of the flow is drawn on the mesh, and the scalar flow along the line is integrated for the calculation of flow rate, as shown in Figure 4. 14.

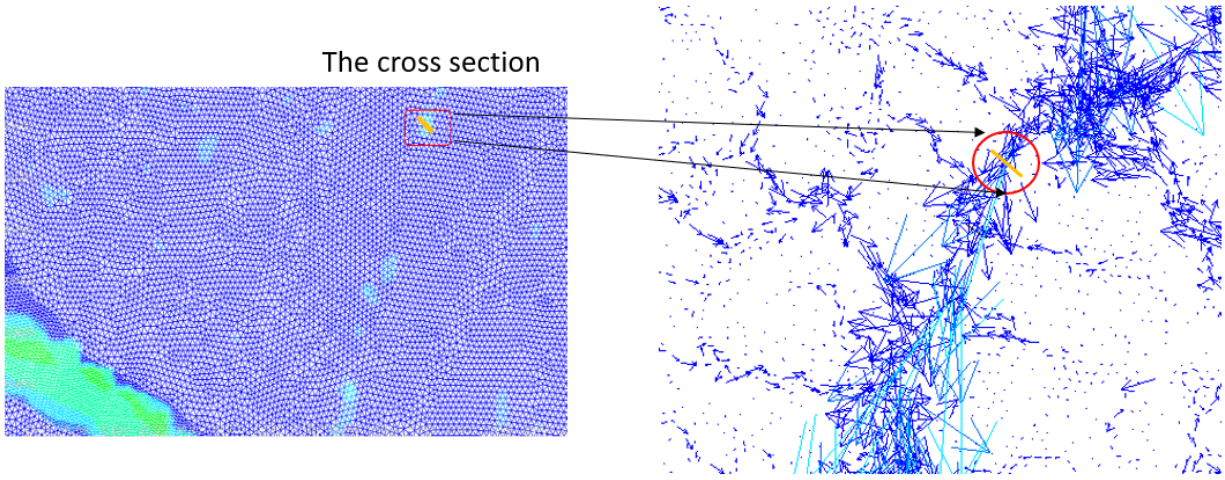

Figure 4. 14 The cross-section location in TELEMAC-2D

Unlike TALEMAC-2D, SWAT model can read flow rate directly from reach files. This project compares measured flow rates on July 22nd and August 8th, as shown in Figure 4. 15. In this figure, the SWAT simulated inflow on August 19 aligns closely to the measured inflow, while the flow simulated by TELEMAC-2D doesn't match either of the measured flows on July 19 or August 9.

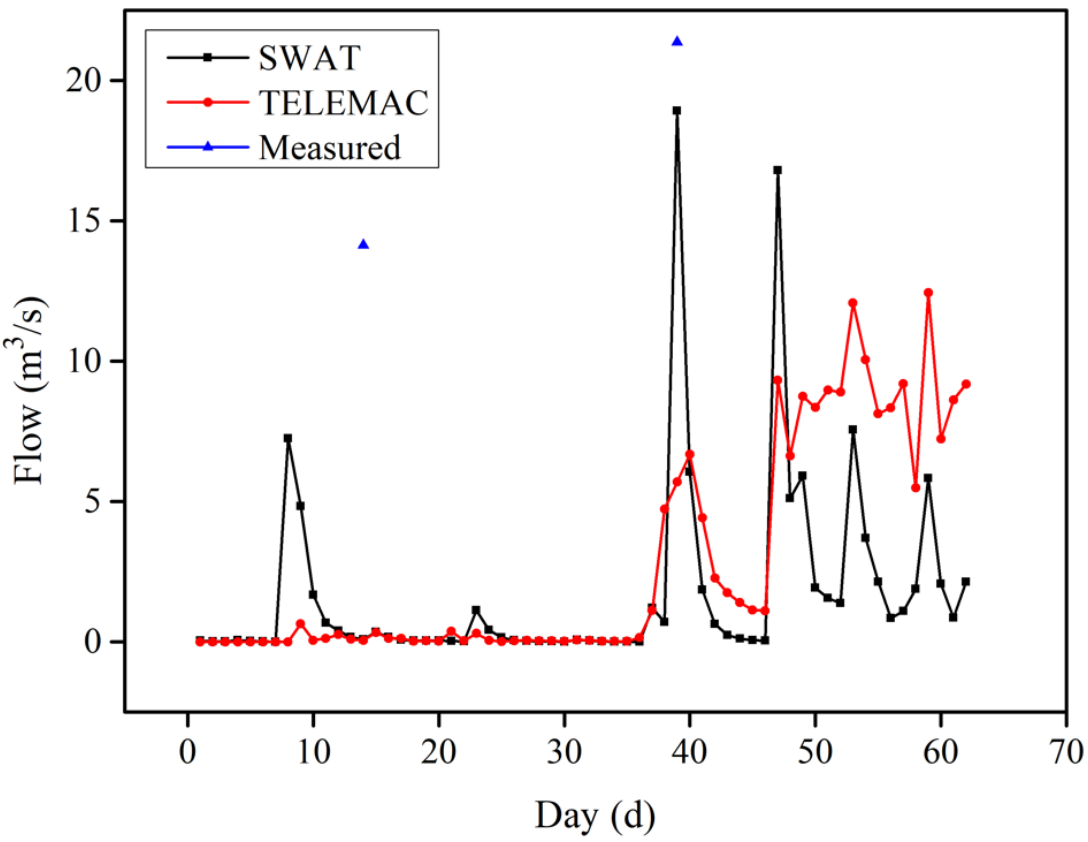

Figure 4. 15 Comparison between measured flow and simulated flow.

By comparing the rainfall hyetograph with the flow time series, the flow rates by both models are found to correlate with the magnitude of the precipitation – the flow rates rise immediately as the precipitation increases. However, it is noticeable that the flow rate simulated by TELEMAC

2D is lower than SWAT simulated inflow from July 1 to August 18. One of the possible reasons is that the tributary on which the monitoring point is located is defined as a depression instead of a channel mesh. While the precipitation accumulates and the depression is filled, the inflow in TELEMAC appears to be higher than SWAT inflow, as evaporation is not considered in TELEMAC 2D simulation. The conclusion, however, requires further validation because the inflow measured on two days is relatively small sample size for calibration. Therefore, future research on the modification of TELEMAC 2D can focus on the improvement of infiltration routine through independent sensitivity analysis and validation with large sample size.

Some of the important features of TELEMAC 2D and SWAT and the differences between the two models for simulating rainfall-runoff during a flood event are listed in Table 4. 8 and described as below:

Table 4. 8 Comparison of TELEMAC-2D and SWAT in simulating rainfall-runoff.

Model	TELEMAC-2D	SWAT
Flow Routine	Finite Element Method	Hydraulic Equations
Computation	Slow	Fast
Simulation Length	Short	Long
Infiltration Method	SCS Method	SCS/ Green & Ampt Method
Minimum Time Step	Second	Day
Hydrologic Consideration	Incomplete	Complete
Antecedent Moisture Condition	CN1, CN2, CN3	CN1, CN2, CN3
Steep Slope Correction	Available	Not Available
Velocity & Water Depth	Available	Not Available

Simulation time: SWAT runs the simulation faster than TELEMAC 2D while it requires more time for model setup. To be specific, while it took SWAT two minutes to run a four-year simulation with a warming-up period of five years, it took TELEMAC-2D 15 days to run a two-month simulation. As a result, hydrologic models are more often used for forecasting a longer period.

Hydrological Condition: SWAT considers a complete hydrological cycle including precipitation, evaporation, infiltration, groundwater exchanging, while TELEMAC-2D takes only precipitation and infiltration into consideration in the infiltration subroutine. Consequently, reasonable results could be obtained from TELEMAC for short time simulations because during which the influence of evaporation on runoff could be neglected. However, runoffs will be overestimated by TELEMAC 2D for long time simulations where the influence of evaporation on runoff can not be ignored .

Fluid motion: one of the advantages of TELEMAC-2D in the simulation of the rainfall-runoff during a flood event is that TELEMAC-2D uses FE or FV to simulate flow movement. Detailed information about water depth and velocities in channel and floodplain can be obtained, which facilitates the analysis of flood inundation area and flood intensity. Conversely, SWAT uses simple hydraulic equations to simulate flows in channels, which makes SWAT inappropriate to model flood events.

Chapter 5 Conclusion and Future Work

5.1 Conclusion

This study developed a hydraulic model TELEMAC-2D and a hydrological model SWAT to simulate rainfall-runoff using the SCS Curve Number method in Niamey city. In the experiment, the infiltration subroutine recently developed for TELEMAC 2D is examined by comparing runoffs generated by TELEMAC 2D and SWAT for a period from July 1st to August 31st in 2019. While the runoffs generated by both models reflect the changes in precipitation promptly and show a similar trend, TELEMAC 2D overestimates the runoff for the infiltration subroutine is not considered in the simulation. Therefore, it is concluded that TELEMAC-2D's infiltration routine is inappropriate for the simulation of the runoff in areas where extensive evaporation exists. Two possible solutions to improve TELEMAC-2D are: 1) couple TELEMAC-2D with a hydrologic model and use net rainfall simulated by the hydrologic as the precipitation input for TELEMAC-2D. 2) build functions in the infiltration subroutine to calculate rainfall amount consumed by other hydrologic phenomena in addition to the infiltration process.

In general, this project is a preliminary study to test the infiltration routine of TELEMAC-2D in simulating rainfall-runoff, and further study on this topic is required.

5.2 Future Work

This project is a preliminary work in this field and future works are ongoing. The direction for further study on this topic can focus on the following area:

1) Calibration and validation: a large sample of flow is required to calibrate the simulated runoff results. Besides, satellite product such as UNU-INWEH's flood mapping tool is suggested for inundation area validation.
2) Input precipitation: instead of measured rainfall, net rainfall can be used to simulate runoff in areas with strong evaporation. Additionally, for studies on a larger watershed, space-distributed rainfall is preferred.
3) Mesh: sensitivity analysis experiments on mesh resolution should be considered in future work.
4) Drainage system: the drainage system should be considered for studies on areas where the drainage system is properly maintained.
5) DEM: high-resolution DEM can be used to capture more urban features.
6) Scenarios: due to lack of data, a single scenario was simulated in this project. Multiple scenarios simulation should be included in future work to complete the study.

Reference

Abaje, I., Ogoh, A., Amos, B., & Abashiya, M. (2015). Climate change, flood disaster assessment and human security in Katsina State, Nigeria. *American Journal of Human Ecology*, *4(4)*, 47-56.

Abbott, M. B., & Basco, D. R. (1989). *Computational fluid dynamics*. Longman Scientific & Technical New-York.

Abdessamed, D., & Abderrazak, B. (2019). Coupling HEC-RAS and HEC-HMS in rainfall–runoff modeling and evaluating floodplain inundation maps in arid environments: case study of Ain Sefra city, Ksour Mountain. SW of Algeria. *Environmental Earth Sciences*, *78*(19), 1-17.

Abily, M., Gourbesville, P., Andres, L., & Duluc, C.-m. (2013). Photogrammetric and LiDAR data for high resolution runoff modeling over industrial and urban sites. 2013 IAHR World Congress,

Al-Sabhan, W., Mulligan, M., & Blackburn, G. A. (2003). A real-time hydrological model for flood prediction using GIS and the WWW. *Computers, Environment and Urban Systems*, *27*(1), 9-32.

Alsdorf, D. E., Rodríguez, E., & Lettenmaier, D. P. (2007). Measuring surface water from space. *Reviews of Geophysics*, *45*(2).

Andreadis, K. M., & Schumann, G. J. (2014). Estimating the impact of satellite observations on the predictability of large-scale hydraulic models. *Advances in water resources*, *73*, 44-54.

Apel, H., Martínez Trepat, O., Hung, N. N., Chinh, D. T., Merz, B., & Dung, N. V. (2016). Combined fluvial and pluvial urban flood hazard analysis: concept development and

application to Can Tho city, Mekong Delta, Vietnam. *Natural Hazards and Earth System Sciences*, *16*(4), 941-961.

Arnold, J. G., Moriasi, D. N., Gassman, P. W., Abbaspour, K. C., White, M. J., Srinivasan, R., Santhi, C., Harmel, R., Van Griensven, A., & Van Liew, M. W. (2012). SWAT: Model use, calibration, and validation. *Transactions of the ASABE*, *55*(4), 1491-1508.

Axworthy, D. H., Ghidaoui, M. S., & McInnis, D. A. (2000). Extended thermodynamics derivation of energy dissipation in unsteady pipe flow. *Journal of Hydraulic Engineering*, *126*(4), 276-287.

Bates, P. D., Anderson, M. G., Baird, L., Walling, D. E., & Simm, D. (1992). Modeling floodplain flows using a two-dimensional finite element model. *Earth surface processes and landforms*, *17*(6), 575-588.

Bates, P. D., Dawson, R. J., Hall, J. W., Horritt, M. S., Nicholls, R. J., Wicks, J., & Hassan, M. A. A. M. (2005). Simplified two-dimensional numerical modeling of coastal flooding and example applications. *Coastal Engineering*, *52*(9), 793-810.

Bates, P. D., & De Roo, A. (2000). A simple raster-based model for flood inundation simulation. *Journal of hydrology*, *236*(1-2), 54-77.

Bates, P. D., Horritt, M. S., & Fewtrell, T. J. (2010). A simple inertial formulation of the shallow water equations for efficient two-dimensional flood inundation modeling. *Journal of hydrology*, *387*(1-2), 33-45.

Benito, G., & Hudson, P. F. (2010). Flood hazards: the context of fluvial geomorphology. *Geomorphological hazards and disaster prevention*, 111-128.

Bennett, B., Leonard, M., Deng, Y., & Westra, S. (2018). An empirical investigation into the effect of antecedent precipitation on flood volume. *Journal of hydrology*, *567*, 435-445.

Bernhofen, M. V., Whyman, C., Trigg, M. A., Sleigh, P. A., Smith, A. M., Sampson, C. C., Yamazaki, D., Ward, P. J., Rudari, R., & Pappenberger, F. (2018). A first collective validation of global fluvial flood models for major floods in Nigeria and Mozambique. *Environmental Research Letters*, *13*(10), 104007.

Betsholtz, A., & Nordlöf, B. (2017). Potentials and limitations of 1D, 2D and coupled 1D-2D flood modeling in HEC-RAS. *TVVR17/5003*.

Beven, K. J. (2011). *Rainfall-runoff modeling: the primer*. John Wiley & Sons.

Bingner, R. (1996). Runoff simulated from Goodwin Creek watershed using SWAT. *Transactions of the ASAE*, *39*(1), 85-90.

Bohorquez, P., & Darby, S. (2008). The use of one-and two-dimensional hydraulic modeling to reconstruct a glacial outburst flood in a steep Alpine valley. *Journal of hydrology*, *361*(3-4), 240-261.

Bomers, A., Schielen, R. M. J., & Hulscher, S. J. (2019). The influence of grid shape and grid size on hydraulic river modeling performance. *Environmental Fluid Mechanics*, *19*(5), 1273-1294.

Boughton, W. (1989). A review of the USDA SCS curve number method. *Soil Research*, *27*(3), 511-523.

Bradbrook, K., Lane, S., Waller, S., & Bates, P. (2004). Two dimensional diffusion wave modeling of flood inundation using a simplified channel representation. *International Journal of River Basin Management*, *2*(3), 211-223.

Bruwier, M., Maravat, C., Mustafa, A., Teller, J., Pirotton, M., Erpicum, S., Archambeau, P., & Dewals, B. (2020). Influence of urban forms on surface flow in urban pluvial flooding. *Journal of hydrology*, *582*, 124493.

Büchele, B., Kreibich, H., Kron, A., Thieken, A., Ihringer, J., Oberle, P., Merz, B., & Nestmann, F. (2006). Flood-risk mapping: contributions towards an enhanced assessment of extreme events and associated risks. *Natural Hazards and Earth System Sciences*, *6*(4), 485-503.

Bulti, D. T., & Abebe, B. G. (2020). A review of flood modeling methods for urban pluvial flood application. *Modeling earth systems and environment*, *6*(3), 1293-1302.

Carr, R. S., & Smith, G. P. (2007). Linking of 2D and Pipe hydraulic models at fine spatial scales. *Water Practice and Technology*, *2*(2).

Carter, V. (1996). "Wetland Hydrology, Water Quality." *National water summary on wetland resources* 2425, 35.

Castro Gama, M., Popescu, I., Mynett, A., Shengyang, L., & Van Dam, A. (2013). Modeling extreme flood hazard events on the middle Yellow River using DFLOW-flexible mesh approach. *Natural Hazards and Earth System Sciences Discussions*, *1*(6), 6061-6092.

Castro, M. J., Ortega, S., De la Asuncion, M., Mantas, J. M., & Gallardo, J. M. (2011). GPU computing for shallow water flow simulation based on finite volume schemes. *Comptes Rendus Mécanique*, *339*(2-3), 165-184.

Caviedes-Voullième, D., Fernández-Pato, J., & Hinz, C. (2020). Performance assessment of 2D Zero-Inertia and Shallow Water models for simulating rainfall-runoff processes. *Journal of hydrology*, *584*, 124663.

Chau, K. W., Wu, C., & Li, Y. S. (2005). Comparison of several flood forecasting models in Yangtze River. *Journal of Hydrologic Engineering*, *10*(6), 485-491.

Chen, A., Hsu, M., Chen, T., & Chang, T. (2005). An integrated inundation model for highly developed urban areas. *Water Science and Technology*, *51*(2), 221-229.

Chen, A. S., Djordjevic, S., Leandro, J., & Savic, D. (2007). The urban inundation model with bidirectional flow interaction between 2D overland surface and 1D sewer networks. *NOVATECH 2007*.

Choo, K.-S., Kang, D.-H., & Kim, B.-S. (2020). Impact Assessment of Urban Flood on Traffic Disruption using Rainfall–Depth–Vehicle Speed Relationship. *Water*, *12*(4), 926.

Cloke, H., & Pappenberger, F. (2009). Ensemble flood forecasting: A review. *Journal of hydrology*, *375*(3-4), 613-626.

Cook, A., & Merwade, V. (2009). Effect of topographic data, geometric configuration and modeling approach on flood inundation mapping. *Journal of hydrology*, *377*(1-2), 131-142.

Costabile, P., Costanzo, C., Ferraro, D., Macchione, F., & Petaccia, G. (2020). Performances of the new HEC-RAS version 5 for 2-D hydrodynamic-based rainfall-runoff simulations at basin scale: Comparison with a state-of-the art model. *Water*, *12*(9), 2326.

Costabile, P., Macchione, F., Natale, L., & Petaccia, G. (2015). Flood mapping using LIDAR DEM. Limitations of the 1-D modeling highlighted by the 2-D approach. *Natural Hazards, 77(1)*, 181-204.

da Costa, R. T., Manfreda, S., Luzzi, V., Samela, C., Mazzoli, P., Castellarin, A., & Bagli, S. (2019). A web application for hydrogeomorphic flood hazard mapping. *Environmental Modeling & Software*, *118*, 172-186.

de Almeida, G. A., Bates, P., & Ozdemir, H. (2018). Modeling urban floods at submetre resolution: challenges or opportunities for flood risk management? *Journal of Flood Risk Management*, *11*, S855-S865.

Demeritt, D., Cloke, H., Pappenberger, F., Thielen, J., Bartholmes, J., & Ramos, M.-H. (2007). Ensemble predictions and perceptions of risk, uncertainty, and error in flood forecasting. *Environmental Hazards*, *7*(2), 115-127.

Demeritt, D., Nobert, S., Cloke, H., & Pappenberger, F. (2010). Challenges in communicating and using ensembles in operational flood forecasting. *Meteorological applications*, *17*(2), 209-222.

Deng, Z., Zhang, X., Li, D., & Pan, G. (2015). Simulation of land use/land cover change and its effects on the hydrological characteristics of the upper reaches of the Hanjiang Basin. *Environmental Earth Sciences*, *73*(3), 1119-1132.

Dessu, S. B., & Melesse, A. M. (2012). Modeling the rainfall–runoff process of the Mara River basin using the Soil and Water Assessment Tool. *Hydrological Processes*, *26*(26), 4038-4049.

Di Baldassarre, G., Schumann, G., & Bates, P. (2009). Near real time satellite imagery to support and verify timely flood modeling. *Hydrological Processes: An International Journal*, *23*(5), 799-803.

Di Baldassarre, G., Schumann, G., Bates, P. D., Freer, J. E., & Beven, K. J. (2010). Flood-plain mapping: a critical discussion of deterministic and probabilistic approaches. *Hydrological Sciences Journal–Journal des Sciences Hydrologiques*, *55*(3), 364-376.

Dimitriadis, P., Tegos, A., Oikonomou, A., Pagana, V., Koukouvinos, A., Mamassis, N., Koutsoyiannis, D., & Efstratiadis, A. (2016). Comparative evaluation of 1D and quasi-2D hydraulic models based on benchmark and real-world applications for uncertainty assessment in flood mapping. *Journal of hydrology*, *534*, 478-492.

Djordjević, S., Ivetić, M., Maksimović, C., & Rajcević, A. (1991). An approach to the simulation of street flooding in the modeling of surcharged flow in storm sewers. *Proceedings: New Technologies in Urban Drainage*, 101-108.

Doocy, S., Daniels, A., Murray, S., & Kirsch, T. D. (2013). The human impact of floods: a historical review of events 1980-2009 and systematic literature review. *PLoS currents*, *5*.

Dottori, F., Di Baldassarre, G., & Todini, E. (2013). Detailed data is welcome, but with a pinch of salt: Accuracy, precision, and uncertainty in flood inundation modeling. *Water Resources Research*, *49*(9), 6079-6085.

Dottori, F., & Todini, E. (2013). Testing a simple 2D hydraulic model in an urban flood experiment. In: Wiley Online Library.

Douglas, I., Alam, K., Maghenda, M., Mcdonnell, Y., McLean, L., & Campbell, J. (2008). Unjust waters: climate change, flooding and the urban poor in Africa. *Environment and urbanization*, *20*(1), 187-205.

Easton, Z., Fuka, D., White, E., Collick, A., Biruk Ashagre, B., McCartney, M., Awulachew, S., Ahmed, A., & Steenhuis, T. (2010). A multi basin SWAT model analysis of runoff and sedimentation in the Blue Nile, Ethiopia. *Hydrology and Earth System Sciences*, *14*(10), 1827-1841.

Ekeu-wei, I. T. and G. A. Blackburn (2018). "Applications of open-access remotely sensed data for flood modelling and mapping in developing regions." *Hydrology 5*(3), 39.

Fereidoon, M., Koch, M., & Brocca, L. (2019). Predicting rainfall and runoff through satellite soil moisture data and SWAT modeling for a poorly gauged basin in Iran. *Water*, *11*(3), 594.

Fernández, D., & Lutz, M. (2010). Urban flood hazard zoning in Tucumán Province, Argentina, using GIS and multicriteria decision analysis. *Engineering Geology*, *111*(1-4), 90-98.

Forster, A., Costi, J., Marques, W. C., Wormsbecher, A. G., & Bendô, A. R. R. (2019). Application of the TELEMAC-2D Model in the fluvial hydrodinamics simulation and reproduction of flood patterns. Defect and Diffusion Forum.

Gaitan, S., van de Giesen, N., & Ten Veldhuis, J. (2016). Can urban pluvial flooding be predicted by open spatial data and weather data? *Environmental Modeling & Software*, *85*, 156-171.

García-Navarro, P., Murillo, J., Fernández-Pato, J., Echeverribar, I., & Morales-Hernández, M. (2019). The shallow water equations and their application to realistic cases. *Environmental Fluid Mechanics*, *19(5)*, 1235-1252.

Ghaffari, G., Keesstra, S., Ghodousi, J., & Ahmadi, H. (2010). SWAT-simulated hydrological impact of land-use change in the Zanjanrood basin, Northwest Iran. *Hydrological Processes: An International Journal*, *24*(7), 892-903.

Ghimire, B., Chen, A. S., Guidolin, M., Keedwell, E. C., Djordjević, S., & Savić, D. A. (2013). Formulation of a fast 2D urban pluvial flood model using a cellular automata approach. *Journal of Hydroinformatics*, *15*(3), 676-686.

Ghimire, E., Sharma, S., & Lamichhane, N. (2020). Evaluation of one-dimensional and two-dimensional HEC-RAS models to predict flood travel time and inundation area for flood warning system. *ISH Journal of Hydraulic Engineering*, 1-17.

Ghimire, S. (2013). Application of a 2D hydrodynamic model for assessing flood risk from extreme storm events. *Climate, 1*(3), 148-162.

Goonetilleke, A., & Jenkins, G. (1999). The role of geographical information systems in urban hydrological modeling. *Water and Environment Journal*, *13*(3), 200-206.

Grahn, T., & Nyberg, L. (2017). Assessment of pluvial flood exposure and vulnerability of residential areas. *International Journal of Disaster Risk Reduction*, *21*, 367-375.

Grimaldi, S., Petroselli, A., & Romano, N. (2013). Green-Ampt Curve-Number mixed procedure as an empirical tool for rainfall–runoff modeling in small and ungauged basins. *Hydrological Processes*, *27*(8), 1253-1264.

Hammond, M. J., Chen, A. S., Djordjević, S., Butler, D., & Mark, O. (2015). Urban flood impact assessment: A state-of-the-art review. *Urban Water Journal*, *12*(1), 14-29.

Haque, M. M., Seidou, O., Mohammadian, A., & Djibo, A. G. (2020). Development of a time-varying MODIS/2D hydrodynamic model relationship between water levels and flooded areas in the Inner Niger Delta, Mali, West Africa. *Journal of Hydrology: Regional Studies*, *30*, 100703.

Hervouet, J.-M. (1999). TELEMAC, a hydroinformatic system. *La houille blanche*(3-4), 21-28.

Hoch, J. M., van Beek, R., Winsemius, H. C., & Bierkens, M. F. (2018). Benchmarking flexible meshes and regular grids for large-scale fluvial inundation modeling. *Advances in water resources*, *121*, 350-360.

Hochrainer-Stigler, S., Mochizuki, J., & Pflug, G. (2016). Impacts of global and climate change uncertainties for disaster risk projections: A case study on rainfall-induced flood risk in Bangladesh. *Journal of Extreme Events*, *3*(01), 1650004.

Hofmann, J., & Schüttrumpf, H. (2020). Risk-Based and Hydrodynamic Pluvial Flood Forecasts in Real Time. *Water*, *12*(7), 1895.

Horritt, M., & Bates, P. (2002). Evaluation of 1D and 2D numerical models for predicting river flood inundation. *Journal of hydrology*, *268*(1-4), 87-99.

Houston, D., Werrity, A., Bassett, D., Geddes, A., Hoolachan, A., & McMillan, M. (2011). Pluvial (rain-related) flooding in urban areas: the invisible hazard.

Hsie, C. H. (1974). *EXPERIMENTAL AND ANALYTICAL EVALUATION OF HYDRODYNAMIC RUNOFF MODELS*. University of Illinois at Urbana-Champaign.

Huang, Q., Wang, J., Li, M., Fei, M., & Dong, J. (2017). Modeling the influence of urbanization on urban pluvial flooding: a scenario-based case study in Shanghai, China. *Natural Hazards*, *87*(2), 1035-1055.

Hunter, N. M., Bates, P. D., Horritt, M. S., & Wilson, M. D. (2007). Simple spatially-distributed models for predicting flood inundation: A review. *Geomorphology*, *90*(3-4), 208-225.

Huţanu, E., Mihu-Pintilie, A., Urzica, A., Paveluc, L. E., Stoleriu, C. C., & Grozavu, A. (2020). Using 1D HEC-RAS modeling and LiDAR data to improve flood hazard maps' accuracy: a case study from Jijia floodplain (NE Romania). *Water*, *12*(6), 1624.

Jamali, B., Bach, P. M., Cunningham, L., & Deletic, A. (2019). A Cellular Automata fast flood evaluation (CA-ffé) model. *Water Resources Research*, *55*(6), 4936-4953.

Jeong, J., Kannan, N., Arnold, J., Glick, R., Gosselink, L., & Srinivasan, R. (2010). Development and integration of sub-hourly rainfall–runoff modeling capability within a watershed model. *Water Resources Management*, *24*(15), 4505-4527.

Jha, A. K., Bloch, R., & Lamond, J. (2012). *Cities and flooding: a guide to integrated urban flood risk management for the 21st century*. The World Bank.

Kadir, M. A. A., Abustan, I., & Razak, M. F. A. (2019). 2D Flood inundation simulation based on a large scale physical model using course numerical grid method. *Int. J. Geomat*, *17*, 230-236.

Kalyanapu, A. J., Shankar, S., Pardyjak, E. R., Judi, D. R., & Burian, S. J. (2011). Assessment of GPU computational enhancement to a 2D flood model. *Environmental Modeling & Software*, *26*(8), 1009-1016.

Kazama, S., Sato, A., & Kawagoe, S. (2010). Evaluating the cost of flood damage based on changes in extreme rainfall in Japan. In *Adaptation and mitigation strategies for climate change* (pp. 3-17). Springer.

Kheradmand, S., Seidou, O., Konte, D., & Batoure, M. B. B. (2018). Evaluation of adaptation options to flood risk in a probabilistic framework. *Journal of Hydrology: Regional Studies*, *19*, 1-16.

Kim, B., Sanders, B. F., Schubert, J. E., & Famiglietti, J. S. (2014). Mesh type tradeoffs in 2D hydrodynamic modeling of flooding with a Godunov-based flow solver. *Advances in water resources*, *68*, 42-61.

King, K. W., Arnold, J., & Bingner, R. (1999). Comparison of Green-Ampt and curve number methods on Goodwin Creek watershed using SWAT. *Transactions of the ASAE*, *42*(4), 919.

Kourgialas, N. N., & Karatzas, G. P. (2011). Flood management and a GIS modeling method to assess flood-hazard areas—a case study. *Hydrological Sciences Journal–Journal des Sciences Hydrologiques*, *56*(2), 212-225.

Kron, W. (2005). Flood risk= hazard• values• vulnerability. *Water international*, *30*(1), 58-68.

Lacasta, A., Morales-Hernández, M., Murillo, J., & García-Navarro, P. (2015). GPU implementation of the 2D shallow water equations for the simulation of rainfall/runoff events. *Environmental Earth Sciences*, *74*(11), 7295-7305.

Leandro, J., Djordjević, S., Chen, A., Savić, D., & Stanić, M. (2011). Calibration of a 1D/1D urban flood model using 1D/2D model results in the absence of field data. *Water Science and Technology*, *64*(5), 1016-1024.

Li, Z., Liu, J., Mei, C., Shao, W., Wang, H., & Yan, D. (2019). Comparative Analysis of Building Representations in TELEMAC-2D for Flood Inundation in Idealized Urban Districts. *Water*, *11*(9), 1840.

Ligier, P.-L. (2016). Implementation of a rainfall-runoff model in TELEMAC-2D. Proceedings of the XXIIIrd TELEMAC-MASCARET User Conference 2016, 11 to 13 October 2016, Paris, France,

Lin, B., Chen, X., Yao, H., Chen, Y., Liu, M., Gao, L., & James, A. (2015). Analyses of landuse change impacts on catchment runoff using different time indicators based on SWAT model. *Ecological Indicators*, *58*, 55-63.

Liu, J., Li, Z., Mei, C., Wang, K., & Zhou, G. (2019). Urban flood analysis for different design storm hyetographs in Xiamen Island based on TELEMAC-2D. *Chinese Science Bulletin*, *64*(19), 2055-2066.

Loi, N. K., Liem, N. D., Tu, L. H., Hong, N. T., Truong, C. D., Tram, V. N. Q., Nhat, T. T., Anh, T. N., & Jeong, J. (2019). Automated procedure of real-time flood forecasting in Vu Gia–Thu Bon river basin, Vietnam by integrating SWAT and HEC-RAS models. *Journal of Water and Climate Change*, *10*(3), 535-545.

Löwe, R., Urich, C., Domingo, N. S., Mark, O., Deletic, A., & Arnbjerg-Nielsen, K. (2017). Assessment of urban pluvial flood risk and efficiency of adaptation options through simulations–A new generation of urban planning tools. *Journal of hydrology*, *550*, 355-367.

Ma, Q., Abily, M., Vo, N., & Gourbesville, P. (2015). High Resolution Rainfall-Runoff Simulation in Urban Area: Assessment of Telemac-2D and Fullswof-2D. E-proceedings of the 36th IAHR World Congress,

Maksimović, Č., Prodanović, D., Boonya-Aroonnet, S., Leitão, J. P., Djordjević, S., & Allitt, R. (2009). Overland flow and pathway analysis for modeling of urban pluvial flooding. *Journal of Hydraulic Research*, *47*(4), 512-523.

Manfreda, S., Sole, A., & Fiorentino, M. (2008). Can the basin morphology alone provide an insight into floodplain delineation? *WIT Transactions on Ecology and the Environment*, *118*, 47-56.

Marin-Perez, R., García-Pintado, J., & Gómez, A. S. (2012). A real-time measurement system for long-life flood monitoring and warning applications. *Sensors*, *12*(4), 4213-4236.

Mark, O., Weesakul, S., Apirumanekul, C., Aroonnet, S. B., & Djordjević, S. (2004). Potential and limitations of 1D modeling of urban flooding. *Journal of hydrology*, *299*(3-4), 284-299.

Massazza, G., et al. (2021). "Recent Changes in Hydroclimatic Patterns over Medium Niger River Basins at the Origin of the 2020 Flood in Niamey (Niger)." *Water 13*(12), 1659.

Medeiros, S. C., & Hagen, S. C. (2013). Review of wetting and drying algorithms for numerical tidal flow models. *International journal for numerical methods in fluids*, *71(4)*, 473-487.

Meng, X., Zhang, M., Wen, J., Du, S., Xu, H., Wang, L., & Yang, Y. (2019). A simple GIS-based model for urban rainstorm inundation simulation. *Sustainability*, *11*(10), 2830.

Mens, M. (2008). Frameworks for flood event management. *T19-07-03*.

Merkuryeva, G., Merkuryev, Y., Sokolov, B. V., Potryasaev, S., Zelentsov, V. A., & Lektauers, A. (2015). Advanced river flood monitoring, modeling and forecasting. *Journal of computational science*, *10*, 77-85.

Merz, R., & Blöschl, G. (2009). A regional analysis of event runoff coefficients with respect to climate and catchment characteristics in Austria. *Water Resources Research*, *45*(1).

Ming, X., Liang, Q., Xia, X., Li, D., & Fowler, H. J. (2020). Real-time flood forecasting based on a high-performance 2-D hydrodynamic model and numerical weather predictions. *Water Resources Research*, *56*(7), e2019WR025583.

Nandi, A., Mandal, A., Wilson, M., & Smith, D. (2016). Flood hazard mapping in Jamaica using principal component analysis and logistic regression. *Environmental Earth Sciences*, *75*(6), 465.

Ndomba, P., Mtalo, F., & Killingtveit, A. (2008). SWAT model application in a data scarce tropical complex catchment in Tanzania. *Physics and Chemistry of the Earth, Parts A/B/C*, *33*(8-13), 626-632.

Neal, J. C., Fewtrell, T. J., Bates, P. D., & Wright, N. G. (2010). A comparison of three parallelisation methods for 2D flood inundation models. *Environmental Modeling & Software*, *25*(4), 398-411.

Pappenberger, F., Beven, K. J., Ratto, M., & Matgen, P. (2008). Multi-method global sensitivity analysis of flood inundation models. *Advances in water resources*, *31*(1), 1-14.

Pau, J. C., & Sanders, B. F. (2006). Performance of parallel implementations of an explicit finite-volume shallow-water model. *Journal of Computing in Civil Engineering*, *20*(2), 99-110.

Pauleit, S., & Duhme, F. (2000). Assessing the environmental performance of land cover types for urban planning. *Landscape and urban planning*, *52*(1), 1-20.

Pilotti, M., Milanesi, L., Bacchi, V., Tomirotti, M., & Maranzoni, A. (2020). Dam-Break Wave propagation in alpine valley with HEC-RAS 2D: Experimental cancano test case. *Journal of Hydraulic Engineering*, *146*(6), 05020003.

Pina, R. D., Ochoa-Rodriguez, S., Simões, N. E., Mijic, A., Marques, A. S., & Maksimović, Č. (2016). Semi-vs. fully-distributed urban stormwater models: model set up and comparison with two real case studies. *Water*, *8*(2), 58.

Ponce, V. M., & Hawkins, R. H. (1996). Runoff curve number: Has it reached maturity? *Journal of Hydrologic Engineering*, *1*(1), 11-19.

Pradhan-Salike, I. and J. R. Pokharel (2017). "Impact of urbanization and climate change on urban flooding: A case of the Kathmandu Valley." *Journal of natural resources and development*, *7*, 56-66.

Pramanik, N., Panda, R. K., & Sen, D. (2010). One dimensional hydrodynamic modeling of river flow using DEM extracted river cross-sections. *Water Resources Management*, *24*(5), 835-852.

Rallison, R. E., & Miller, N. (1982). Past, present, and future SCS runoff procedure. Rainfall-runoff relationship/proceedings, International Symposium on Rainfall-Runoff Modeling held May 18-21, 1981 at Mississippi State University, Mississippi State, Mississippi, USA/edited by VP Singh,

Rawat, J., & Kumar, M. (2015). Monitoring land use/cover change using remote sensing and GIS techniques: A case study of Hawalbagh block, district Almora, Uttarakhand, India. *The Egyptian Journal of Remote Sensing and Space Science*, *18*(1), 77-84.

Rehman, S., Sahana, M., Hong, H., Sajjad, H., & Ahmed, B. B. (2019). A systematic review on approaches and methods used for flood vulnerability assessment: framework for future research. *Natural Hazards*, *96*(2), 975-998.

Revilla-Romero, B., Hirpa, F. A., Pozo, J. T.-d., Salamon, P., Brakenridge, R., Pappenberger, F., & De Groeve, T. (2015). On the use of global flood forecasts and satellite-derived inundation maps for flood monitoring in data-sparse regions. *Remote Sensing*, *7*(11), 15702-15728.

Rizeei, H. M., Pradhan, B., & Saharkhiz, M. A. (2018). Surface runoff prediction regarding LULC and climate dynamics using coupled LTM, optimized ARIMA, and GIS-based SCS-CN models in tropical region. *Arabian Journal of Geosciences*, *11*(3), 1-16.

Robins, P., & Davies, A. (2011). Application of TELEMAC-2D and SISYPHE to complex estuarine regions to inform future management decisions. *Proceedings of the XVIIIth Telemac & Mascaret User Club 2011, 19-21 October 2011, EDF R&D, Chatou*, 86-91.

Romali, N. S., Yusop, Z., & Ismail, A. Z. (2018). Application of HEC-RAS and Arc GIS for floodplain mapping in Segamat town, Malaysia. *International Journal*, *14*(43), 125-131.

Rosenzweig, B., Herreros Cantis, P., Kim, Y., Cohn, A., Grove, K., Brock, J., Yesuf, J., Mistry, P., Welty, C., & McPhearson, T. (2021). The value of urban flood modeling. *Earth's Future*, *9*(1), e2020EF001739.

Rosenzweig, B. R., McPhillips, L., Chang, H., Cheng, C., Welty, C., Matsler, M., Iwaniec, D., & Davidson, C. I. (2018). Pluvial flood risk and opportunities for resilience. *Wiley Interdisciplinary Reviews: Water*, *5*(6), e1302.

Rostamian, R., Jaleh, A., Afyuni, M., Mousavi, S. F., Heidarpour, M., Jalalian, A., & Abbaspour, K. C. (2008). Application of a SWAT model for estimating runoff and sediment in two mountainous basins in central Iran. *Hydrological Sciences Journal*, *53*(5), 977-988.

Rozalis, S., Morin, E., Yair, Y., & Price, C. (2010). Flash flood prediction using an uncalibrated hydrological model and radar rainfall data in a Mediterranean watershed under changing hydrological conditions. *Journal of hydrology*, *394*(1-2), 245-255.

Salami, R. O., Von Meding, J. K., & Giggins, H. (2017). Vulnerability of human settlements to flood risk in the core area of Ibadan metropolis, Nigeria. *Jàmbá: Journal of Disaster Risk Studies*, *9*(1), 1-14.

Samadi, S., Tufford, D., & Carbone, G. (2017). Assessing Parameter Uncertainty of a Semi-Distributed Hydrology Model for a Shallow Aquifer Dominated Environmental System. *JAWRA Journal of the American Water Resources Association*, *53*(6), 1368-1389.

Samuels, P. (1990). Cross section location in one-dimensional models. International Conference on river flood hydraulics,

Sanders, B. F., Schubert, J. E., & Detwiler, R. L. (2010). ParBreZo: A parallel, unstructured grid, Godunov-type, shallow-water code for high-resolution flood inundation modeling at the regional scale. *Advances in water resources*, *33*(12), 1456-1467.

Santoro, V., Crimì, A., & Pezzinga, G. (2018). Developments and limits of discrete vapor cavity models of transient cavitating pipe flow: 1D and 2D flow numerical analysis. *Journal of Hydraulic Engineering*, *144*(8), 04018047.

Sanyal, J., & Lu, X. X. (2006). GIS-based flood hazard mapping at different administrative scales: A case study in Gangetic West Bengal, India. *Singapore Journal of Tropical Geography*, *27*(2), 207-220.

Sayama, T., Ozawa, G., Kawakami, T., Nabesaka, S., & Fukami, K. (2012). Rainfall–runoff–inundation analysis of the 2010 Pakistan flood in the Kabul River basin. *Hydrological Sciences Journal*, *57*(2), 298-312.

Schumann, G., Bates, P. D., Horritt, M. S., Matgen, P., & Pappenberger, F. (2009). Progress in integration of remote sensing–derived flood extent and stage data and hydraulic models. *Reviews of Geophysics*, *47*(4).

Seyoum, S. D., Vojinovic, Z., Price, R. K., & Weesakul, S. (2012). Coupled 1D and noninertia 2D flood inundation model for simulation of urban flooding. *Journal of Hydraulic Engineering*, *138*(1), 23-34.

Shustikova, I., Domeneghetti, A., Neal, J. C., Bates, P., & Castellarin, A. (2019). Comparing 2D capabilities of HEC-RAS and LISFLOOD-FP on complex topography. *Hydrological Sciences Journal*, *64*(14), 1769-1782.

Sitterson, J., Knightes, C., Parmar, R., Wolfe, K., Avant, B., & Muche, M. (2018). An overview of rainfall-runoff model types.

Smith, L. C. (1997). Satellite remote sensing of river inundation area, stage, and discharge: A review. *Hydrological Processes*, *11*(10), 1427-1439.

Soares-Frazão, S., Lhomme, J., Guinot, V., & Zech, Y. (2008). Two-dimensional shallow-water model with porosity for urban flood modeling. *Journal of Hydraulic Research*, *46*(1), 45-64.

Sörensen, J., & Mobini, S. (2017). Pluvial, urban flood mechanisms and characteristics–assessment based on insurance claims. *Journal of hydrology*, *555*, 51-67.

Stoesser, T., Wilson, C., Bates, P., & Dittrich, A. (2003). Application of a 3D numerical model to a river with vegetated floodplains. *Journal of Hydroinformatics*, *5*(2), 99-112.

Tan, W.-Y. (1992). *Shallow water hydrodynamics: Mathematical theory and numerical solution for a two-dimensional system of shallow-water equations*. Elsevier.

Tarhule, A. (2005). Damaging rainfall and flooding: the other Sahel hazards. *Climatic change*, *72*(3), 355-377.

Tariq, M. A. U. R., & Van De Giesen, N. (2012). Floods and flood management in Pakistan. *Physics and Chemistry of the Earth, Parts A/B/C*, *47*, 11-20.

Tayefi, V., Lane, S., Hardy, R., & Yu, D. (2007). A comparison of one-and two-dimensional approaches to modeling flood inundation over complex upland floodplains. *Hydrological Processes: An International Journal*, *21*(23), 3190-3202.

Teng, J., Jakeman, A. J., Vaze, J., Croke, B. F., Dutta, D., & Kim, S. (2017). Flood inundation modeling: A review of methods, recent advances and uncertainty analysis. *Environmental Modeling & Software*, *90*, 201-216.

Termeh, S. V. R., Kornejady, A., Pourghasemi, H. R., & Keesstra, S. (2018). Flood susceptibility mapping using novel ensembles of adaptive neuro fuzzy inference system and metaheuristic algorithms. *Science of the Total Environment*, *615*, 438-451.

Testa, G., Zuccalà, D., Alcrudo, F., Mulet, J., & Soares-Frazão, S. (2007). Flash flood flow experiment in a simplified urban district. *Journal of Hydraulic Research*, *45*(sup1), 37-44.

Tiepolo, M. and S. Braccio (2018). " Flood Risk Preliminary Mapping in Niamey, Niger."

Tingsanchali, T. (2012). Urban flood disaster management. Procedia engineering, 32, 25-37.

Tramblay, Y., Bouvier, C., Ayral, P.-A., & Marchandise, A. (2011). Impact of rainfall spatial distribution on rainfall-runoff modeling efficiency and initial soil moisture conditions estimation. *Natural Hazards and Earth System Sciences*, *11*(1), 157-170.

Tramblay, Y., Bouvier, C., Martin, C., Didon-Lescot, J.-F., Todorovik, D., & Domergue, J.-M. (2010). Assessment of initial soil moisture conditions for event-based rainfall–runoff modeling. *Journal of hydrology*, *387*(3-4), 176-187.

Tsakiris, G., & Bellos, V. (2014). A numerical model for two-dimensional flood routing in complex terrains. *Water Resources Management*, *28*(5), 1277-1291.

Tsubaki, R., & Fujita, I. (2010). Unstructured grid generation using LiDAR data for urban flood inundation modeling. *Hydrological Processes: An International Journal*, *24*(11), 1404-1420.

UNISDR, C. (2015). "The human cost of natural disasters: A global perspective."

van Dijk, E., van der Meulen, J., Kluck, J., & Straatman, J. (2014). Comparing modeling techniques for analysing urban pluvial flooding. *Water Science and Technology*, *69*(2), 305-311.

Vaze, J., Jordan, P., Beecham, R., Frost, A., & Summerell, G. (2011). Guidelines for rainfall-runoff modeling: towards best practice model application.

Vojinovic, Z. (2015). *Flood Risk: The Holistic Perspective*. IWA Publishing.

Vojinovic, Z., & Tutulic, D. (2009). On the use of 1D and coupled 1D-2D modeling approaches for assessment of flood damage in urban areas. *Urban Water Journal*, *6*(3), 183-199.

Vu, M., Raghavan, S. V., & Liong, S. Y. (2012). SWAT use of gridded observations for simulating runoff–a Vietnam river basin study. *Hydrology and Earth System Sciences*, *16*(8), 2801-2811.

Vu, T. T., Nguyen, P. K., Chua, L. H., & Law, A. W. (2015). Two-dimensional hydrodynamic modeling of flood inundation for a part of the mekong river with telemac-2d. *British Journal of Environment and Climate Change*, *5*(2), 162-175.

Wallach, R., Grigorin, G., & Byk, J. R. (1997). The errors in surface runoff prediction by neglecting the relationship between infiltration rate and overland flow depth. *Journal of hydrology*, *200*(1-4), 243-259.

Winsemius, H. C., Aerts, J. C., Van Beek, L. P., Bierkens, M. F., Bouwman, A., Jongman, B., Kwadijk, J. C., Ligtvoet, W., Lucas, P. L., & Van Vuuren, D. P. (2016). Global drivers of future river flood risk. *Nature Climate Change*, *6*(4), 381-385.

Wong, C. (2015). A framework for 'City Prosperity Index': linking indicators, analysis and policy. *Habitat International*, *45*, 3-9.

Wu, C., & Chau, K. W. (2006). A flood forecasting neural network model with genetic algorithm. *International journal of environment and pollution*, *28*(3-4), 261-273.

Wu, W., Rodi, W., & Wenka, T. (2000). 3D numerical modeling of flow and sediment transport in open channels. *Journal of Hydraulic Engineering*, *126*(1), 4-15.

Xiao, Y., Yi, S., & Tang, Z. (2017). Integrated flood hazard assessment based on spatial ordered weighted averaging method considering spatial heterogeneity of risk preference. *Science of the Total Environment*, *599*, 1034-1046.

Xing, Y., Liang, Q., Wang, G., Ming, X., & Xia, X. (2019). City-scale hydrodynamic modeling of urban flash floods: the issues of scale and resolution. *Natural Hazards*, *96*(1), 473-496.

Xu, J., & Small, E. E. (2002). Simulating summertime rainfall variability in the North American monsoon region: The influence of convection and radiation parameterizations. *Journal of Geophysical Research: Atmospheres*, *107*(D23), ACL 22-21-ACL 22-17.

Yamazaki, D., O'Loughlin, F., Trigg, M. A., Miller, Z. F., Pavelsky, T. M., & Bates, P. D. (2014). Development of the global width database for large rivers. *Water Resources Research*, *50*(4), 3467-3480.

Yan, J., Jin, J., Chen, F., Yu, G., Yin, H., & Wang, W. (2018). Urban flash flood forecast using support vector machine and numerical simulation. *Journal of Hydroinformatics*, *20*(1), 221-231.

Yao, L., Wei, W., Yu, Y., Xiao, J., & Chen, L. (2018). Rainfall-runoff risk characteristics of urban function zones in Beijing using the SCS-CN model. *Journal of Geographical Sciences*, *28*(5), 656-668.

Ye, X., Zhang, Q., & Viney, N. (2011). The effect of soil data resolution on hydrological processes modeling in a large humid watershed. *Hydrological Processes*, *25*(1), 130-140.

Yin, J., Yu, D., Yin, Z., Liu, M., & He, Q. (2016). Evaluating the impact and risk of pluvial flash flood on intra-urban road network: A case study in the city center of Shanghai, China. *Journal of hydrology*, *537*, 138-145.

Yu, D. (2010). Parallelization of a two-dimensional flood inundation model based on domain decomposition. *Environmental Modeling & Software*, *25*(8), 935-945.

Yu, D., & Coulthard, T. J. (2015). Evaluating the importance of catchment hydrological parameters for urban surface water flood modeling using a simple hydro-inundation model. *Journal of hydrology*, *524*, 385-400.

Yu, D., & Lane, S. N. (2006). Urban fluvial flood modeling using a two-dimensional diffusion-wave treatment, part 1: mesh resolution effects. *Hydrological Processes: An International Journal*, *20*(7), 1541-1565.

Zakizadeh, H., Ahmadi, H., Zehtabian, G., Moeini, A., & Moghaddamnia, A. (2020). A novel study of SWAT and ANN models for runoff simulation with application on dataset of metrological stations. *Physics and Chemistry of the Earth, Parts A/B/C*, *120*, 102899.

Zhang, L., Meng, X., Wang, H., & Yang, M. (2019). Simulated runoff and sediment yield responses to land-use change using the SWAT model in northeast China. *Water*, *11*(5), 915.

Zhu, J., Dai, Q., Deng, Y., Zhang, A., Zhang, Y., & Zhang, S. (2018). Indirect damage of urban flooding: Investigation of flood-induced traffic congestion using dynamic modeling. *Water*, *10*(5), 622.

Appendix

Table A. 1 Soil description in SCS method.

Soil Group	Runoff Potential	Description	Final Infiltration Rate (mm/h)
A	Lowest runoff potential	Includes deep sands with very little silt and clay, also deep, rapidly permeable losses.	8-12
B	Moderately low runoff potential	Mostly sandy soils less deep than A, loess less deep or less aggregated than A, but the group has above-average infiltration after thorough wetting	4-8
C	Moderately high runoff potential	Comprises shallow soils and soils containing considerable clay and colloids, though less than those of group D. The group has below-average infiltration after pre-saturation.	1-4
D	Highest runoff potential	Includes mostly clays of high swelling percent, but the group also includes some shallow soil with nearly impermeable sub-horizons near the surface	0-1

Table A. 2 Reference for AMC in SCS method.

AMC	Precipitation in previous 5 days	
	Dormant Season	Growing Season
I	Less than 13 mm	Less than 36 mm
II	13 to 25 mm	36 to 53 mm
III	More than 28 mm	More than 53 mm

Table A. 3 Runoff curve number for urban areas.

Cover Description		Curve Numbers for Hydrologic Group			
Cover Type and Hydrologic Condition	Average Percent Impervious Area	A	B	C	D
Fully developed urban areas (vegetation established)					
Open space (lawns, parks, golf courses, cemeteries, etc.)					
Poor condition (grass cover < 50%)		68	79	86	89
Fair condition (grass cover 50% to 75%)		49	69	79	84
Good condition (grass cover > 75 %)		39	61	74	80
Impervious areas					
Pave parking lots, roofs, driveways, etc. (Excluding right-of-way)		98	98	98	98
Streets and roads:					
Paved; curbs and storm sewers. (Excluding right-of-way)		98	98	98	98
Paved; open ditches. (Including right-of-way)		83	89	92	93
Gravel (Including right-of-way)		76	85	89	91
Dirt (Including right-of-way)		72	82	87	89
Western desert urban areas					
Natural desert landscaping (Previous areas only)		63	77	85	88
Artificial desert landscaping (Impervious weed barrier, desert shrub with 1- to 2-inch sand or gravel mulch and basin borders)		96	96	96	96
Urban districts					
Commercial and business	85	89	92	94	95
Industrial	72	81	88	91	93
Residential districts by average lot size:					
1/8 Acre or less (town house)	65	77	85	90	92
1/4	38	61	75	83	87
1/3	30	57	72	81	86
1/2	25	54	70	80	85
1	20	51	68	79	84
2	12	46	65	77	82
Developing urban areas					
Newly grade areas (previous areas only, no vegetation)		77	86	91	94
Idle lands					

1 Average runoff condition, and IA = 0.2S.

2 The average percent impervious area shown was used to develop the composite CN's. Other assumptions are as follows: impervious areas are directly connected to the drainage system, impervious

areas have a CN of 98, and pervious areas are considered equivalent to open space in good hydrologic condition.

3 CN's shown are equivalent to those of pasture. Composite CN's may be computed for other combinations of open space cover type.

Table A. 4 Runoff Curve Numbers for cultivated agricultural lands.

Cover description			Curve Number for Hydrologic Group			
Cover Type	Treatment	Hydrologic Condition	A	B	C	D
Fallow	Bare soil	--	77	86	91	94
	Crop residue cover (CR)	Poor	76	85	90	93
		Good	74	83	88	90
Row Crops	Straight row (SR)	Poor	72	81	88	91
		Good	67	78	85	89
	SR + CR	Poor	71	80	87	90
		Good	64	75	82	85
	Contoured (C)	Poor	70	79	84	88
		Good	65	75	82	86
	CON + CR	Poor	69	78	83	87
		Good	64	74	81	85
	Contoured & Terraced (C&T)	Poor	66	74	80	82
		Good	62	71	78	81
	C&T + CR	Poor	65	73	79	81
		Good	61	70	77	80
Small Grain	SR	Poor	65	76	84	88
		Good	63	75	83	87
	SR + CR	Poor	64	75	83	86
		Good	60	72	80	84
	C	Poor	63	74	82	85
		Good	61	73	81	84
	C + CR	Poor	62	73	81	84
		Good	60	72	80	83
	C&T	Poor	61	72	79	82
		Good	59	70	78	81
	C&T + CR	Poor	60	71	78	81
		Good	58	69	77	80
Close-Seeded or Broadcast	SR	Poor	66	77	85	89
		Good	58	72	81	85
		Poor	64	75	83	85

Legumes or	C	Good	55	69	78	83
Rotation		Poor	63	73	80	83
Meadow	C&T	Good	51	67	76	80

Table A. 5 Runoff Curve Number for agricultural lands.

Cover description		Curve Number for hydrologic group			
Cover Type	Hydrologic Condition	A	B	C	D
Pasture, grassland, or range-continuous forage or grazing	Poor	68	79	86	89
	Fair	49	69	79	84
	Good	39	61	74	80
Meadow---continuous grass, protected from grazing and generally mowed for hay.	---	30	58	71	78
Brush---brush-weed-grass mixture with brush the major element	Poor	48	67	77	83
	Fair	35	56	70	77
	Good	30	48	65	73
Woods—grass combination (Orchard or Tree Farm)	Poor	57	73	82	86
	Fair	43	65	76	82
	Good	32	58	72	79
Woods	Poor	45	66	77	83
	Fair	36	60	73	79
	Good	30	55	70	77
Farmsteads---building, lanes, driveways, and surrounding lots	---	59	74	82	86

1 Average runoff condition, and Ia = 0.2S.

2 Poor: 75% ground cover and lightly or only occasionally grazed.

3 Poor: 75% ground cover.

4 Actual curve number is less than 30; use CN = 30 for runoff computations.

5 CN’s shown were computed for areas with 50% woods and 50% grass (pasture) cover. Other combinations of conditions may be computed from the CN’s for woods and pasture.

6 Poor: Forest litter, small trees, and brush are destroyed by heavy grazing or regular burning. Fair: Woods are grazed but not burned, and some forest litter covers the soil. Good: Woods are protected from grazing, and litter and brush adequately cover the soil.

Table A. 6 TELEMAC-2D keywords used in this project.

Keyword	Value
EQUATIONS	
BOTTOM SMOOTHINGS	0
FRICTION COEFFICIENT	0.1
PROPAGATION	TRUE
LAW OF BOTTOM FRICTION	4
DIFFUSION OF VELOCITY	TRUE
ADVECTION OR TRACERS	FALSE
TURBULENCE MODEL	1
BOUNDARY CONDITIONS	
PRESCRIBED FLOWRATES	1; 0
PRESCRIBED ELEVATIONS	0; 1
LIQUID BOUNDARIES FILE	'INFLOW.txt'
STAGE-DISCHARGE CURVES FILE	'OUTFLOW.txt'
VELOCITY PROFILES	1;1
OPTION FOR LIQUID BOUNDARIES	1;2
INITIAL CONDITIONS	
INITIAL ELEVATION	182
INITIAL CONDITIONS	CONSTANT ELEVATION
INITIAL TIME SET TO ZERO	TRUE
INPUT&OUTPUT FILES	
GEINETRY FILE	'NIAMEY_GEO.slf'
STEERING FILE	'NIAMEY_STEERING.cas'

BOUNDARY CONDITION FILE	‘NIAMEY_BD.cli’
RESULTS FILE	‘RESULTS.slf’
FORMATTED DATA FILE 1	‘RAINFALL.txt’
FORTRAN FILE	‘RUNOFF_SCS_CN.f’
GRAPHICS AND LISTINGS	
COMPUTATION CONTINUED	FALSE
LISTING PRINTOUT PERIOD	300
INFORMATION ABOUT SOLVER	YES
TITLE	‘NIAMEY RIVER_TELEMAC2D’
TIME STEP	4
NUMBER OF TIME STEPS	410400
DISCRETIZATION IN SPACE	11;11
SUPG OPTION	0;0
TYPE OF ADVECTION	1;5
PRECONDITIONING	2
MASS-LUMPING ON H	1
ORIGINAL DATE OF TIME	2019;07;01
ORIGINAL HOUR OF TIME	00;00;00
TIDAL FLATS	TRUE
OPTION FOR THE TRAT OF TIDAL FLATS	1
NUMERICAL PARAMETERS	
TREATMENT OF THE LINERAR SYSTEM	2
SOLVER	1
SOLVER OPTION	2
SOLVER ACCURACY	1.E-3
MAXIMUM NUMBER OF ITERATION FOR SOLVER	1000
TREATMENT OF NEGATIVE DEPTHS	2

THRESHOLD DEPTH FOR RECEDING PROCEDURE	0.5
IMPLICITATION FOR DEPTH	1
IMPLICITATION FOR VELOCITY	1
RAINFALL	
RAIN OR EVAPORATION	YES
RAINFALL-RUNOFF MODEL	1
ANTECEDENT MOISTURE CONDITIONS	2
OPTION FOR INITIAL ABSTRACTION RATIO	1
NUMBER OF PRIVATE ARRAYS	4
NAMES OF PRIVATE VARIABLES	‘CN’